Stereoselective preparation of 1-phenylmenthol from (-)-menthone as a template for molecularly imprinting and its subsequent adsorption from liquid solutions

By

Mugeri Masala

A dissertation submitted to the School of Mathematical and Natural Sciences Department of Chemistry as the minimum requirements for the fulfilment of Master of Science (MSc) degree in Chemistry at the University of Venda

June 2021

Declaration

I, **Mugeri Masala (11634470)** hereby declare that the work presented under this dissertation titled ‘Stereoselective preparation of 1-phenylmenthol from (-)-menthone as a template for molecularly imprinting and its subsequent adsorption from liquid solutions’’ is my original work under the supervision of Dr. SS Mnyakeni Moleele and Dr. NT Tavengwa and has never been submitted before to this or any other university for any degree and it is presented for a Master of Science degree at the University of Venda.

Candidate’s signature ..... Date 30 JUNE 2021

Dedication

This master's research dissertation is dedicated to my mother Maria Magaisa for being there for me throughout my career. She waited patiently for me to finish, prayed hard for me, and wished me to accomplish and archive all the best I want in my life.

To my sister and brother Nkhetheni and Khodathau, you were physically far from me when I was at school, but I knew you were very close with your love and care each day of my studies.

Lastly, this work also goes straight to my daughter Alita, in the middle of this project I became so strained, but she picked me up and gave me a reason not to give up no matter how hard or slow things were.

They must thank the LORD for his constant love, for the wonderful things he did for them. **(Psalms 107: 15)**

Abstract

Extraction and purification of target compound or analytes from the matrices is always a goal to achieve in different industries and fields of study. Therefore, there is always a need to purify the desired product to get rid of other unwanted products or contaminants. However, to get 100% purity, proper selection of good extraction method and the sorbent with high selectivity is required. Molecularly imprinted polymers (MIPs) as sorbent have demonstrated its usefulness for recognition and separation of the target molecules by improving the quality and selectivity of analytical methods. The aim of the study was to synthesize 1-phenylmenthol by reducing chiral menthone with Grignard reagent, then use it as a template for the preparation of MIPs by precipitation polymerisation.

Menthol was oxidized to menthone by the Jones reagent and then treated with phenyl magnesium bromide (PhMgBr) to give 1-phenylmenthol which was then purified by column chromatography. The major product 1-phenylmenthol was used as a template to prepare MIPs by precipitation polymerization. During polymerization methacrylic acid (MAA) was used as a functional monomer, ethylene glycol di-methacrylate (EGDMA) as cross-linker, azobisisobutyronitrile (AIBN) as an initiator in methanol as a solvent. The non-imprinted polymer was synthesized with the same reagents but without a template. Imprinted polymers were washed to elute or remove the 1-phenylmenthol, with a mixture of methanol/acetic acid (90:10, v/v), all wash out solution was collected and analysed for the presence of 1-phenylmenthol using UV-vis spectroscopy for the total of 10 cycles. The four elution were considered enough to wash out the template.

The product (1-phenylmenthol) was characterized by Fourier transform infra-red (FIRT), carbon and proton MNR spectroscopy. The results from ^{13}C NMR confirmed the presence of the two quaternary carbons at 148.6 ppm and 78.4 ppm, while ^{1}H NMR confirmed the presence of OH peak at 2.2 ppm. FTIR showed a broad O-H peak at 3592 cm^{-1}, strong C-H at 2924 cm^{-1} and 3052 cm^{-1} from alkanes and benzene, respectively. The polymers (unwashed MIPs, washed MIPs, and washed NIPs) were characterized by Brunauer-Emmett-Teller (BET), Fourier Transform Infra-red (FTIR), thermogravimetric analyser (TGA), and ultraviolet (UV) spectroscopy. The BET results showed higher surface area (17.85 $m^2\ g^{-1}$), pore size (85.27 Å), and pore volume (0.038 $cm^3\ g^{-1}$) for the MIP as compared to NIP with the surface area of (10.05 $m^2\ g^{-1}$), pore size (70.69 Å) and pore volume (0.018 $cm^3\ g^{-1}$). TGA confirmed the stability of washed MIP and NIPs up to 300°C as compared to unwashed MIP which was gradually

decreasing in weight from 100°C. FTIR results shows the presence of template by broad O-H peak at a higher wavenumber of 3573 cm^{-1} and strong C-H stretching peaks from alkane groups on unwashed MIPs as compared to washed MIPs and NIPs which did not have the template. A series of parameters such as the effect of concentration, the effect of polymer mass, effect of sample pH, and effect of the contact time were investigated. The high enrichment factor was achieved at samples pH 7 as the optimum pH. In the effect of concentration, the optimum concentration were 11 mg L^{-1} and 7 mg L^{-1} for MIP and NIP, respectively. The optimum mass of the polymer was determined to be 50 and 80 mg for MIP and NIP, respectively. The optimum time for the adsorption of the 1-phenylmenthol was at 180 min.

(-)-Menthone and 1-phenylmenthol were successfully synthesised and purified using column chromatography with silica gel. Unlike other essential oils (menthol and menthone), 1-phenylmenthol was found to have these properties as they were never reported before: it has no minty odour, colour is yellowish and not soluble in water. Molecularly imprinted polymer was successful synthesized using precipitation polymerization. The method can be applied to real samples based on high enrichment factors obtained.

Keywords: Menthone, stereoselective, Grignard reaction, 1-phenylmenthol, molecularly imprinted polymers (MIPs), adsorption studies

Acknowledgments

First and foremost, I would like to thank God almighty my refuge, for giving me grace, strength, knowledge, and ability to pursue this research study and to persevere and complete it satisfactorily. Without His blessings, this achievement would not have been possible. Special and deep gratitude goes to my supervisor and co-supervisor Dr. SS Mnyakeni Moleele and Dr. NT Tavengwa for providing me with the opportunity to work on this research and their encouragement, support, and supervision at all levels. I want to express my appreciation to the chemistry technicians, Mr. F. Mutshaeni and Mr. Pandelani for assisting me with laboratory chemicals and NMR sample analysis. I cannot express how grateful I am to the National Research Foundation (NRF), Sasol Inzalo Foundation, and University of Venda research and publications committee (RPC) for funding my project. I also want to thank all my friends from Chemistry and Biochemistry departments for their support, patience, and guidance in the laboratory. To be honest, these guys helped from that point where I did not know a thing. A special thanks to my mother, my sister, and brother, for the encouragement, love, patience, and for always being there, no matter what.

Finally, I would like to thank my Roman Catholic Church father Benoit, he could not understand why I was always absent from youth meetings, but he finally understood that I was busy studying hard to complete my MSc studies.

THANK YOU ALL!

Table of contents

List of figures

List of tables

List of schemes

List of abbreviations

^{13}C NMR	Carbon nuclear magnetic resonance
^{1}H NMR	Proton nuclear magnetic resonance
ACC	1,1-azobis (cyclohexane-1-carbonitrile)
AIBN	Azobisisobutyronitrile
BET	Brunauer-Emmett-Teller
BGE	Background electrolyte
$CDCl_3$	Chloroform-d
CDs	Cyclodextrins
CE	Capillary electrophoresis
CEC	Capillary electrochromatography
$CeCl_3$	Cerium chloride
CO_2	Carbon dioxide
CSIR	Council for scientific and industry research
CSP	Chiral stationary phase
CZE	Capillary zone electrophoresis
DLLME	Dispersive liquid-liquid micro-extraction
DMPA	2,2 dimethoxy-2-phenylacetophenone
DVB	1,4 divinylbenzene
EGDMA	Ethylene glycol di-methacrylate
EKC	Electro-kinetic chromatography
FPSE	Fabric phase sorptive extraction
FTIR	Fourier-transform infrared spectroscopy

GC	Gas chromatography
GLC	Gas-liquid chromatography
GSC	Gas- solid chromatography
H_2NNH_2	Hydrazine
H_2SO_4	Sulphuric acid
HCl	Hydrochloric acid
HPLC	High-performance liquid chromatography
iPD	*Trans*-isopiperitonol dehydrogenase
iPI	*cis*-isopulegone isomerase
iRP	isopiperitonone reductase
L_3OH	Limonene-3-hydroxylase
$LiAlH_4$	Lithium aluminium hydride
LLE	Liquid-liquid extraction
LPME	Liquid phase micro-extraction
LS	Limonene synthase
MAA	Methacrylic acid
MEKC	Micellar electro-kinetic capillary chromatography
MEPS	Micro-extraction by packed sorbents
MHz	Mega hertz
MIPs	Molecularly imprinted polymers
MISPE	Molecularly imprinted solid-phase extraction
MMR	Menthone: menthol reductase
MNR	Menthone: neomenthol reductase
MOF	Metal organic framework

MS	Mass spectrometer
$Na_2Cr_2O_7 \cdot 2H_2O$	Sodium dichromate dihydrate
Na_2SO_4	Sodium sulphate
$NaBH_4$	Sodium borohydride
NACE	Non-aqueous capillary electrophoresis
NADH	Nicotinamide adenine dinucleotide
NADPH	Nicotinamide adenine dinucleotide phosphate
$NaHCO_3$	Sodium hydrogen carbonate
NH_4Cl	Ammonium chloride
NIPs	Non-imprinted polymers
NMR	Nuclear magnetic resonance
NSAIDs	Non-steroidal anti-inflammatory drugs
PETE	Pentaerythritol triacrylate
PETEA	Pentaerythritol tetra-acrylate
PhLi	Phenyl lithium
PhMgBr	Phenyl magnesium-bromide
Ppm	Parts per million
PR	(+)-pulegone reductase
PS-DVB	Polystyrene divinylbenzene
SBSE	Stir bar sorptive extraction
SDME	Single drop micro-extraction
SEM	Scanning electron microscopy
SFC	Supercritical fluid chromatography
SPE	Solid-phase extraction

SPME	Solid phase micro-extraction
TFA	Trifluoroacetic acid
TGA	Thermogravimetric analysis
THF	Tetrahydrofuran
TLC	Thin-layer chromatography
TRIM	Trimethylolpropane triacrylate

Chapter 1

Introduction

This chapter "introduction" gives the general background introduction of the study, problem statement, aims and objectives of the project.

1.1. Background

Most of the essential oil including menthone and menthol are chiral compounds. Like many molecules of biological enzymes, proteins, neurotransmitter, hormones, and drugs contain several stereogenic centers, hence, they have so many health benefits in humans. However, the quantitative analysis of chiral molecules remains challenging, for more complex molecules such as 1-phenylmenthol [1]. The synthesis of 1-phenylmenthol was investigated via the reduction of monoterpene menthone. 1-phenylmnethol is now a novel derivative of menthol where phenyl group is added by Grignard reagent instead of hydrogen by $NaBH_4$. Menthol and menthone are natural compounds extracted from the peppermint plant, *Mentha x piperita*, in which the peppermint leaves have several health benefits, for example, it can be used to treat common cold, headaches and as an aromatherapy [2]. They are known for their minty odour, refreshing and cooling sensation [3]. Menthol is mostly used but both menthone and menthol are abundant in all essential oil extracts [4].

Diluted extracts can be applied to the skin for relief from itching, muscle pain, and the perception of airflow in your nasal cavity when inhaling their vapours [5, 6]. They can be also used as flavouring agent in foods, soaps, and cosmetic products [7]. Leaves from pennyroyal tea (*Mentha pulegium*) can be used as herbs or tea which also have best health benefits [8]. Pennyroyal tea has antibacterial and anti-inflammatory properties; thus, it can fight flu and blocked sinuses due to bacterial infections [9]. After consuming anything containing menthol, it gives the cooling sensation and noticeably minty scent (freshen your breath), same reason why menthol is a common flavouring for toothpastes, mouthwashes, chewing gums, sweets, tea, and skin products [3, 9, 10].

A variety of methods are used for the extraction of essential oils from plants [8] such as steam distillation [11], hydro-distillation [12, 13], microwave extraction [14] and supercritical fluid extraction [15–17]. Therefore, after extraction from the plants, separation, recovery, and identification of compound of interest is required. Thus, sample preparation plays several roles: to reduce the complexity (selective from the mixture), to pre-concentrate target of compound with high extraction efficiency and enrichment factors [18].

There are many reported and used pre-concentration extraction techniques of compound from different fields (environmental, pharmaceutical, biological, food and analytical laboratories) [19–21] such as: solid phase extraction (SPE) [22–24], and liquid-liquid extraction (LLE) [25], solid phase micro-extraction (SPME) [26], stir bar sorptive extraction (SBSE) [27, 28], micro-

extraction by packed sorbent (MEPS) [29], fabric phase sorptive extraction (FPSE) [30, 31], and dispersive liquid-liquid micro-extraction (DLLME) [32], liquid-phase micro-extraction (LPME) [33].

Although these methods were used by different researchers in different application, they have some limitations. For example, SPME, suffers from relatively low operating temperature, instability and swelling of the coating if exposed to organic solvents, low sorbent loading and poor extraction sensitivity and it can only be used where low sample volume is needed, but limited in applications where large sample volumes are required [19]. SBSE suffers from poor extraction sensitivity. MEPS is like SPME, it permits its application in analyses where only small volumes are needed but limited in applications where higher volumes are required such as environmental fields. Furthermore, applications are relatively limited for food supplements due to difficult application of MEPS, which requires a longer time in the pre-analytical steps [21]. LLE has been replaced long time ago due to well experienced disadvantages: the used of large volume of toxic organic solvents, high time-consuming and expensive [34]. SPE also uses large volume of extraction solvents, besides, it involves a multistep procedure and may cause blockage when handling real samples [20].

Adsorption is one of the most effective, suitable, economic, and healthy methods for the removal of target compounds, organic compounds, drugs, heavy metals, etc from different matrices [35]. Adsorption process has attracted attention of many researchers because of low cost, design flexibility, and high efficiency [36, 37]. Another advantage is availability of adsorbents but, effectiveness of adsorption process needs to be considered while selecting adsorbent material [35]. Adsorbents are of different types, and examples include silica-based sorbents [38, 39], activated carbon [40], polystyrene-divinylbenzene (PS-DVB) [41–43], porous graphitic carbon [44–46], molecular imprinted polymers (MIPs) [47, 48], metal organic framework (MOF) [49, 50], and zeolites [36, 51, 52].

However, great attention has now been paid towards molecularly imprinting polymer (MIP) sorbent to improve the quality and selectivity of analytical methods [48]. The development of molecularly imprinting polymers (MIPs) demonstrated its usefulness for recognition and separation of target molecules. Unlike other sorbents materials, MIPs have advantages such as stability, selectivity, easy application and preparation, which has promoted an increasing number of applications in various areas [53–55]. Following proper selection of great extraction method, the best sorbent is also selected to get high selectivity of pre-concentrated target

compound. Selective and highly adsorptive MIPs are influenced by the functional monomers and cross-linkers used. Appropriate functional monomers and cross-linking strongly determine the effectiveness of MIPs interacting with target molecules and polymer complex stability formed during the polymerization process [56]. MAA has ability to interact with the template through hydrogen bonds whereas, EGDMA is highly reactive, which produce polymers with high stiffness so that it is more stable [57].

In this study, menthol was oxidized to menthone by the Jones reagent and then treated with phenyl-magnesium bromide (PhMgBr) to give 1-phenylmenthol. 1-phenylmenthol was found to be a yellowish oil, but, without minty odour like menthone and menthol. The synthesized 1-phenylmenthol was then used as a template in the synthesis of molecularly imprinted polymers (MIPs). During polymerization, MAA was used as a functional monomer, EGDMA as cross-linker, AIBN as an initiator in methanol as a solvent.

1.2. Problem statement

Most organic synthetic reactions are known to produce one or two products due to the stereoselectivity of starting material, for instance, a chiral menthone is known to form two diastereomers product, but only one major product is isolated and the other is an impurity. Therefore, there is always a need to purify the desired product to get rid of the unwanted products. Analytes at times occur in trace amounts which is a problem because they will be detected by most analytical instruments. Therefore, there is a need to pre-concentrate before instrumental analysis.

Purification by extraction and recovery of analytes becomes important to many industrial, environmental, pharmaceutical, biological, and analytical laboratories, because they cannot take anything below 100% purity. This is where diverse extraction methods and extraction sorbent materials are used. Most of these extraction methods suffer from instability, the use of large volumes of toxic organic solvents, time-consuming and they are expensive, while most of sorbent materials suffer from lack of selectivity and some cannot be reused. It is against this background that this research will attempt to develop molecularly imprinted polymers (MIPs) as the selective sorbent used in solid phase extraction. Unlike other sorbents, MIPs has ability to recognise (selectivity) and separation of target compound from the matrix.

1.3. Aim and objectives.

1.3.1. Aim

Synthesis of 1-phenylmenthol by Grignard reduction of (-)-menthone as the template for the preparation of molecularly imprinted polymers (MIPs) by precipitation polymerisation. The MIPs was then used for the removal of 1-phenylmenthol from spiked solutions.

1.3.2. Objectives

- Carrying out Grignard reaction for the synthesis of 1-phenylmenthol.
- Characterization of the Grignard reaction product(s) using ^{13}C-, ^{1}H-NMR and FTIR.
- Synthesis of the MIP using 1-phenylmenthol by precipitation polymerization.
- Characterization of the MIP and NIP using UV-Vis, TGA, FTIR and BET.
- Optimization of the adsorption of 1-phenylmenthol (effect of concentration, the effect of polymer mass, effect of sample pH, and effect of the contact time).
- Carrying out reusability studies of the prepared imprinted polymers.

Chapter 2

Literature review

This chapter gives a detailed literature review concerning reaction schemes of how menthone, the starting compound is enzymically and chemically synthesized. Synthesis of 1-phenylmenthol and examples of other organometallic reactions was highlighted. Drawbacks associated with chiral or racemic organic compounds, importance of chiral compound separation and methods to separate them including MIPs as sorbent material for extraction technique were also discussed. Synthesis of MIPs, preparative approaches and polymerization reagents used during template imprinting was fully discussed.

2.1. Extraction of peppermint essential oils

The genus Mentha consists of variety of species, which includes: *mentha x peperita, and mentha pulegium* etc. Peppermint essential oils are extracted from the leaves of *mentha x peperita* plant, composition depends on the type of verities at different stages of its production and extraction conditions. The active components found in peppermnt oil are menthol, menthone, isomenthone, limonene, neomenthol, geranyl giphosphate and (+)-Pulegone [8]. However, the major component is menthol and menthone, they are well recognised due to their refreshing minty flavour and odour which they give to plants[58–60].

This section talks more about the biological production and storage of essential oils on the leaf of peppermint. The essential oils of peppermint and other Mentha species is produced and accumulated specifically on the leaf of peppermint plant, which is made from peltate glandular trichomes (oil glands) found on the surface of the leaf. These epidermal oil glands are composed radially dispersed secretory cells that is embedded in the surface, in which the essential oils are synthesized [61]. The oil gland cells (where essential oils are produced and stored) are isolated, then once they are isolated, they can provide a clarify biosynthesis pathway steps and relevant biosynthetic enzymes needed which also permit basic purification and detailed characterization of menthol pathway catalysts. The biosynthesis of (−)-menthol from primary metabolism requires eight enzymatic steps [62]. The biosynthesis pathway route was described to show biological extraction of essential oils into which menthone, and menthol are isolated and purified. Therefore, they can be used as starting material in further organic reactions such as synthesis of 1-phenylmenthol. Unlike other compounds that are commercially available or that can be derived from the purification of essential oil mixtures, 1-phenylmenthol is not commercially available.

2.1.1. Enzyme-catalysed biosynthesis of menthol from peppermint (*Mentha x piperita*)

Biosynthesis of menthol was reviewed, which menthol and related monoterpenes are produced and accumulated at the upper peppermint leaf surface. Different compounds of peppermint oils are produced in different plant cells and organs. Eight enzymes shows in schemes below catalysed the production of major peppermint constituents (menthone and menthol) [63].

The biosynthesis (Scheme 1) starts with (-)-limonene synthase (LS) enzymes which catalysed conversion of geranyl diphosphate by conducting the cyclization leading to (-)-limonene. (-)-Limonene itself is an important precursor in the peppermint plant pathway [63]. The next step is the NADPH- and O_2-dependent hydroxylation of (-)-limonene to form (-)-trans-isopiperitenol, followed by allylic oxidation of (-)-trans-Isopiperitenol to form the α, β- unsaturated ketone (-)-isopiperitenone. Double

bond in the α,β-unsaturated ketone now activated, for the stereospecific, 1.4 addition of NADPH to form (+)-cis-isopulegone by the enzyme (-)-isopiperitenone reductase, the last step on this scheme is formation of (+)-pulegone by movement of a double bond of (+)-cis-isopulegone [64].

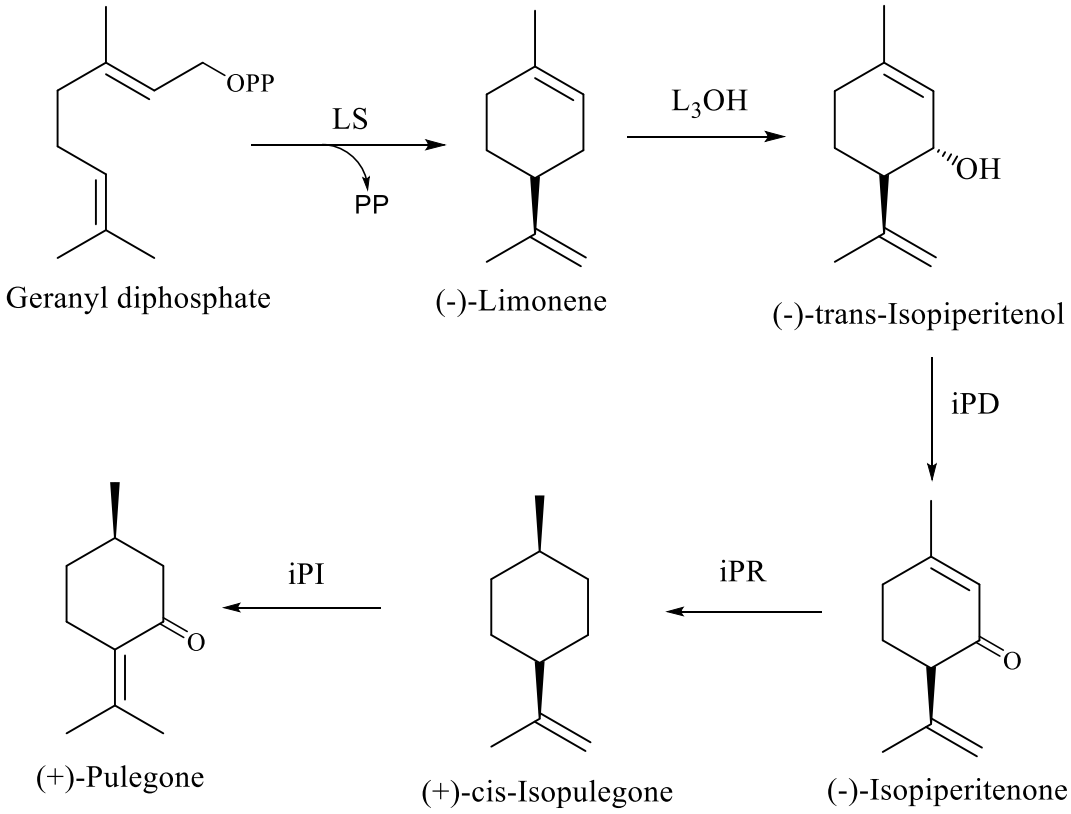

Scheme 1: Conversion of geranyl diphosphate to (+)-pulegone. The enzymatic steps are catalysed by (-)-limonene synthase (LS), (-)-limonene-3-hydroxylase (L_3OH), (-)-trans-isopiperitenol dehydrogenase (iPD), (-)-isopiperitenone reductase (iPR), and (+)-cis-isopulegone isomerase (iPI).

Via (+)-pulegone, (+)-pulegone reductase (PR) converts (+)-pulegone to (+)-isomenthone, and (-)-menthone (Scheme 2) [63, 64]. (+)-pulegone plays an important role in peppermint metabolism pathway as the precursor of (-)-menthone and (+)-isomenthone. However, previous studies had suggested that pulegone reductase lacked stereoselectivity in the formation of both (-)-menthone and (+)- isomenthone [65], instead (-)-menthone and (+)-isomenthone were produced by recombinant or NADH-dependent reductase [62, 65].

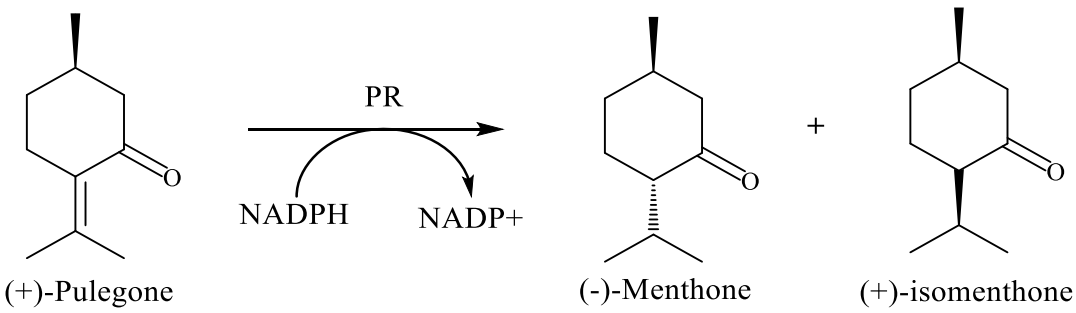

Scheme 2: Conversion of (+)-pulegone to (+)-isomenthone and (-)-menthone. The enzymatic steps are catalysed by (+)-pulegone reductase (PR).

With (-)-menthone as a starting point, the last step in the biosynthesis of menthol is the formation of menthol and its isomers, menthone is reduced by (-)-menthone:(-)-menthol reductase (MMR) and menthone: (+)-neomenthol reductase (MNR) enzymes to form (-)-menthol and (+)-neomenthol respectively (Scheme 3). Likewise, with (+)-isomenthone as the substrate, (+)-neoisomenthol and (+)-isomenthol are produced with the same enzymes (Scheme 4) [63, 66]. Based on genetic implication and direct demonstration, two different NADPH dependent keto-reductases operate on (−)-menthone and (+)-isomenthone, one NADPH-dependent reductase convert (-)-menthone to (-)-menthol and (+)-neomenthol, the other converts (+)-isomenthone to (+)-neoisomenthol and (+)-isomenthol [64, 67, 68]

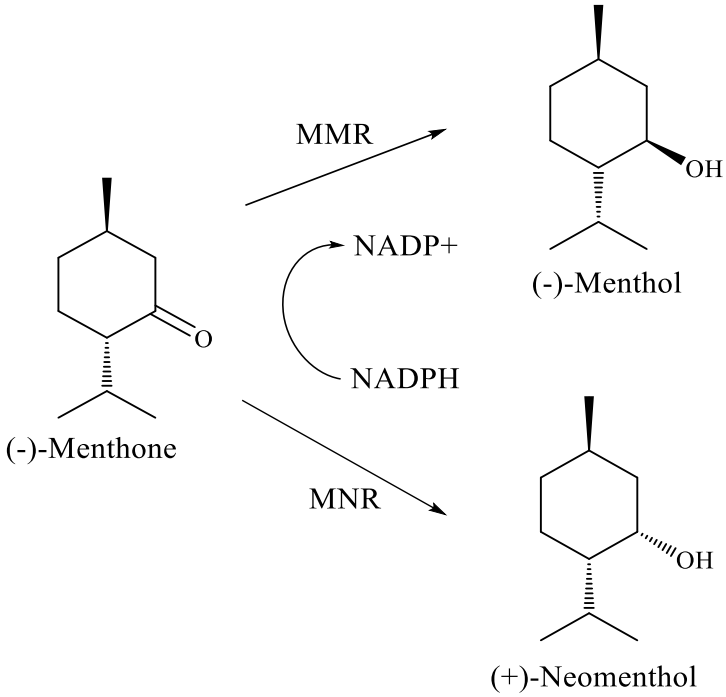

Scheme 3: Conversion of (+)-menthone to (-)-menthol and (+)-neomenthol. The enzymatic steps are catalysed by (−)-menthone:(−)-menthol reductase (MMR) and menthone: (+)-neomenthol reductase (MNR)

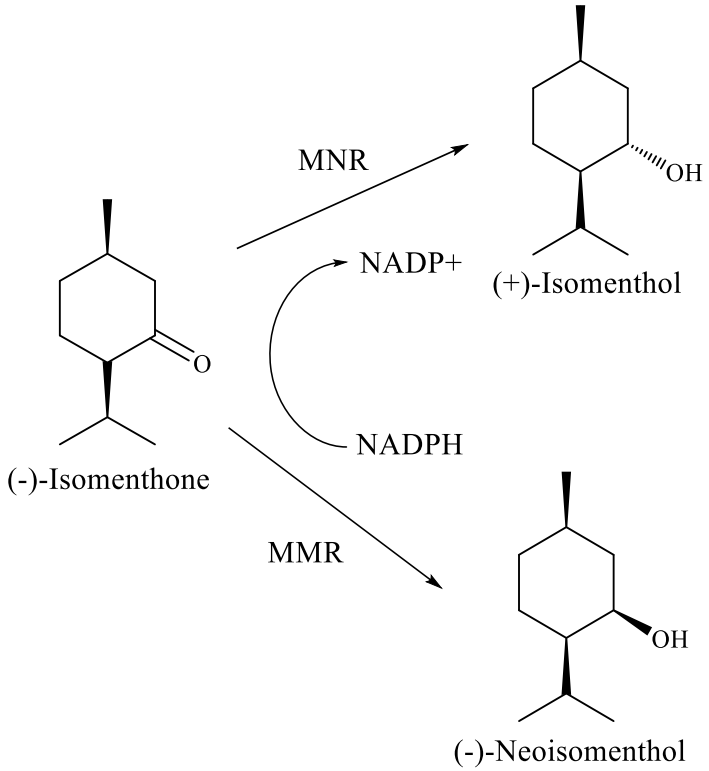

Scheme 4: Conversion of (+)-isomenthone to (+)-isomenthol and (+)-neoisomenthol. The enzymatic steps are catalysed by (−)-menthone:(−)-menthol reductase (MMR) and menthone: (+)-neomenthol reductase (MNR)

2.2. Stereoselective addition of organometallic (R-MgX) reagents to (-)-menthone

Menthone and menthol are now commercially available, meaning to get them one should not go through the biosynthesis again. This has drove the attention of many researchers for the further investigation on the chemical synthetic and stereoselectivity reduction of chiral menthone. However, most of the interest was on the addition of organometallics (R-MgX) to (-)-menthone instead of other reducing agents (e.g. $NaBH_4$, $LiAlH_4$, H_2NNH_2 etc.) [68].

The first synthesis of menthone was via oxidation of menthol by chromic acid [69]. There are not many records about the chemical synthesis of menthone from pulegone. The only reported reaction was the addition of organotin anions to (+)-pulegone, i.e., compounds with tin-metal bonds [70]. Otherwise more interest in previous studies was the addition of organometallic reagents to ketones including menthone. Since menthone is an enolizable and hindered ketone (due to bulk isopropyl group), as compared to cyclohexanol, it always made it difficult to be reduced into two isolated diastereomers as theoretically hypothesized [71]. Lecomte *et al*. [72] described the addition of phenyl lithium to (-)-

fenchone (Scheme 5), (-)-menthone, and (+)-camphor where the aim was to increase the stereoselectivity yields of the products.

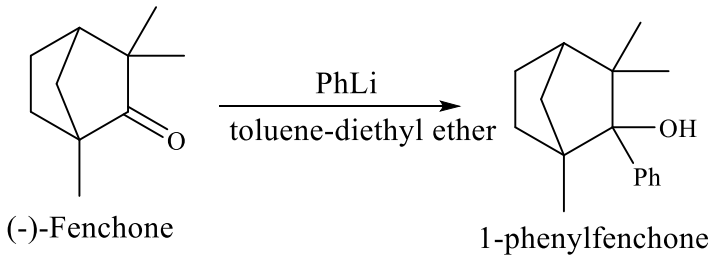

Scheme 5: Stereoselective addition of phenyl lithium (PhLi) to (-)-fenchone.

The reduction of menthone by organometallic reagents was also described by Panev and Dimitrov [69]. They investigated the addition of several organometallic reagents to (-)-menthone with and without $CeCl_3$ to improve the synthetic method for the preparation of neomenthol derivatives in high yields as well as studying their stereoselectivity. These examples from the literature drive the experimental procedure reaction of our project and emphasize how challenging this reaction was.

In this study, the proposed reaction scheme was the stereoselective reduction of menthone by PhMgBr to yield 1-phenylmenthol as the major product (Scheme 6).

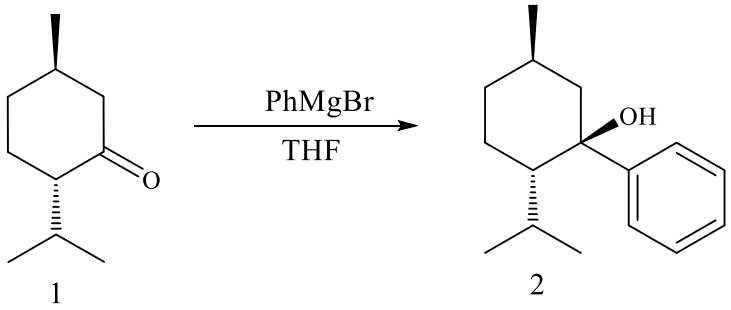

Scheme 6: Stereoselective addition of PhMgBr to (+)-menthone.

2.2.1. Formation of the two diastereomers

This section describes the stereoselective nucleophilic addition of Grignard reagent to menthone. The axial attack makes hydroxyl group (-OH) be equatorial and form menthol derivative (Scheme 7) [73]. The equatorial attack makes hydroxyl group (-OH) be axial and form neomenthol derivative (Scheme 8). In most addition reactions published, the attack by the PhMgBr has been described to proceed exclusively from the equatorial side of the carbonyl C-atom, resulting in the formation of neomenthol derivatives [69].

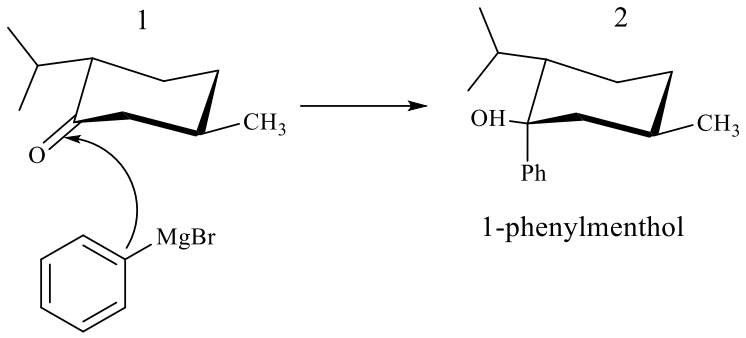

Scheme 7: Formation of 1-phenylmenthol by axial addition of PhMgBr.

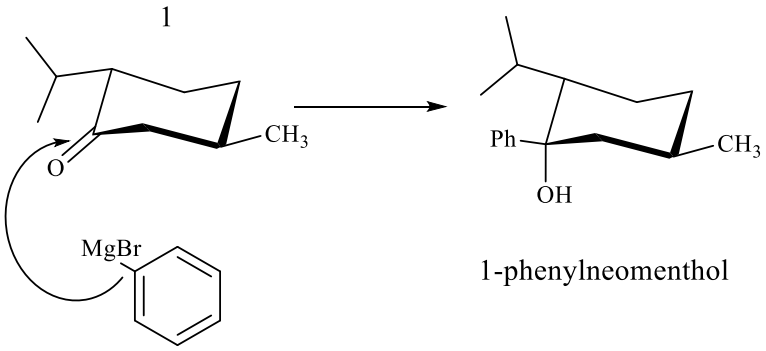

Scheme 8: Formation of 1-phenylneomenthol by equatorial addition of PhMgBr.

2.3. Chirality of organic compounds

Most chiral organic compounds e.g., pesticides and therapeutic drugs, after synthesis, are sold on the market as racemic mixtures. The enantiomers in the racemates do not exhibit the same bioactivity towards target diseases, Table 1 shows some examples of chiral compounds with their contrasting [74–76]. Because of this chirality, living organisms show different biological responses to one of the pair of enantiomers in drugs, pesticides, or any other organic compound [77]. As a result, two enantiomers of certain drugs will exhibit different pharmacokinetics activities such as toxicology, absorption, distribution, and metabolism in the human body [74]. Thus, one isomer may produce the desired therapeutic activities, while the other may be inactive or produce unwanted effects [77]. The problem with side effects and environmental issues caused by racemic drugs or pesticides encouraged researchers to separate two racemates into enantiopure products. Besides, removal of unwanted, inactive isomer will reduce metabolic drug load in patients' bodies, avoid bio-inversion, reduce drug interactions and it will make organic reactions simpler [78, 79].

Table 1: Contrast pharmacokinetics activities of chiral compounds

Enantiomer 1	**Enantiomer 2**
S-propranolol 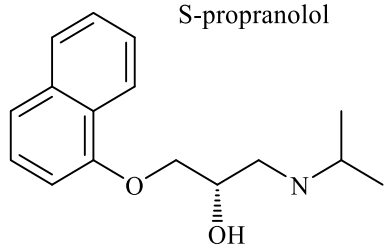 S(-)-Propranolol is a beta-blocker used to treat hypertension (high blood pressure), and other diseases [80]	R-propranolol 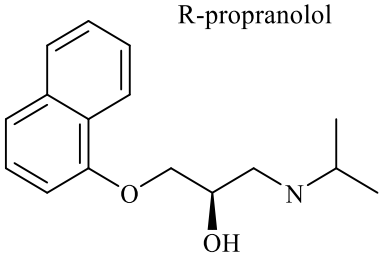 R- (+)-propranolol is inactive
L-dopa 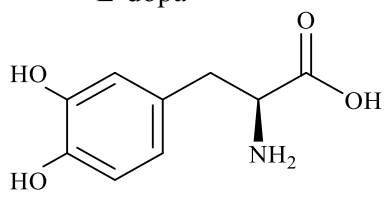 L-Dopa is used in therapeutics treatment of Parkinson disease [81]	D-dopa 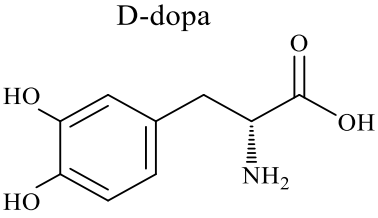 D-dopa is inactive
S-ketamine 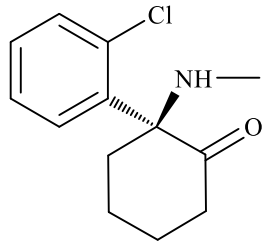 S-(+)-ketamine is used to induce loss of consciousness or anesthesia [80]	R-ketamine 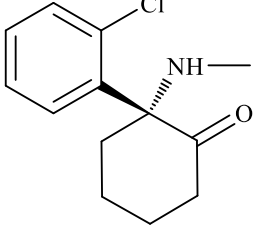 R-(-)-ketamine has negative effects of causing agitation and hallucination
(-)-Menthol 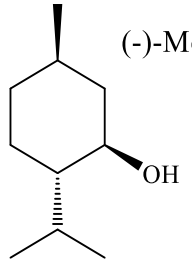 (-)-Menthol has a strong minty odor and cooling sensation [63, 66, 82]	(+)-Neomenthol 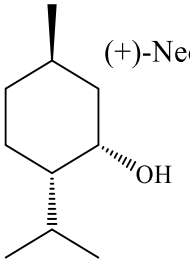 (+)-Menthol and (+)-neomenthol are less minty with a strong musty odor

2.4. Chiral separation techniques

As already discussed above, it is important to separate chiral compounds. Thus, this section concentrated on separation methods. These have been used in chiral separations of the different compounds.

2.4.1. High-performance liquid chromatography with chiral columns

Due to its remarkable properties like reproducibility, selectivity, sensitivity, rapidness, and the availability of a wide range of chiral stationary phases (CSPs), high-performance liquid chromatography (HPLC) has achieved a great reputation in chiral resolution [83]. HPLC is a highly improved form of column liquid chromatography. Instead of a solvent being allowed to flow through a column under gravity, it is forced through under high pressures of up to 400 atmospheres which makes it much faster. HPLC is carried out at around room temperature, thus, it is suitable for chiral resolution [84].

For chiral separation, HPLC is divided into two categories: namely, direct resolution using chiral stationary phase (CSP) [85] and indirect resolution employing chiral derivatization reagents. Chiral derivatization is explained under gas chromatography (GC) [85]. In the direct resolution, CSP is added into the column interacting continuously with the enantiomers to be separated. CSPs are categorised into polysaccharide-based CSPs, cyclodextrin-based CSPs [86], macrocyclic antibiotic-based CSPs, ion-exchange-type CSPs, crown ether-based CSPs, protein-based CSPs, brush/pirkle-type CSPs and molecularly imprinted polymer (MIP) CSPs [87, 88].

Rebizi *et al*. [88] investigated the chiral separation of cefadroxil by using HPLC with UV detection using polysaccharide-based CSPs, namely cellulose and amylose derivatives as chiral selectors. Cefadroxil is a *β-lactam* antibiotic, a chiral compound with three stereogenic centres that allow eight possible stereoisomers. Among eight diastereomers. only one isomer of cefadroxil is active as an antibiotic. Therefore, to ensure the quality of cefadroxil, the determination of optical impurities is required. This was achieved by using commercially available different coated and immobilized polysaccharide derivatives of both cellulose and amylose as CSPs. It resulted in the separation of stereoisomers with good resolution on cellulose CSPs (Chiralpak IB column) using hexane–2-propanol (60: 40 v/v) as the mobile phase, but poorly resolved on amylose CSPs.

Fedorova *et al*. [89] reported a new protein-based CSP. They synthesized new silica-based, mixed-binary chiral sorbent grafted with the macrocyclic antibiotic eremomycin and bovine serum albumin (BSA). The eremomycin-BSA sorbent was filled into the HPLC column for enantio-separation of racemic profens (ketoprofen, ibuprofen, and indoprofen). The results showed that mixed sorbent

(eremomycin-BSA) provided a higher resolution of enantiomers as compared with results obtained using a sorbent with only eremomycin as the chiral selector.

Yang *et al*. [90] conducted enantio-separation of eleven 3,5-disubstituted hydantoins in HPLC under the normal phase mode using Chiralpak IA, a polysaccharide-based CSP. Hydantoin is an organic heterocyclic compound used in organic chemistry. 3,5-disubstituted hydantoins were reported to be chiral auxiliaries. Therefore, to obtain high optical purity of a chiral auxiliary chiral HPLC column was used to successfully separate them.

Fanali *et al*. [91] conducted the enantio-separations experiment of flavanone derivatives using polysaccharide-based CSP by HPLC in the normal- and polar organic phase mode. Based on the results both cellulose 3, 5-dichlorophenylcarbamate, and amylose 3,5-dimethyl phenyl carbamate were useful CSP, but the problem was mobile phases that were making it difficult to achieve the best enantiomers elution.

Sun *et al*. [92] performed the first chiral separation of haloxyfop (herbicide) enantiomers on a pirkle type CSP called (R, R) Whelk-O1 chiral column coated with 1-(3, 5-dinitrobenzamido)-1, 2, 3, 4-tetrahydro phenanthrene as CSP by HPLC. Haloxyfop is a chiral herbicide used to control annual and perennial grasses in broadleaf crops. It has pair of enantiomers, R-haloxyfop and S-enantiomer, as known that the use of active enantiomer helps reduce the amounts of pesticides released into the environment, the separation was done and CSP showed excellent enantioselectivity toward the two enantiomers.

2.4.2. Gas chromatography with chiral columns

Gas chromatography (GC) uses carrier gas as a mobile phase, usually an inert gas such as helium or nitrogen [93]. The mobile phase carries the vaporized sample through a stationary phase in the column than to the detector, mainly mass spectrometer (MS) [93]. Due to the chiral stationary phase and chiral derivatization reagent, chiral GC is well recognized as a powerful, simple, convenient, fast, and efficient method for the separation of enantiomeric compositions of volatile and thermally active components [86, 94]. Chiral GC stationary phases were mainly classified into three categories: cyclodextrin derivatives, chiral amino acid derivatives, and metal coordination complexes. However, some chiral GC stationary phases have been developed such as chiral ionic liquids, polysaccharides, cyclopeptides, and metal-organic frameworks [95].

It has been applied for many different analytes, such as essential oils, fragrances, intermediates, organic compounds, metabolites, pharmaceuticals drugs, and pesticides [84, 94]. Furthermore, indirect resolution is the method of converting enantiomers to diastereomers via chemical reactions with chiral

derivatizing reagents, which are then separated by GC using achiral columns [96, 97]. This is because different molecular properties displaced by diastereomers make it simple to be separated by usual chromatographic techniques, while enantiomers can be resolved only by using the specific column with a CSP [98].

Patil *et al*. [95] demonstrated how the ability of cyclodextrin-based GC stationary phases was improved by derivatization. Using permethylated, acetyl, dimethyl, trifluoro acetyl, and dipentyl as derivatization reagents, cyclodextrins (CDs) were derivatized to improve their enantioselectivities, to decrease melting points, and to improve solubilities.

Derwich *et al.* [58] extracted and analysed the chemical composition of essential oils from *Mentha pulegium* leaves, a traditional herbal medicine in Morocco. They were extracted by hydro distillation and analysed by GC-FID and GC–MS. Twenty-eight compounds were identified, and the yield of essential oils was 1.66%. The total identified compounds accounted for about 97.34% of the oil.

Almalki *et al.* [99] Synthesized and analysed six N-(dimethoxybenzyl)-4-Bromo-2,5-dimethoxyphenethylamine isomers. GC–MS methods were used to differentiate and specifically identify all six members of this dimethoxy-benzyl 25B-NBOMe derivatives. Halogenated and non-halogenated derivatives (N-(2′,5′-dimethoxybenzyl)-2,5-dimethoxyphenethylamine) were prepared and subjected to EI-MS analysis, as a result, all six of these isomer derivatives showed equivalent EI-MS fragment ions. The combination of different base peak ions (m/z 151 or 242/244), unique fragment ions (m/z 136 and m/z 263), along with differences in the relative abundance of ions at m/z 121 and m/z 91, allowed for differentiation and specific identification of all six of the isomeric derivatives [99].

2.4.3. Supercritical fluid chromatography

SFC is another technique, related to HPLC, which uses a supercritical fluid as the mobile phase, i.e., fluid at a pressure and temperature above the critical point [100]. Supercritical mobile phases (typically CO_2) have properties that are intermediate between those of gases and those of liquid. Supercritical CO_2 is created by subjecting the gas to high pressures. The high diffusivity and low viscosity of supercritical fluids allow the use of high flow rates without any harmful effects on separation efficiency [101]. The use of a CO_2 as mobile phase gives the technique its advantages such as higher flow rates, faster separations, and lower organic solvent consumption. Furthermore, after pressure reduction, CO_2 may be easily evaporated, recycled, and reused, which reduces costs and the amount of generated waste [102, 103].

The enantioselective separation performance of SFC is influenced by the column, mobile phase flow rate and composition, pressure, and temperature. An organic polar solvent must be added to the mobile

phase to elute analytes from the column [101]. CSPs used in SFC are mainly the same as those used in HPLC. Polysaccharide derivative CSPs have been commonly used for the chiral separation of pesticides, i.e. amylose tris(3,5-dimethyl phenyl carbamate) and cellulose tris (3,5- dimethyl phenyl carbamate) CSPs [104, 105].

Tao *et al*. [102] developed an SFC-MS/MS method for simultaneous detection of fenbuconazole (fungicide) and its chiral metabolites in fruit, vegetable, cereal, and soil. Baseline separation of six stereoisomers was achieved on ACQUITY UPC2 Trefoil AMY 1 column (amylose and Chiralpark IB-3 cellulose polysaccharide CSPs). Recoveries for the six target analytes were between 76.3% and 104.6%.

Yan *et al*. [106] developed two-step method for the separation of β-cypermethrin (pesticide) stereoisomers by SFC with polysaccharide chiral stationary phases. The effects of chiral stationary phases, mobile phases were also considered. Through a two-step separation, β-cypermethrin was firstly separated by using a cellulose-derived chiral stationary phase to obtain two stereoisomeric pairs, and further resolved on an amylose-based chiral stationary phase to produce four enantiopure stereoisomers.

Heiland *et al*. [107] presented the first microchip-based SFC. Chip-SFC was developed and tested with two analytes: chiral herbicide napropamide using Chiralpak IC-3/cellulose tris-(3, 5-dichlorophenylcarbamate) as stationary phase and pirkle's alcohol using Chiralpak IB-5 material as the stationary phase. Napropamide has two isomers (-) and (+)-napropamide in which the (−)-isomer is more toxic toward biological factors, like root growth and fresh weight. Elution of isomers after separation was done by mixtures of supercritical carbon dioxide with methanol CO_2/MeOH streams (pinch and eluent). It resulted in fast racemic herbicide enantiomer separation of fewer than 20 s.

2.4.4. Capillary electrophoresis

Capillary electrophoresis (CE) and other capillary electromigration techniques are often used for chiral separation, namely electro-kinetic chromatography (EKC), micellar electro-kinetic capillary chromatography (MEKC), non-aqueous capillary electrophoresis (NACE), and capillary electrochromatography (CEC) [101, 108]. These techniques are based on the interaction of enantiomers with a chiral stationary selector added to the background also called background electrolyte (BGE) [109]. The simplicity and availability of chiral selectors such as surfactants, macrocyclic antibiotics, polysaccharides, and cyclodextrins, make these CE techniques the best for chiral separation [110].

However, CEC combines features of capillary electrophoresis (CE) and liquid chromatography (LC), i.e. combining chromatographic and electrokinetic separation principles [111]. Although CEC is characterized by high selectivity and efficiency, it is associated with a limited number of specific stationary phases developed for it, the low number of commercially available CEC columns, the frits to maintain the stationary phase, which makes CEC not very useful for industrial application [110]. Generally, an electrical field is applied over a capillary that is filled with stationary (CSP) and a mobile phase to perform separations [112].

Lancioni *et al*. [113] developed a method to optimize the ligand concentrations in the BGE of CE. Four chiral pharmaceutical drugs (pindolol, propranolol, oxprenolol, and homatropine methyl bromide) were chosen as analytes. The separation was done using 2-hydroxypropyl-β-cyclodextrin (2-HP-β- cyclodextrins) as a ligand or chiral sector. As a result, the concentration ligand was found as optimum.

Amin *et al*. [109] investigated diastereomeric separations of chiral antimalarials by capillary zone electrophoresis (CZE), variety of chiral selectors were used to successfully separate antimalarial enantiomers i.e. oligosaccharides (cyclodextrins and oligomaltodextrins).

García *et al*. [112] developed a capillary micellar electrokinetic chromatography (MEKC) method that enables the stereoselective separation of the insecticide bioallethrin stereoisomers. Amounts of different cyclodextrins surfactant, cyclodextrin, and urea were added in the BGE. Bioallethrin is an insecticide belonging to the pyrethroids family which is used in agriculture, forestry, household, and public health. The method was developed also to evaluate the toxicity of bioallethrin stereoisomers on the growth of the green alga *Pseudokirchneriella subcapitata*, and the germination of plant *Sorghum bicolor* (non-target organisms). Based on the results, bioallethrin stereoisomers were separated with a resolution of 7.4 in 6.5 min. The racemic bioallethrin resulted in more toxicity than S-bioallethrin for green algae and 100% inhibition of seeds germination. Thus, both racemate and pure S-bioallethrin are classified as toxic to algae.

2.4.5. Pre-concentration

The first extraction technique developed was liquid-liquid extraction (LLE), but due to lots of disadvantages, it has been replaced from laboratories by new extraction techniques such as solid-phase extraction (SPE) and solid-phase micro-extraction (SPME). These techniques are employed before the analytical instrument for pre-concentrating the target compounds from aqueous media [114, 115].

2.4.6. MIPs in sample pre-emptying (solid-phase extraction)

The ability to isolate and pre-concentrate the compounds of interest from complex sample matrix [116] makes MIPs excellent sorbent materials for SPE and SPME sample preparation techniques [117].

In the SPE approach, MIP particles are packed inside an empty cartridge. The MIP SPE cartridges are pre-conditioned and loaded with a sample [118, 119]. Before analyte elution, the MIPs are washed with solvents commonly methanol to remove all interferences and not the bound analyte. Elution is carried out by a solvent that can release the bound analyte from the imprinted sites [115, 120].

Xu *et al*. [121] prepared double water-compatible molecularly imprinted polymers (DWC-MIPs) and applied them as solid-phase extraction (SPE) sorbent for selective pre-concentration and specific recognition of triazines herbicides in water samples. Although four types of atrazine imprinted WC-MIPs were successfully prepared, WC-MIPs displayed excellent recognition ability in aqueous media. The SPE based on DWC-MIPs was successfully used for simultaneous pre-concentration, separation, and determination of four triazine compounds in tap water and river water samples.

Manesiotis *et al*. [122] prepared MIPs using S-ibuprofen as a template. The imprinted polymers were employed as an HPLC stationary phase and complete enantiomeric separation of racemic ibuprofen. The synthesized polymers were subsequently tested in MI-SPE as selective sorbents for the extraction of ibuprofen from complex samples.

Zunngu *et al*. [123] synthesized selective MIPs using ketoprofen as a template, which was applied as an SPE sorbent. SPE technique was optimized and used with HPLC for the quantitative determination of ketoprofen in wastewater treatment plants located in the southern part of Durban City, South Africa. Ketoprofen is a drug used to treat inflammatory diseases and it is being consumed by many humans, therefore it is widely detected with other nonsteroidal anti-inflammatory drugs (NSAIDs) in wastewater and surface water. Based on the results, ketoprofen was detected in all samples and its concentrations were higher when compared with what has been reported for WWTPs located in Europe.

Tavengwa *et al*. [124] successfully synthesized magnetic MIPs by bulk polymerization for the extraction of nitroaromatic compounds (NACs). Prepared magnetic MIPs were packed in solid-phase extraction cartridges for the extraction of selected NACs i.e., 2,4-dinitrotoluene (2,4-DNT), nitrobenzene (NB), and 2-nitrotoluene (2-NT). After SPE, the filtrate was subjected to HPLC-UV for further analysis. Magnetic MIPs were used instead to overcome some of the problems that are found in MIPs, such as greater selectivity and shorter contact time with the analyte solution.

2.4.7. Solid-phase micro-extraction

In SPME, a syringe-like with a sorbent-coated fiber at the end of the needle is applied for the analyte extraction from sample solutions, after extraction, it is injected directly into the analytical instrument i.e. GC or HPLC [118]. An excellent coating material is very important to obtain high extraction efficiency [125]. Several SPME coating materials have been used including, MIP-coated fibers [119], polydimethylsiloxane (PDMS) [126], polyacrylate (PA), polydimethylsiloxane divinylbenzene (PDMS-DVB) and carbowax polydivinylbenzene (CW-DVB) [125]. However, great attention has now been paid towards molecularly imprinting polymer (MIP) sorbent to improve the quality and selectivity of analytical methods. The development of molecularly imprinting polymer (MIP) demonstrated its usefulness for recognition and separation of target molecules, unlike other sorbents materials, MIP has advantages such as stability, selectivity, easy application and preparation, which has promoted an increasing number of applications in various areas [127–129].

2.5. Molecularly imprinting technology

Molecularly imprinting is a template-directed technique that allows the design and synthesis of polymers with well-defined artificial recognition sites that are complementary in the functional group, size, and shape of the target molecule [130, 131]. Figure 1 shows the molecular imprinting process. Firstly, a pre-polymerization complex is formed between the template and the functional monomer in a porogenic solvent [132]. Secondly, the complex is mobilized by the cross-linker, and the initiator is used to obtain a polymerization complex. Lastly, after synthesis, different removal of template methods are used such as pressurized hot water extraction (PHWE), Soxhlet extraction or microwave extraction [133–135]. Thereafter, MIPs binding sites are formed which are sterically and chemically complementary to the template molecule, enabling the polymer to selectively rebind the imprint molecule and its analogues from a mixture [130, 136].

MIPs are synthesized by different polymerization techniques, such as bulk polymerization [57, 137, 138], precipitation polymerization [1, 139, 140], suspension polymerization [141], emulsion polymerization [142], and sol-gel polymerization [143].

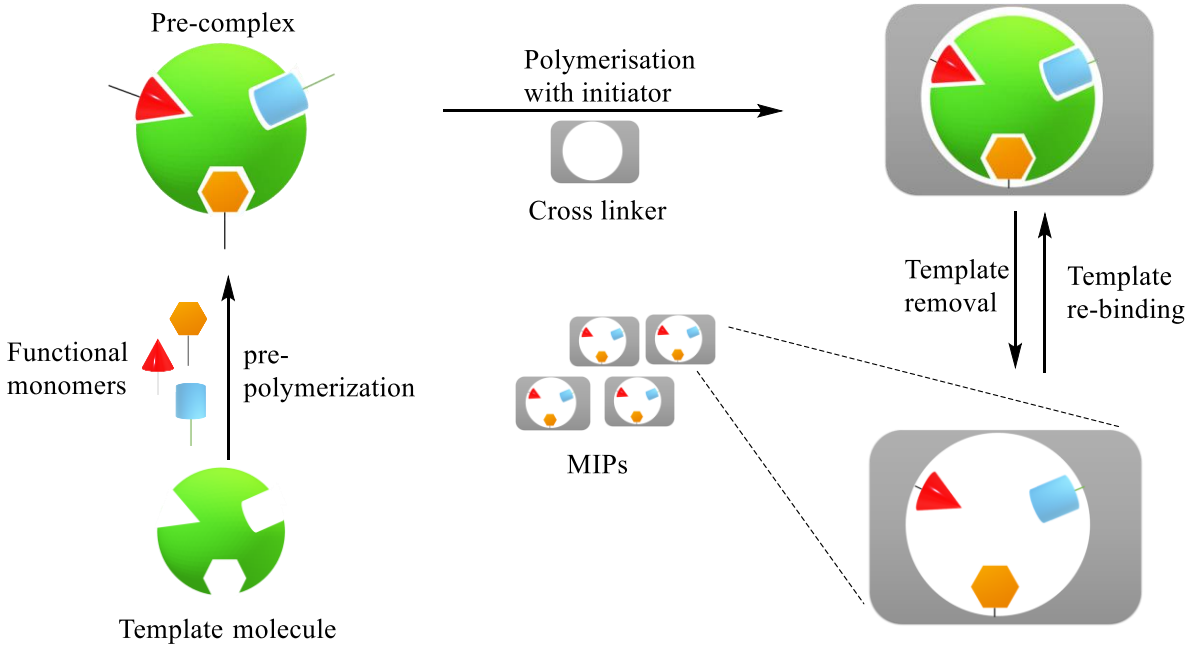

Figure 1: General method for the synthesis of MIPs [134].

2.5.1. Application and uses of molecularly imprinted polymers (MIPs)

MIPs have been applied in many areas [144], as CSP in chromatographic separation [145–147] as a sorbent in samples preparation [123, 124] chemical sensors [148], capillary electro-chromatography enantioselective [67, 149] catalysis [150–152] for its remarkable advantages. The recognition sites of MIP mimic the binding sites of antibodies and enzymes [153, 154]. However, in contrast to those biological enzymes, MIPs are physically robust, stable in a broad range of pH, pressure, and temperature and they have high selectivity and sensitivity [155, 156]. Additionally, those polymeric materials are easier to synthesize for a wide range of template molecules and are less expensive than antibodies [116]. Furthermore, MIPs can be stored for several years at room temperature and they can be reused several times without loss of the memory effect [130].

In most the chromatographic analysis, MIPs have been used as CSP. For example, Ansell *et al*. [147] successfully synthesized (−)-ephedrine imprinted polymers in the enantio-separation of (±)-ephedrine. (−)-Ephedrine imprinted polymers were used as stationary phases in supercritical fluid chromatography. Liao *et al*. [146] prepared (S)-ornidazole molecularly imprinted monolithic through a single-step thermal copolymerization, a new monolithic stationary phase for the rapid chiral separation of anti-parasitic drugs by pressurized CEC.

2.5.2. Pre-polymerization reagents of MIPs

2.5.2.1. Template

The template is the target molecule or compound that plays a vital role in the process of imprinting. It is the molecule for which the imprinted polymers are synthesized. Generally, an ideal template molecule should satisfy three requirements: firstly, it should have no groups involved to prevent polymerization, it should exhibit excellent chemical stability in the polymerization reaction, and lastly, it should contain functional groups well adapted to assemble with functional monomers [157–159]. Examples of templates that were used before include chiral compounds (e.g. (-)-menthol [67], 2,4-dinitrotoluene (2,4-DNT) [124], S-citalopram (SCIT) [160] and R-mandelic acid [149]), enzymes (e.g. chymotrypsin [161]), pharmaceutical drugs (e.g. non-steroidal anti-inflammatory drugs (NSAIDs) [162], propranolol [163], oseltamivir (OS) [164], and S-amlodipine (S-AML) [165]), biological compounds (e.g. (-)-ephedrine [166], steroids [167], and protein [168]) and pesticides (e.g. bifenthrin and diazinon [169]).

2.5.2.2. Functional monomers

Functional monomers create binding sites on the imprinted polymer forming a pre-polymerization complex via monomer-template interaction by providing a functional group. They should contain functional groups like carboxylic acid, alcohol, and amide or any group with N-H, O-H, or F-H bonds, which are responsible of forming hydrogen bond with the template [132]. The choice of functional monomers affects the polymer of the recognition site and the concentration influence the number of binding sites. Generally, functional monomers are used in the molar excess to template molecules, which permits to favour the formation of functional monomer-template complexes [170]. Xia *et al.* [1] synthesized MIP microspheres by precipitation polymerization using 4-vinylpyridine as functional monomer and EGDMA as cross-linker. They showed particle morphology of the MIP prepared from 1 to 10% (w/v) concertation of 4-vinylpyridine. Moreover, monodisperse MIP microspheres were isolated when 1 and 2% (w/v) of co-monomer was used but, at higher concentrations of 4, 6, and 8% (w/v) the spherical particles started to agglomerate. Figure 2 shows common functional monomers used during imprinting.

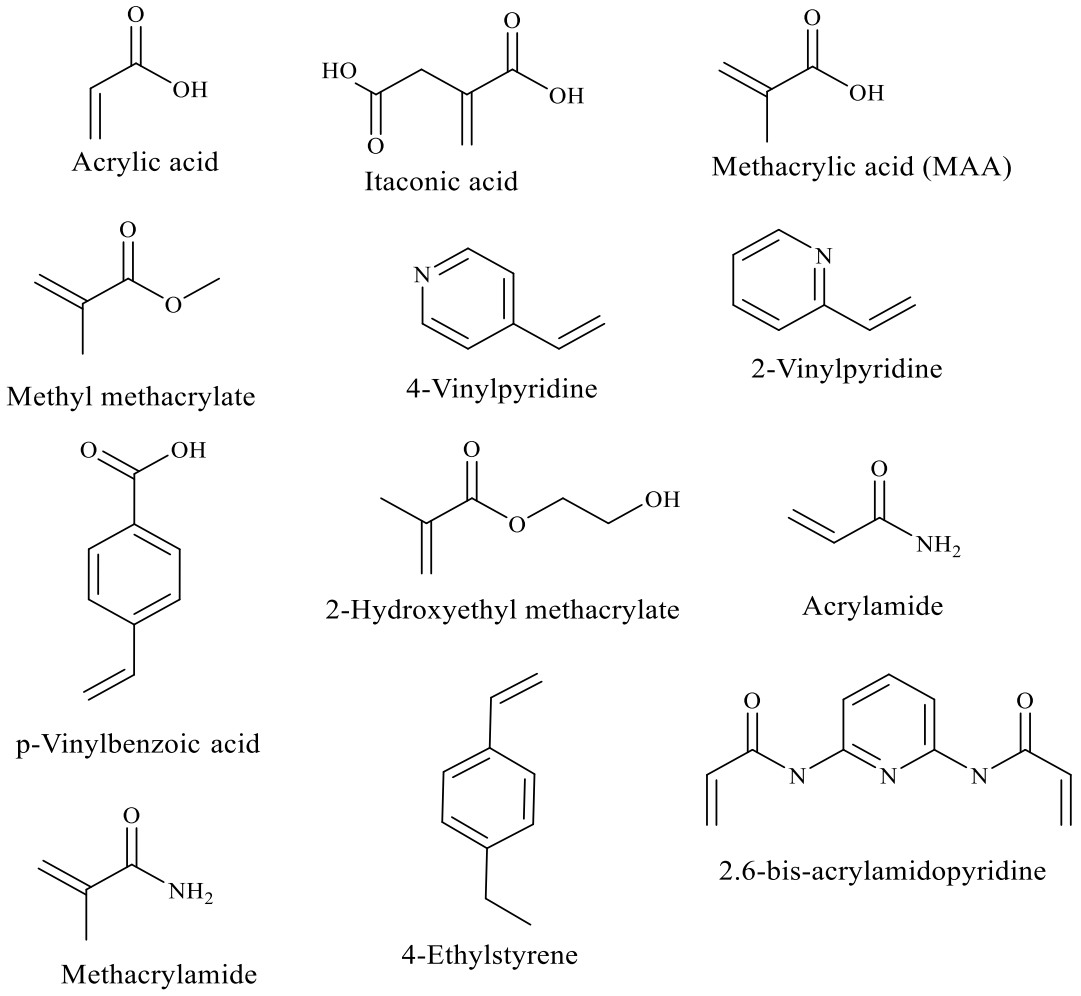

Figure 2: Structures of common functional monomers.

2.5.2.3. Cross-linkers

The cross-linker is primarily responsible for the morphology of the polymer matrix, it stabilizes the imprinted binding sites, and also provides mechanical and thermal stability to the polymer [171]. High cross-linking ratios are generally used to obtain permanently macroporous materials with good mechanical stability [78, 87]. Xia *et al* [1] indicated that to control the morphology and specific binding characters of the imprinted polymer, high percentage of cross-linker: monomers ratio must be used. From their results, monodisperse MIP were formed in molar ratios of 1:4 and 1:2, thus, when EGDMA is 4 times and 2 times higher than 4-vinylpyridine. But when the molar ratios changed to 2:1, and 4:1, thus when EGDMA is lower than the 4-vinylpyridine, MIP microspheres became agglomerated. This indicate that with the decrease in the amount of EGDMA, the agglomeration becomes heavier, then high percentage of cross-linker in the co-monomers mixture is crucial to prevent polymer agglomeration [1]. Different cross-linker reagents can be used during molecular imprinting as is shown in Figure 3, the most popular cross-linker is ethylene glycol dimethacrylate (EGDMA).

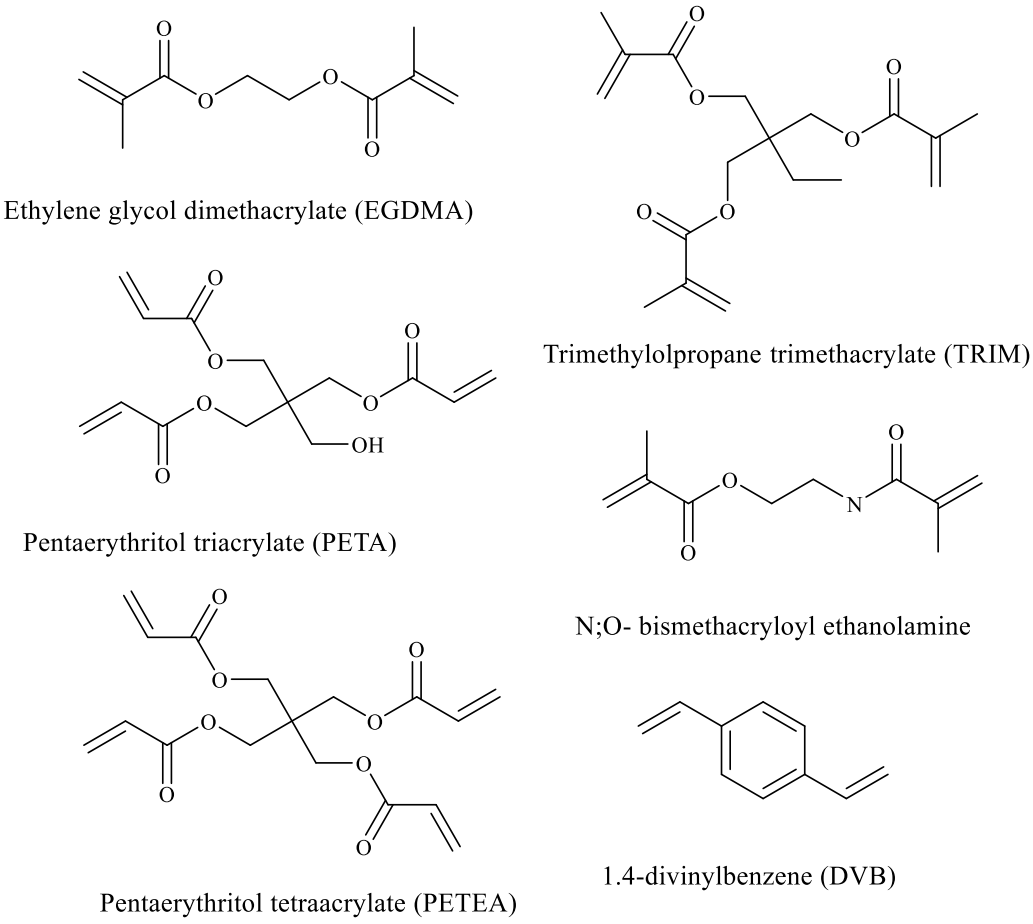

Figure 3: Structures of cross-linkers used in molecular imprinting.

2.5.2.4. Solvents

Porogenic solvents play an important role in the formation of the porous structure of MIPs, and they dissolve all the components (template, functional monomer, cross-linker and initiator) in a single phase during the polymerisation process [172]. Another role of solvents is to disperse the heat of the reaction produced during polymerization; otherwise, the temperature will increase [158, 173]. The increasing amount of solvent used result in increasing of pores size, so a proper amount of solvent will improve the formation of specific cavities designed for binding template molecules [174]. Less polar solvents improve the formation of functional monomer-template complexes (stabilization of hydrogen bonds), while the more polar solvent disturbs interactions in the formed complexes. Examples of solvents used during imprinting are acetonitrile, chloroform, dichloromethane, N, N-dimethylformamide, methanol, 2-methoxy ethanol, tetrahydrofuran, and toluene [136, 171, 175].

2.5.2.5. Initiator

Initiators start the process of polymerization. The appropriate use of the initiators controls the degree of the exothermic process of polymerization. In some cases before and after addition of initiator, the dissolved oxygen is removed from polymerization solutions by bubbling an inert gas like nitrogen or argon [158]. Each initiator has its specific decomposition rate at a given temperature and concentration [166]. When a high concentration of initiator is used, it increases the temperature generated during polymerization which negatively impacts the recognition properties of MIPs. This is because the high temperatures reached with high concentrations of initiator worsen the quality of the imprints formed [1, 166] . So, to achieve the best selective rigid polymers, MIPs should be synthesized over a long period using low concentrations of initiator and low temperatures [176]. In addition, when lower amounts of initiator are used, the peak temperature inside the polymerization mixture decreases, generating polymers with quality imprinting cavities [130]. Common initiators are listed in Figure 4, among them, azobisisobutyronitrile (AIBN) is most conveniently used at the decomposition temperatures of 50–70℃.

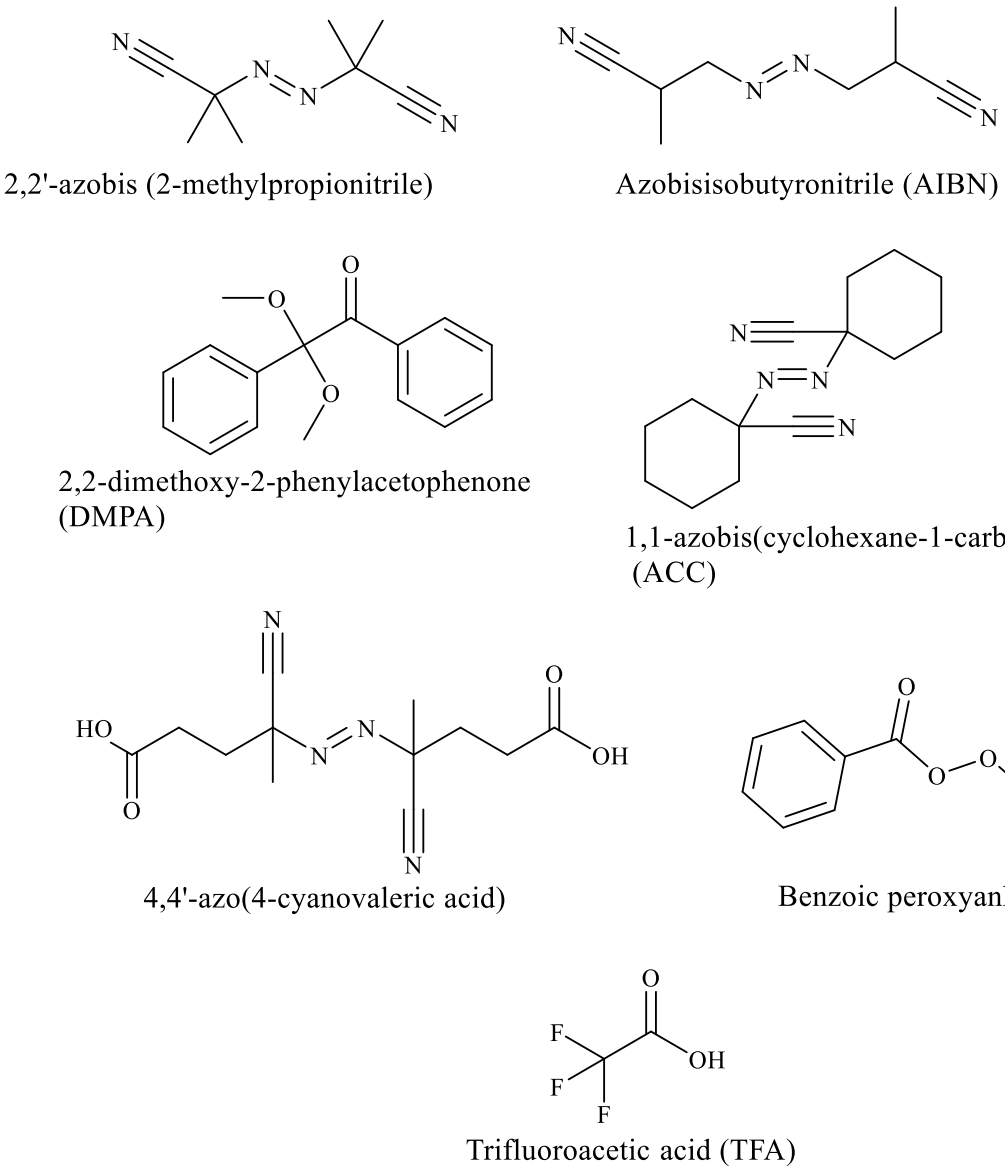

Figure 4: Common initiators used in molecular imprinting.

2.5.3. MIP preparative approaches

Three different approaches have been proposed for MIPs preparation, that is the covalent, non-covalent, and semi-covalent approaches, differing from the way the template is linked to the functional monomer [127]. Of the three approaches, the non-covalent approach has been used more extensively but, the semi-covalent approach combines the advantages of the other two [114].

2.5.3.1. Covalent approach

The covalent approach involves the formation of reversible covalent bonds between the template and monomers before polymerization (Figure 5). To remove the template, synthesized polymers are treated with reagents in solution or is refluxed in a soxhlet extraction, then MIPs will rebind template molecules again via the same covalent interactions. However, the difficulty of designing an appropriate template–monomer complex in which covalent bond formation and cleavage are readily reversible under mild conditions makes this approach rather restrictive [126, 127].

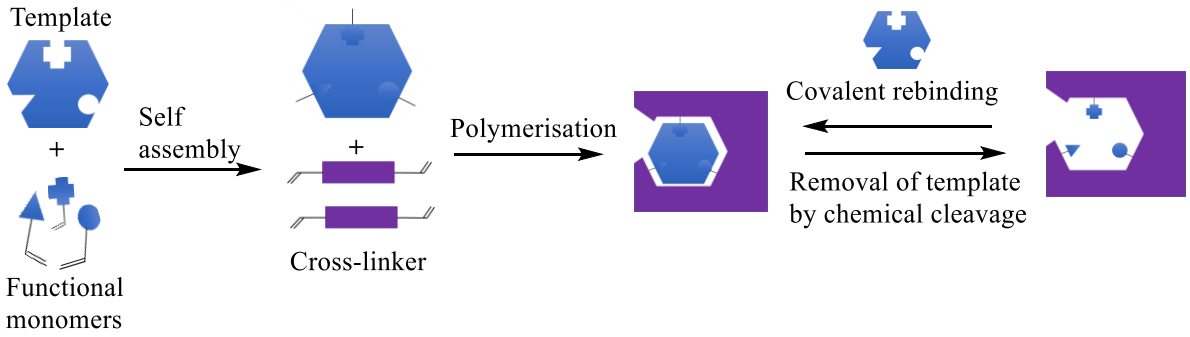

Figure 5: Covalent molecular imprinting [176].

2.5.3.2. Non-covalent approach

It is obtained by mixing the template with a suitable functional monomer in an appropriate porogen by the formation of weak non-covalent interactions, such as hydrogen bonding or van der Waals forces, before polymerization. The template molecule is removed from the synthesized polymer matrix by washing with solvents (Figure 6) [176, 177]. This approach becomes the most widely used because it is relatively simple to prepare the template–monomer complex and easy to remove the templates from the polymer matrix [178].

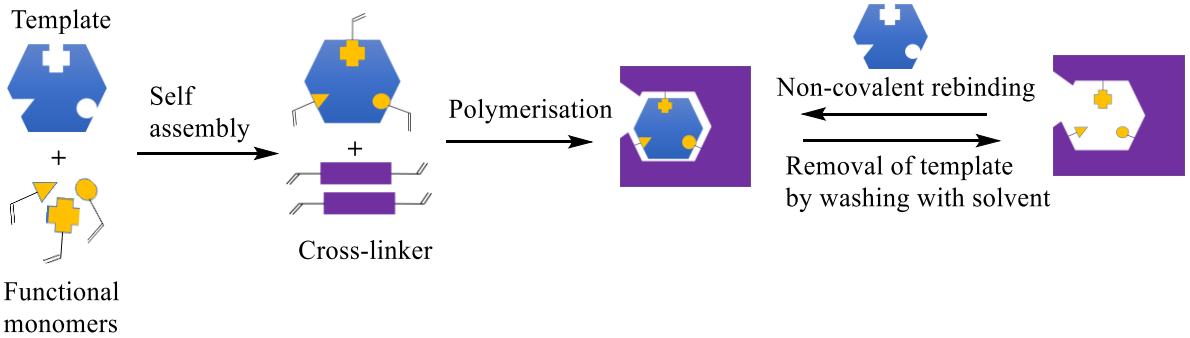

Figure 6: Non-covalent molecular imprinting [176].

2.5.3.3. Semi-covalent approach

Semi-covalent imprinting combines the advantages of the above two approaches, thus, co-polymerization during imprinting formation is done by covalent bonds, and re-binding of the target molecule to the MIP is done by non-covalent bonds [179]. In other words, the stable and stoichiometric complex in covalent imprinting and the template re-binding in non-covalent imprinting (Figure 7) [180, 181].

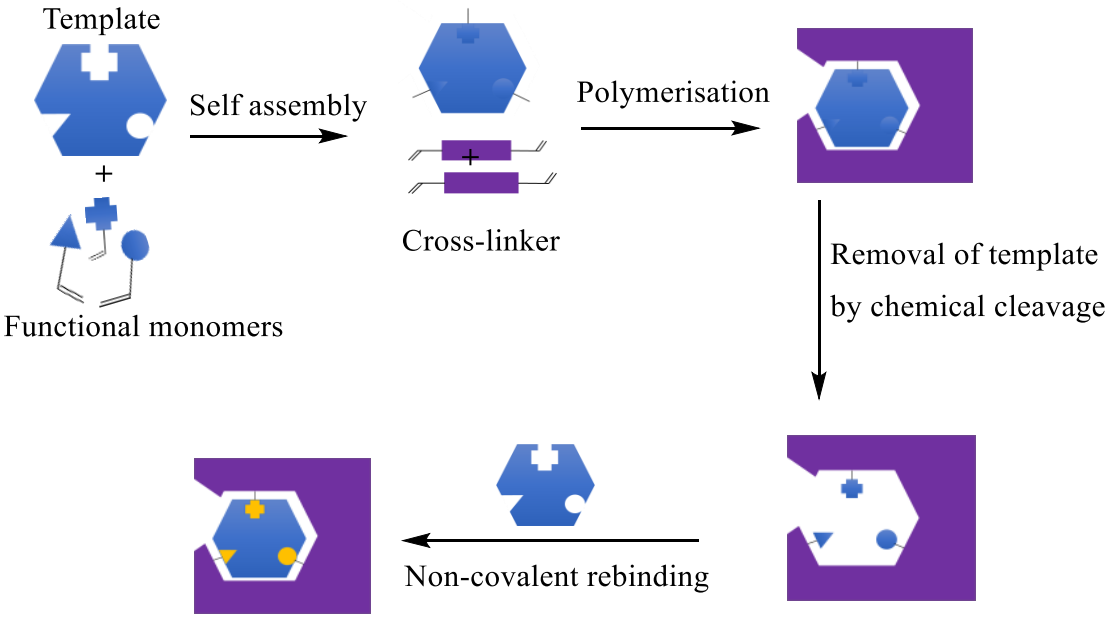

Figure 7: Semi-covalent molecular imprinting [177].

Chapter 3

Materials and methods

This chapter gives detailed information of all material and reagents, characterisation instruments and methods used to the synthesis of 1-phenylmenthone and synthesis of MIPs. Adsorption and reusability studies of MIPs procedure was also explained.

3.1. Chemicals and reagents

Methanol, toluene, methacrylic acid (MAA), ethylene glycol dimethacrylate (EGDMA), and azobisisobutyronitrile (AIBN) were purchased from Sigma-Aldrich (Darmstadt, Germany). (-)-Menthone (90%), (+)-menthol, THF, NH_4Cl, dichloromethane (DCM), sodium chloride, magnesium sulfate ($MgSO_4$), p-anisaldehyde, acetone, ethanol (99%), hydrochloric acid (37%), acetic acid, sodium borohydride ($NaBH_4$), diethyl ether, were also purchased from Sigma-Aldrich (Darmstadt, Germany). Magnesium, phenyl bromide and phenyl magnesium bromide were purchased from Rochelle Chemicals (Johannesburg, South Africa). Iodide, ethyl acetate, hexane, potassium permanganate, potassium carbonate, sodium hydroxide, silica gel, vanillin, toluene, $NaHCO_3$, Na_2SO_4, $Na_2Cr_2O_7{\cdot}2H_2O$, H_2SO_4 and chloroform ($CDCl_3$) were purchased from Sigma-Aldrich (Darmstadt, Germany).

Anhydrous THF was prepared by drying THF with molecular sieves. All reactions were carried out in oven dried Schlenk flasks under a nitrogen atmosphere. The following starting materials (-)-menthone and PhMgBr were commercially available or prepared according to the literature. Centrifugation was carried out by a Beckman Coulter Avanti J-E centrifuge (4000 x g) for 3 min at 20°C.

3.2. Characterisation instruments

NMR spectroscopy: Structures of all organic compounds were analysed by ^{1}H and ^{13}C NMR recorded on a Bruker 400 MHz instrument (USA Massachusetts) using chloroform ($CDCl_3$) as a solvent and tetramethylsilane (TMS) at 0.00 ppm as an internal standard. Values for the chemical shifts were expressed in parts per million (ppm).

Thin-layer chromatography (TLC): TLC was used to monitor the reactions using DC-Fertigfolien pre-coated TLC-sheets ALUGRAM Xtra Silica Gel/UV_{254} plate and the mobile phase was ethyl acetate and hexane (10:90, v/v). All TLC plates were visualized by p-anisaldehyde and vanillin stains. P-anisaldehyde was prepared as follows: 5 mL of concentrated sulfuric acid, 1.5 mL of glacial acetic acid, and 3.7 mL of *p*-anisaldehyde were dissolved into 135 mL absolute ethanol, then the solution was stirred vigorously to ensure homogeneity. The resulting staining solution was then stored in a 500 mL beaker and covered with aluminium foil. Vanillin stain was prepared by adding 15 g vanillin in 250 mL ethanol and 2.5 mL concentrated sulfuric acid.

Column chromatography: All the crude products in all reactions were purified by column chromatography using silica gel as a stationary phase and ethyl acetate and hexane (10:90, v/v to 30:70, v/v) as mobile phase.

TGA Q500 V20.13 Build 39 (CSIR Pretoria, South Africa) was used to determine weight loss vs temperature of imprinted polymers. Thermograms were recorded using a heating rate of 20℃ per minute from 0-1000℃, under nitrogen atmosphere at a rate of 40 mL per min. **FTIR** was used to analyse the functional group of compounds using an FT-IR spectrometer (Bruker platinum 22 vector) in a frequency range of 400–4000 cm^{-1}. Solid and liquid samples were analysed as they are. The surface area, total pore volume, and average pore diameter of the MIPs were analysed by the TriStar II 3020 Version 3.02 (serial # 215) **BET** instrument from CSIR lab analysis, Pretoria. MIPs sample were degassed for 4 h at 100°C before analysis.

3.3. Synthesis of menthone (1)

Sodium chromate ($Na_2Cr_2O_7{\cdot}2H_2O$ (15.0 g, 50.33 mmol)) was added to 30 mL water in an Erlenmeyer flask, the reaction was cooled in ice and treated with 10 mL concentrated sulphuric acid (H_2SO_4 98%, d = 1.84) as a source of hydrogen to form chromic acid. This solution was transferred to a measuring cylinder and diluted with water to make it 75 mL. Menthol (23.44 g, 150 mmol) and a solution of chromic acid (75 mL) were mixed slowly in a three-necked round-bottomed flask, the internal temperature was maintained between 20-25℃ and the reaction mixture was stirred for 24 h at room temperature until green-black pigment was formed. The mixture was separated and extracted with Et_2O (2 x 90 mL). The organic layer was washed with 10% aq. $NaHCO_3$ (3 x 40 mL) and water (3 x 50 mL). The organic extracts were then dried (Na_2SO_4) and concentrated by a rotavapor to give the desired compound 1 as a colourless liquid like oil (20.6 g, 95%).

^{1}H NMR (400 MHz, $CDCl_3$): δ (ppm) 0.776 (3H, d, H-9, J = 6.8 Hz), 0.837 (3H, d, H-10, J = 6.8 Hz), 0.937 (3H d, H-7, J = 6.4 Hz)), 1.256-1.330 (2H, m, H-4), 1.751-1.846 (2H, m, H-3), 1.883-1.917 (1H, m, H-5), 1.946-2.025 (1H, m, H-8), 2.042-2.098 (2H, m, H-6), 2.249-2.296 (1H, ddd, H-2, J = 12.8, 4, 2.4 Hz)), **^{13}C NMR (400 MHz, $CDCl_3$) δC (ppm)** 18.63 (C-7), 21.15 (C-9), 22.23 (C-10), 25.82 (C-8), 27.80 (C-3), 33.86 (C-4), 35.42 (C-5), 50.80 (C-6), 55.77 (C-2), 212.22 (C-1).

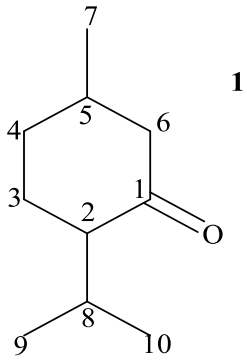

1

3.4. Synthesis of 1-phenylmenthol

Grignard reagent (PhMgBr) (10.3 mL, 64.82 mmol) was added dropwise at -10℃ to a solution of menthone (1) (5.0 g, 32.24 mmol) and 45 mL anhydrous THF in a round-bottomed flask. The reaction was stirred for 24 h at room temperature under nitrogen gas and then heated under reflux for another 24 h. After been allowed to cool down to room temperature, the mixture was hydrolysed by adding 5 drops of 2 M HCl and extracted with Et_2O (3 x 40 mL). The organic layer was washed with 5% aq. $NaHCO_3$, H_2O (50 mL), dried with Na_2SO_4 and concentrated by rotavapor to give compound 2 as a yellowish oil.

^{1}H NMR: δ (ppm) 0.753 (3H, d, H-7, J = 6.8 Hz), 0.848 (3H, d, H-9, J = 6.8 Hz), 0.919 (d, H-10, J = 6.4 Hz), 0.989-1.096 (2H, m, H-4), 1.256-1.282 (2H, m, H-3,), 1.434-1.599 (2H, m, H-5, H-8), 1.623-1.700 (2H, m, H-6), 1.860-1.918 (1H, m, H-2), 2.198 (1H, s, H-15). 7.25 (1H, t, H-14, J= 8), 7.37 (1H, t, H-12, J= 8), 7.48 (1H, t, H-13, J =8 Hz). **^{13}C NMR (400 MHz, $CDCl_3$) δC (ppm)** 18.38 (C-7), 21.30 (C-3), 22.22 (C-9), 23.73 (C-10), 26.70 (C-8), 28.52 (C-5), 35.18 (C-4), 49.90 (C-2), 51.61 (C-6), 78.41 (C-1), 124.60 (C-12), 126.12 (C-13)128.08 (C-14), 148.61 (11).

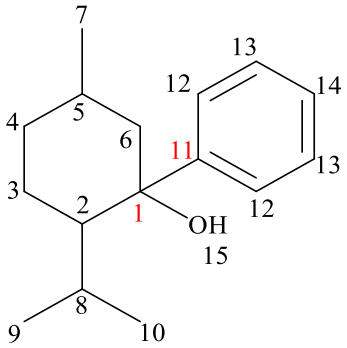

2

3.5. Synthesis of molecularly imprinted polymers (MIPs)

A modified method by Xia *et al*. [1]. was used. Briefly, in 250 mL one neck round-bottomed flask, 70 mL methanol was added followed by 1-phenylmenthol (0.116 g, 0.5 mmol) the template and the functional monomer MAA (422 µL, 5 mmol). The mixture was stirred for 10 min and cross-linker EGDMA (2 mL, 10 mmol) was added. The pre-polymerization mixture was purged with N_2 for 2 min to remove oxygen before addition of initiator AIBN (50 mg, 0.3 mmol). After addition of initiator, it was purged again with N_2 for 2 min. The flasks were greased with oil and closed loosely with the lid then covered by parafilm and placed in an oil bath and the temperature was slowly increased to 80°C and maintained for 24 h. The obtained products (MIPs containing the template) were dried at 90℃ oven to remove the excess solvent. Non imprinted polymers (NIPs) were prepared using the same procedure but without the template. Table 2 shows the synthesis of MIPs and NIPs experimental conditions.

Table 2: Experimental conditions for the synthesis of MIP

MIPs	Solvent (70 mL)	Functional monomer (MAA, µL)	Cross-linker (EGDMA, mL)	Initiator (AIBN, mg)	Template (g)
MIP 1	Methanol	422	2.0	50	0.116
MIP 2	Toluene	422	2.0	50	0.116
MIP 3	Methanol	844	7.5	100	0.232
NIP 1	Methanol	422	2.0	50	0.000

3.6. Template elution

After polymerization of MIPs, a part of imprinted MIPs was washed to remove the template (1-phenylmenthol) from the polymers. Although non-imprinted polymers (NIPs) were not template-imprinted they did not skip the ‘removal step’. To verify the absence of 1-phenylmenthol template into the imprinted polymer, 2 g of dried MIPs were washed with the mixture of methanol: acetic acid (90:10 v/v) for the total of 10 washing cycles. A mass of 2 g and 1 g of MIPs and NIPs were transferred into 50 mL centrifuge tubes then, 20 mL solvent was added into the tubes. The tubes were placed on a shaker at 150 rpm for 20 min and they were centrifuged at 20℃ for 3 min, then 2 mL aliquot of the supernatant was transferred into Eppendorf tubes. This procedure was repeated 10 times in all MIPs and NIPs. The wet washed polymers were dried at 90℃ overnight.

3.7. Adsorption studies

Parameters that affect the adsorption of 1-phenylmenthol onto MIP were optimized. The optimization was demonstrated through the application of MIPs and NIPs as sorbents in solid-phase extraction. It was done using methanol because template (1-phenylmenthol) has poor solubility in water. Adsorption parameters in the batch mode, such as sample pH (2 to 11), polymer mass (10 to 80 mg), contact time (30 to 180 min) and concentration of 1-phenylmenthol (7 to 54 mg L^{-1}), were optimized for the adsorption of 1-phenylmenthol by MIPs and NIPs sorbent from 30 mL methanol solutions. It was done by holding all the other parameters constant while varying one. For example, when monitoring the effect of pH, the pH was adjusted to 2, 7 and 11, while time, adsorption solvent, mass of sorbent and concentration of 1-phenylmenthol were kept constant. For the first pH experiment, 30 mL solution of methanol was adjusted to pH of 2 and placed into 50 mL tube, followed by addition of 11 mg L^{-1} template and 30 mg of sorbent. The tubes were shaken on an elliptical benchtop shaker at 150 rpm for 60 min. After the adsorption of the 1-phenylmenthol, the whole solution of polymers was loaded in SPE cartridges where the solution was drained, leaving the sorbent sitting on the bottom of the cartridge. After elution with 3 mL methanol, the eluents were analysed by UV to measure the absorbance. Each experiment was repeated 3 times (triplicates). In each case, the enrichment factor (EF) was calculated using equation 1.

$$EF = \frac{C_{ads}}{C_o} \qquad (1)$$

where C_o is initial concentration in mg L^{-1} and C_{ads} is the amount of 1-phenylmenthol enriched into the imprinted polymers in mg L^{-1}

Chapter 4

Results and discussion

This chapter looks at the detailed results and discussion obtained from characterization techniques used during the study of this project. NMR and FTIR results for the synthesis of 1-phenylmenthol was discussed. UV-vis spectrum for the validation and calibration of 1-phenylmenthol was explained. Synthesis of MIPs and elution of template molecules was also shown. FTIR, TGA and BET results for the synthesized MIPs and NIPs, optimization of the template molecule and reusability of the imprinted polymers was also discussed.

4.1. Reduction of menthone to 1-phenylmenthol (2)

This study was about the reduction of (-)-menthone (1) to yield 1-phenylmenthol (2). It began by simply treating commercially available menthone (1) with a strong oxidizing reagent (PhMgBr) in THF as a solvent under inert environment (Scheme 9). The reaction was monitored by thin layer chromatography (TLC). Unfortunately, nuclear magnetic resonance (NMR) spectroscopy analysis of the isolated product showed that the reactions did not take place.

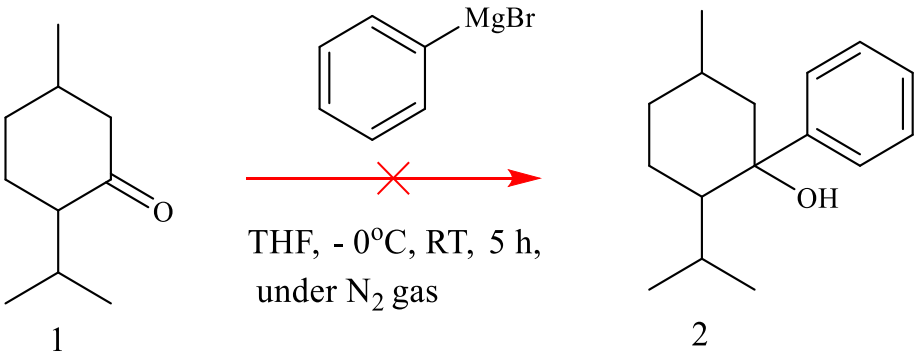

Scheme 9: Grignard reaction addition of PhMgBr to (-)-menthone.

Figure 8 shows ^{13}C NMR spectrum of the product obtained in the reaction scheme 9, the reaction did not take place, starting material did not react to form new expected compound. This was supported by the absence of two quaternary carbon C1 at 78 ppm and C11 at 148 ppm, it was also supported by the presence of ketone peak at 211 ppm from the menthone, which means that it was not reduced to alcohol as expected. The reaction might have failed due to the duration of reaction and temperature. The same reaction was repeated in section 4.2.

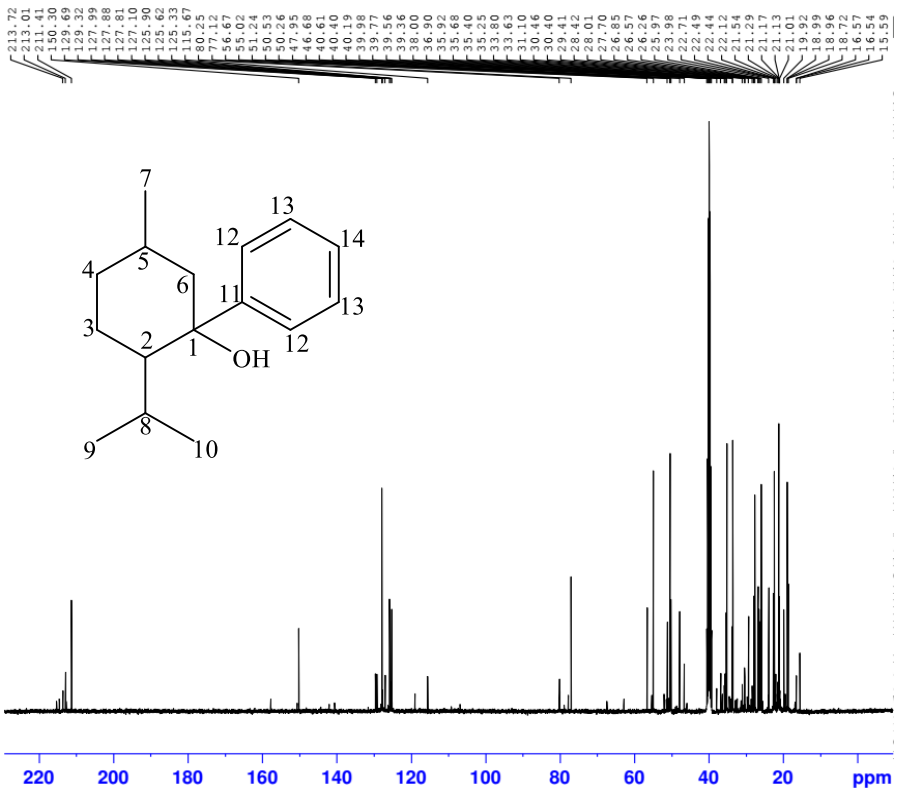

Figure 8: ^{13}C NMR spectrum of 1-phenylmenthol (2) synthesised according to scheme 9.

4.2. Alternative approach towards the synthesis of 1-phenylmenthol (2)

Scheme 10 shows an alternative approach where the different method (procedure) was used and reaction conditions were changed, also considering that the Grignard reagent is sensitive to water and oxygen. The reaction was monitored by TLC after every 4 h, it was purified by column chromatography and analysed ^{13}C NMR, but the reaction failed, and it was confirmed by NMR spectrum (Figure 9).

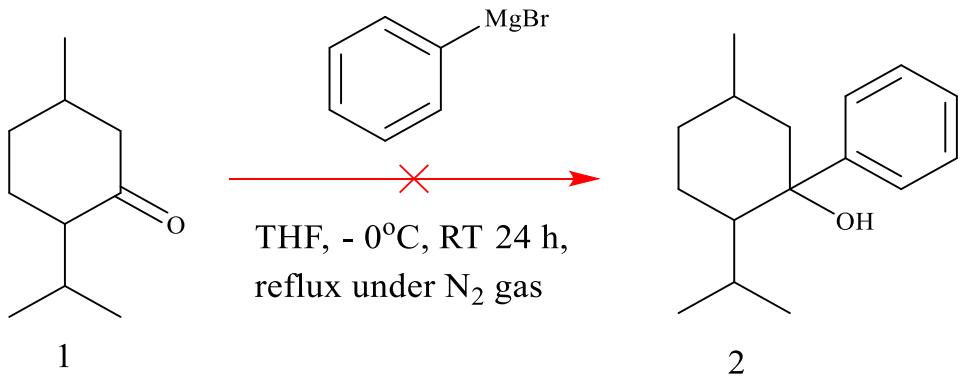

Scheme 10: Alternative approach towards the synthesis of 1-phenylmenthol (2).

Figure 9 shows ^{13}C NMR spectrum of compound 2 synthesized according to scheme 10. The spectrum shows that the ketone peak at 212 ppm is still present in the product, which meant that menthone was not fully converted and it was difficult to separate. Although, two quaternary carbon C11 at 148 ppm and C1 at 78 ppm were observed, but the product was still contaminated and too little after double column purification. In the next section 4.3 and 4.4, the starting materials menthone and phenyl magnesium bromide were prepared in the lab because the purchased reagents might be the problem hence, the reactions were failing.

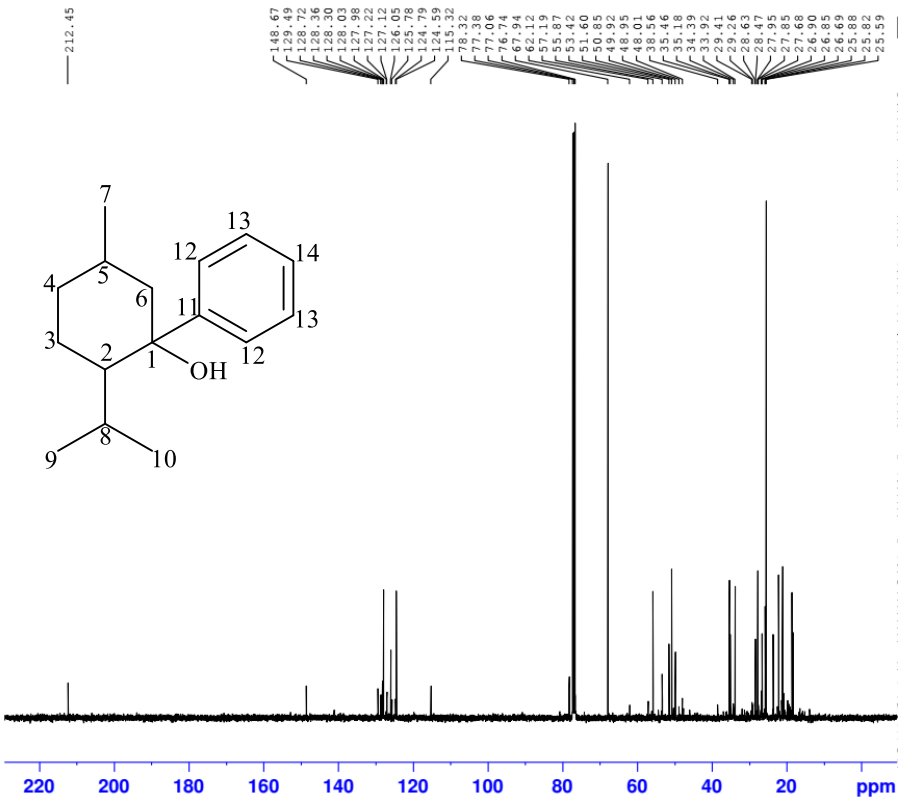

Figure 9: ^{13}C NMR spectrum of 1-phenylmenthol (2) synthesised according to scheme 10.

4.3. Oxidation of menthol to menthone (1)

Menthone (1) was successfully prepared by treating commercially available menthol (3) with a hot solution of chromic acid in diethyl ether as a solvent (Scheme 11). The product 1 was obtained as a colourless oil with a percentage yield of 85%. The structure of synthesized product 1 was purified by column chromatography and analysed by ^{13}C NMR (Figure 10), ^{1}H NMR (Figure 11), and IR (Figure 12) spectroscopies.

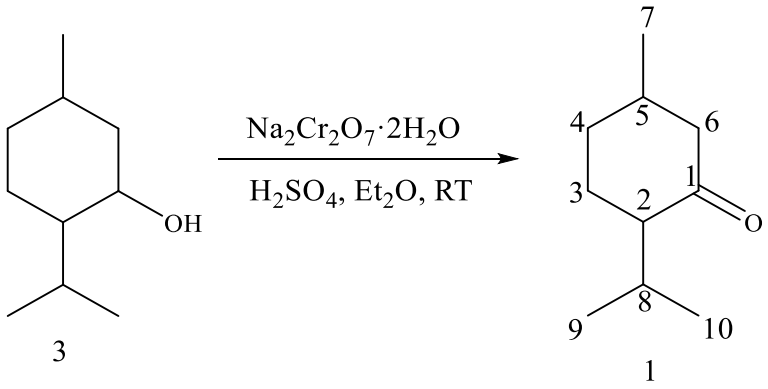

Scheme 11: Oxidation of menthol (3) by chromic acid to form menthone (1).

Figure 10 (a) shows ^{13}C NMR spectrum of menthone (1), the compound that was synthesised according to scheme 11. The product was characterized by the presence of the quaternary carbon peak C1 at 212 ppm, which meant that alcohol (menthol) was converted to the expected ketone (menthone). Figure 10 (b) shows dept 135 carbon NMR spectrum of menthone (1). This spectrum confirmed all methylene carbon peaks such as C3, C4, and C6 were below the base line, and absence of C1 confirmed that indeed it was quaternary carbon (carbon bonded to no hydrogens). Both spectra show successful conversation of alcohol (menthol) to ketone (menthone) by chromic acid, also known as Jones reagent. Some reactions have used pyridinium chlorochromate (PCC) for the same conversion [182]. Almost all living organisms require aldehydes or ketones, in the chemical industry, simple aldehydes and ketones are produced in large quantities for then to be used as solvents and as starting materials to prepare other important compounds [183] hence, menthone was prepared as starting material for the synthesis of the target compound (1-phenylmenthol).

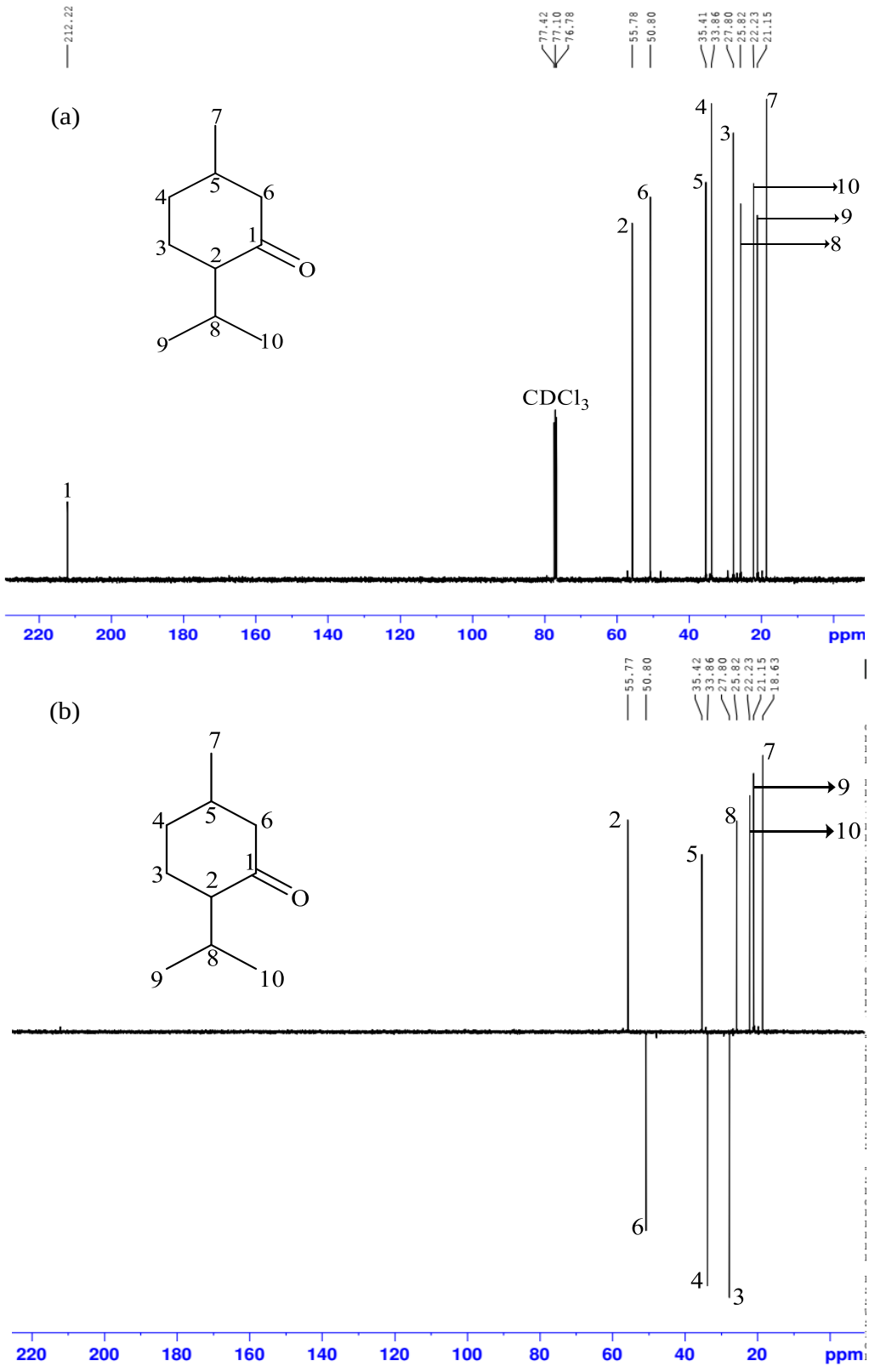

Figure 10: ^{13}C NMR full spectrum (a) dept 135 NMR spectrum (b) of menthone synthesized according to scheme 11.

Figure 11 shows ^{1}H NMR spectrum of menthone (1) which was characterized by the absence of singlet alcohol peak confirming that menthol had been oxidized to ketone. Integration of all proton peaks were calculated to determine how many protons were there also the multiplicity of all protons were also interpreted. Starting from the upfield side, H7, H9 and H10 are all doublets with 3 hydrogens each. Although H9 and H10 seems equivalent, they were all detected and splitted as two non-equivalent peaks. Peak H3 and H4 shows multiplets with two hydrogens each. Peak H2 represented doublet of doublet of a doublet (ddd) with one hydrogen, and peak H5 and H8 shows multiplet with one hydrogen each. The integration of peak H6 was supposed to be at peak H8 representing one hydrogen since peak H6 has two hydrogens. Proton H2 and H6 are deshielded due to the high electronegative oxygen next to them.

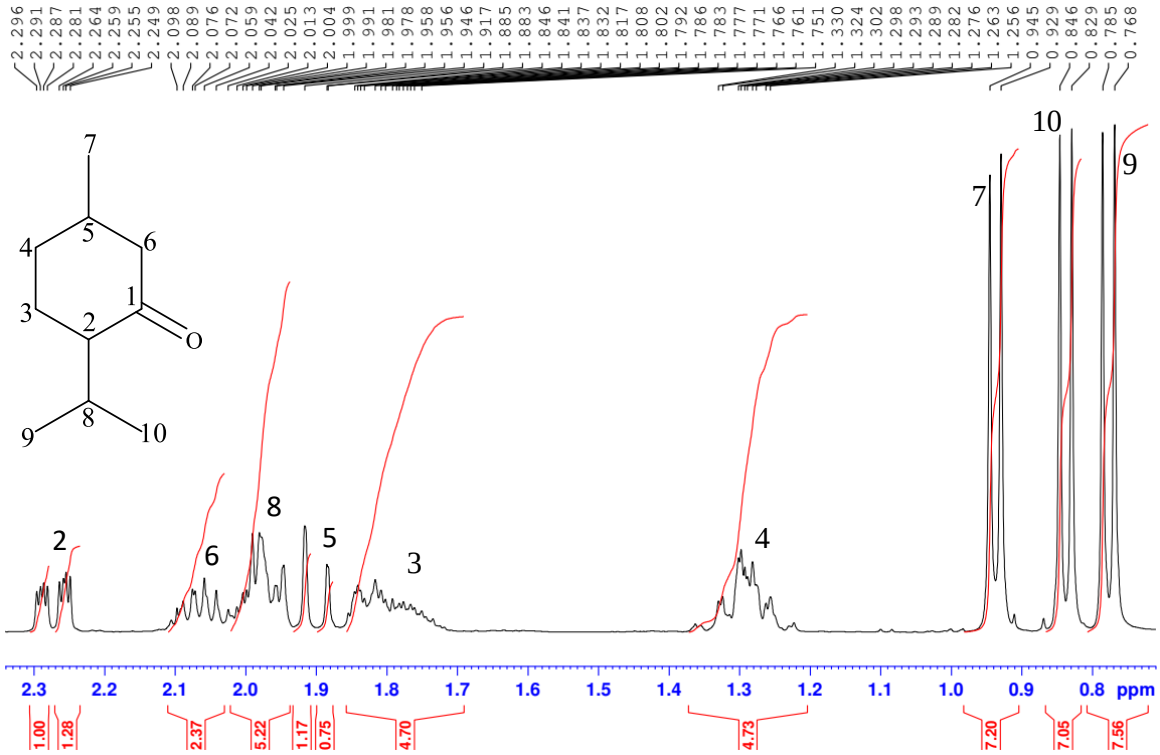

Figure 11: ^{1}H NMR spectrum of menthone, product obtained in scheme 11.

Figure 12 shows the infrared (IR) spectrum of synthesized menthone (1) according to scheme 11. The structure of the product 1 was characterised by IR, which showed that a strong C=O peak at 1707 cm^{-1} was due to ketone and strong C-H peak at 2954 cm^{-1} was due to alkane from the cyclohexane.

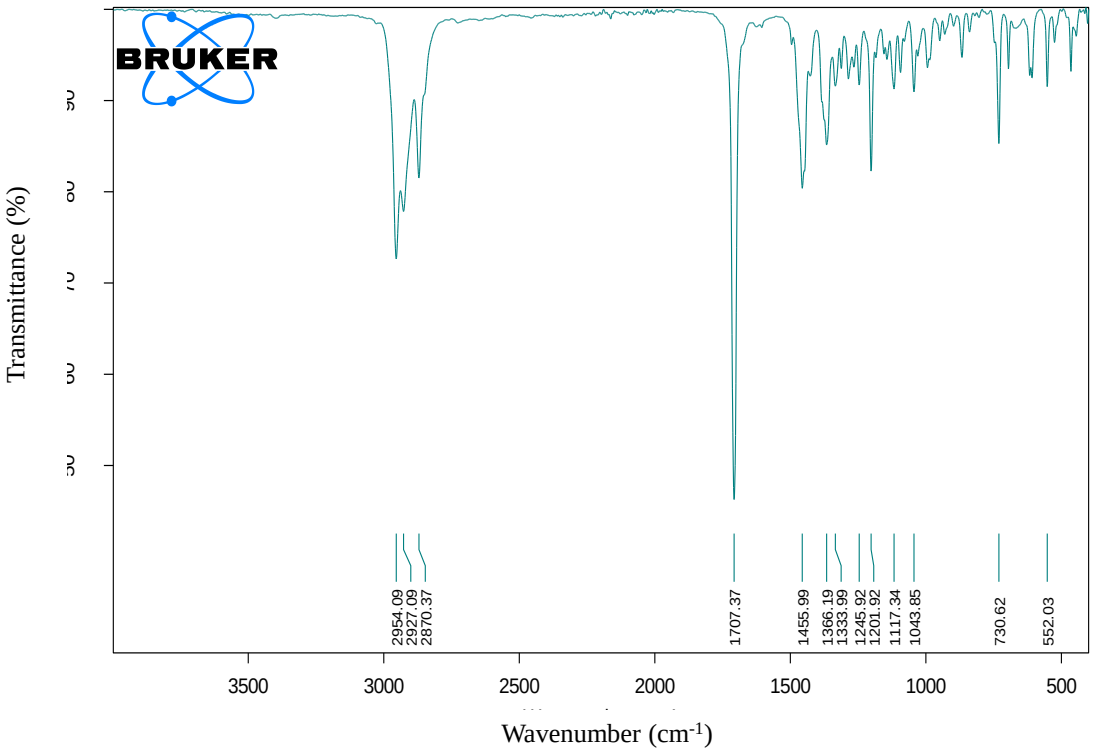

Figure 12: IR spectrum of synthesized menthone according to scheme 11.

4.4. Proposed method for the synthesis of 1-phenylmenthol (2)

Scheme 12 shows the synthesis of 1-phenylmenthol (2) through two step reaction. Previously synthesized compound 1 (Scheme 11) and freshly prepared Grignard reagent (PhMgBr) were used. The Grignard reagent was prepared as needed, by reacting bromobenzene (4) with magnesium metal in THF as a solvent in the presence of iodine as a catalyst, followed by addition of menthone. The first reaction was supposed to reflux by itself, but iodine was used to assist. Unfortunately, the reaction was not successful, and it was confirmed by ^{13}C NMR (Figure 13).

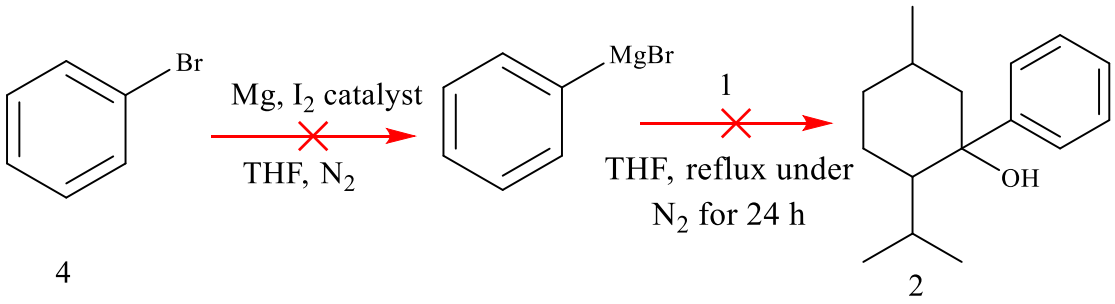

Scheme 12: Proposed method for the synthesis of 1-phenylmenthol (2)

Figure 13 shows ^{13}C NMR of compound 2 synthesised in scheme 12. Based on the spectrum, the first reaction did not happen as expected which ended up with all stating material in the product. Perhaps the freshly prepared Grignard reaction was unreactive because it was exposed in oxygen or contaminated by water which destroy the reagent. Reaction condition and procedure to prepare the Grignard reagent also affect the reduction of menthone. Even though quaternary carbon C1, and C11 peaks at 78 ppm and 148 ppm were observed and ketone carbon peak at 212 ppm was not observed, the product was too contaminated and not convincing. The same reaction was repeated in section 4.5.

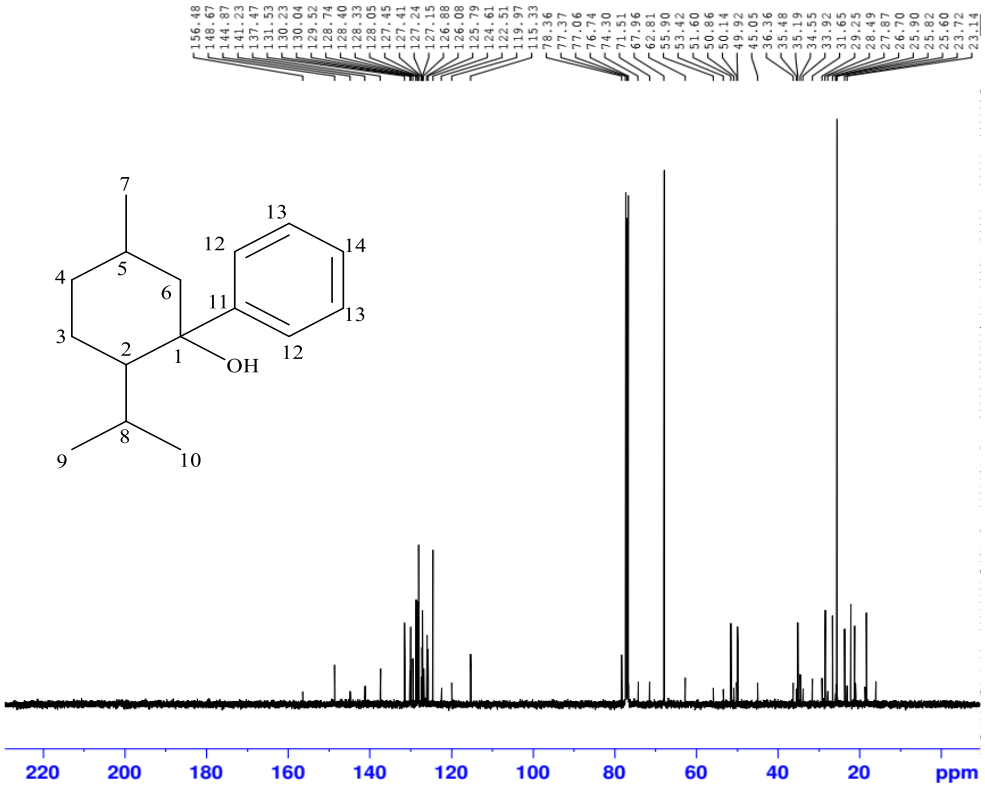

Figure 13: ^{13}C NMR full spectrum of 1-phenylmenthol synthesized according to scheme 12.

4.5. Alternative approach following the synthesis of 1-phenylmenthol (2) in 4.4.

Since, reaction scheme 12 failed, a different procedure was applied, including carefully monitoring the reaction with TLC, observing colour changes and temperature. The reaction of bromobenzene and magnesium metals is highly exothermic with addition iodine, the reaction heated up by its own. While refluxing it showed different colour change, black soon after addition of iodide, yellow when it started to heat up, then cream white. The reaction could cool down to room temperature, followed by addition of menthone, which was then stirred for 24 h. Addition of menthone to PhMgBr is now an endothermic, so the reaction needed external heat, i.e., it was heated under reflux for another 24 h. NMR analysis (Figure 14) of the isolated product showed that the reaction was successful.

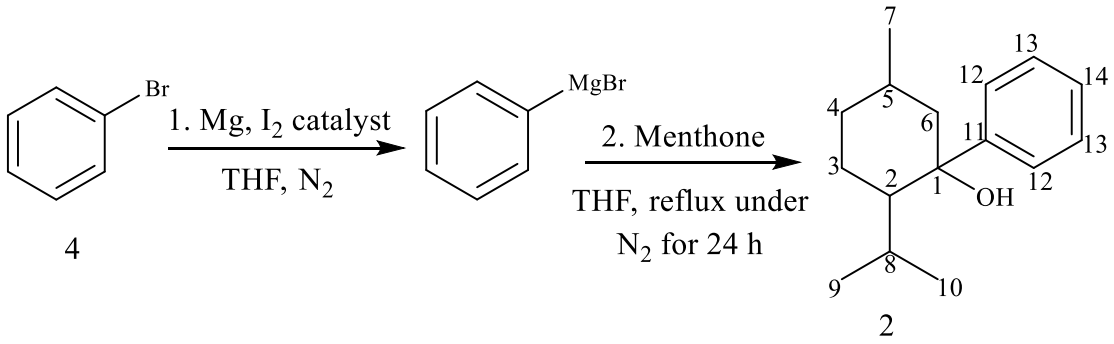

Scheme 13: Alternative approach towards the synthesis of 1-phenylmenthol (2)

Figure 14 shows the ^{13}C NMR spectrum of 1-phenylmenthol synthesized according to scheme 13. The spectrum shows all CH peaks from the benzene ring, C12 at 124 ppm, C14 at 127 ppm, and C13 at 128 ppm. The two new quaternary carbons C1 and C11 at 78 ppm and 148 ppm respectively also emphasized that indeed the product was formed. This spectrum was recorded after the product was purified twice trying to clean and get pure product. However, the product was still contaminated, and it became too little after purification, meaning the percentage yield was very small, so it needed to be upscaled.

It was up to this point where it started to show that reduction of (-)-menthone (1) by organometallic reagent is not as easy as it is presented on the scheme, this was also supported by few papers [69, 71, 72], which all emphasized on saying (-)-menthone (1) is an enolizable and a hindered ketone due to the bulky isopropyl making it difficult for it to be reduced into an alcohol. Paven and Dimitrov [69] investigated the addition of organometallic reagents to compound 1 with and without cerium chloride ($CeCl_3$) as a catalyst and THF as a solvent, PhMgBr was one of the reagents. Their results indicated that conversion of compound 1 to compound 2 by most organometallic reagents was not complete resulting in some difficulty in isolating both products (1-phenylmenthol and its isomer 1-

phenylneomenthol). Lecomte *et al*. [72] investigated how they could improve the reduction of hindered ketones by using phenyl lithium (PhLi) in a non-polar solvent (toluene-diethyl ether) (see scheme 5). Their results and discussion indicated that the addition of organometallic reagent to a hindered ketone, including menthone could be easily achieved by using a non-polar solvent (toluene) because non-polar solvents favour addition versus enolization when working with ketone like compound menthone. They also indicated that the percentage yields of the product can be increased using PhMgBr in THF as a solvent with or without cerium chloride ($CeCl_3$) as a catalyst.

The reaction scheme 13 worked after using synthesized starting reagents. This confirmed that purchased reagents used in section 4.1 and 4.2 had badly affected the formation of compound 2, which was because the reagents were old and were not stored in a suitable environment, especially PhMgBr, it was unreactive due to the exposure to oxygen and water.

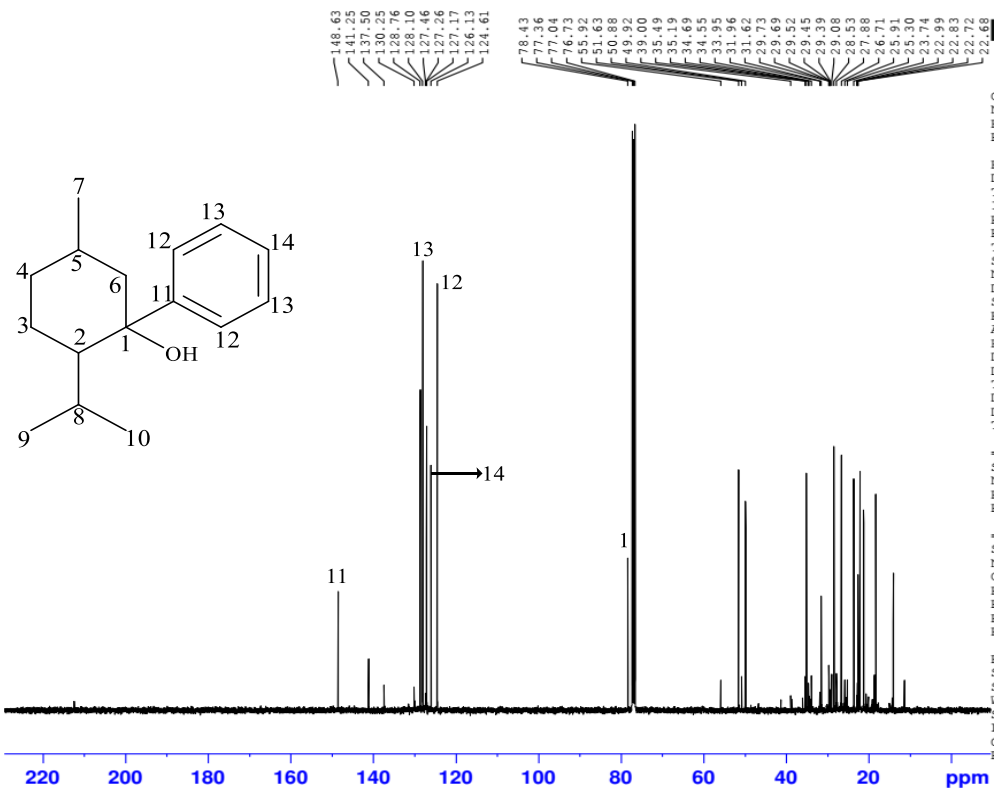

Figure 14: ^{13}C NMR full spectrum of 1-phenylmenthol synthesized according to scheme 13.

4.6. Modified method towards the synthesis of 1-phenylmenthol (2)

Although the reaction scheme 13 worked, the reaction was repeated in this section to upscale the product yield and to get pure product without contaminations. New Grignard reagent (PhMgBr) was purchased and another modified method by Paven and Dimitrov [69] was adopted for the preparation of compound 2. PhMgBr reagent was added dropwise at 10℃ into THF solution of menthone, then the reaction mixture was stirred for 24 h at room temperature, then refluxed for another 24 hours. The crude product mixture was hydrolysed by 2 M HCl and extracted to form the desired product as yellowish oil. The product was purified by column chromatography and the percentage yield was 68%. Furthermore, the product was analyzed by ^{13}C NMR (Figure 15), ^{1}H NMR (Figure 16) and IR (Figure 17) spectroscopies.

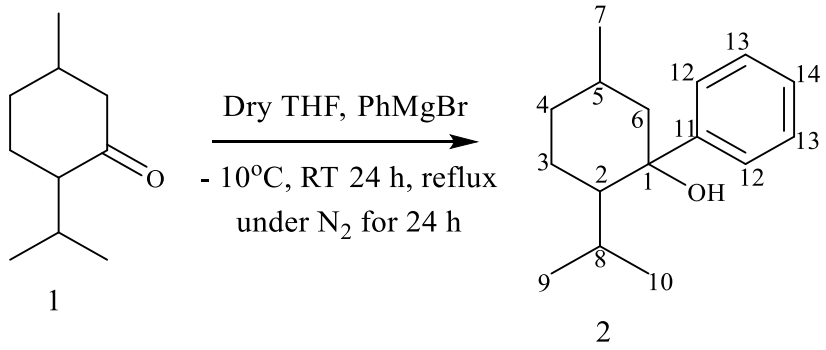

Scheme 14: Modified method towards the synthesis of 1-phenylmenthol (2).

Figure 15 (a) shows the ^{13}C NMR full spectrum of menthone, the compound that was synthesised according to scheme 14. The spectrum shows the presence of two quaternary carbon peaks C1 and C11 at 78 ppm and 148 ppm, thus the product has formed. Carbon C12, C13 and C14 peaks confirmed the presence of CH from the phenyl group. The two C12 carbons and two C13 carbons are equivalent, hence they have higher peak intensity as compared to C14 peak. Other carbon peaks from the cyclohexane have changed (in terms of chemicals shifts) as compared to the ^{13}C spectrum of starting material (menthone), thus another indication that all starting material were converted to product. Figure 15 (b) shows dept 135 carbon NMR spectrum of 1-phenylmenthol, this spectrum is the one which makes it clear on which carbon is which. Dept 135 do not show quaternary carbons, C1 and C11. However, it clearly showed the CH_2 carbons C3, C4 and C6 below the base line and all CH and CH_3 are above the base line, but CH carbons from phenyl group are deshielded (called aromatic region) as compared to other CH from cyclohexane group. Both spectra showed successful reduction of menthone by phenyl-magnesium bromide reagent to form 1-phenylmenthol.

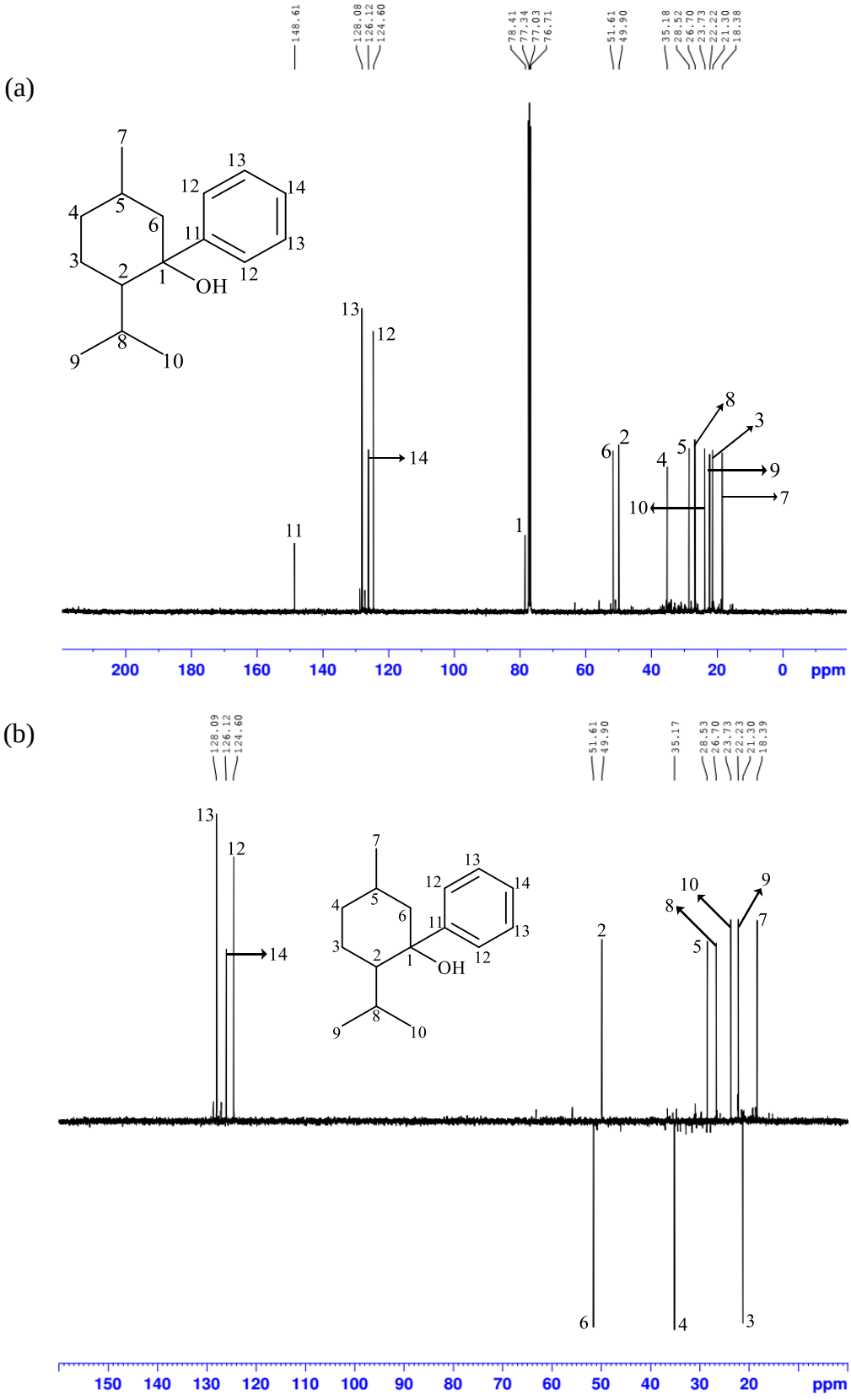

Figure 15: ^{13}C NMR full spectrum (a) dept 135 NMR spectrum (b) of 1-phenylmenthol synthesized according to scheme 14.

Figure 16 (a) shows ^{1}H NMR spectrum of 1-phenylmenthol (2) synthesized according to scheme 14. Compound 2 was bit complicated in terms of protons, as far as the spectrum is showing, most of the signals were overlapping making it difficult to read the multiplicity. However, the spectrum shows peak H15 at 2.2 ppm, broad singlet due to alcohol, this was the most expected peak to confirm the convention of ketone to alcohol. Figure 16 (b) shows an expansion spectrum of aromatic region where all protons due to phenyl group were observed. As shown in the spectrum, H12 at 7.37 ppm is doublet due to H13, H13 at 7.48 ppm is triplet due to H14 and H12. Moreover, H14 at 7.25 ppm is triplet due to two H13 hydrogens.

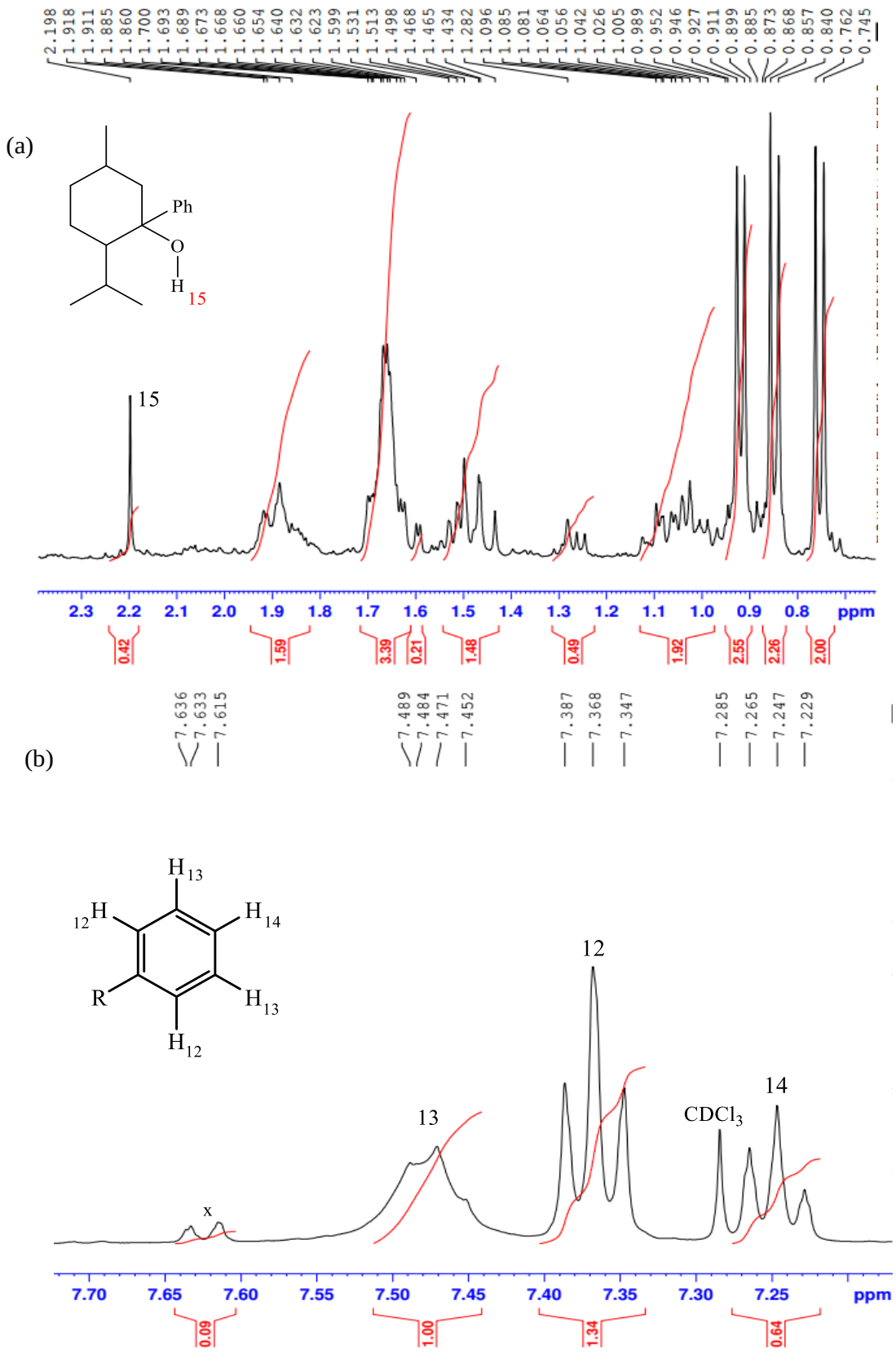

Figure 16: ^{1}H NMR spectrum (a) aromatic expansion (b) of 1-phenylmenthol as synthesized according to scheme 14.

Figure 17 shows IR spectrum of 1-phenylmenthol synthesized according to scheme 14. The spectrum confirmed all the functional groups that were found on the product 2. A broad O-H peak at wavenumber 3492 cm^{-1} confirmed the presence of alcohol, strong C-H stretching peaks at 2924 cm^{-1} and 3052 cm^{-1} were from the cyclohexane and benzene. The C=O ketone peak was observed to be weak as compared to IR spectrum of menthone on Figure 12 which represented the conversion of ketone to alcohol.

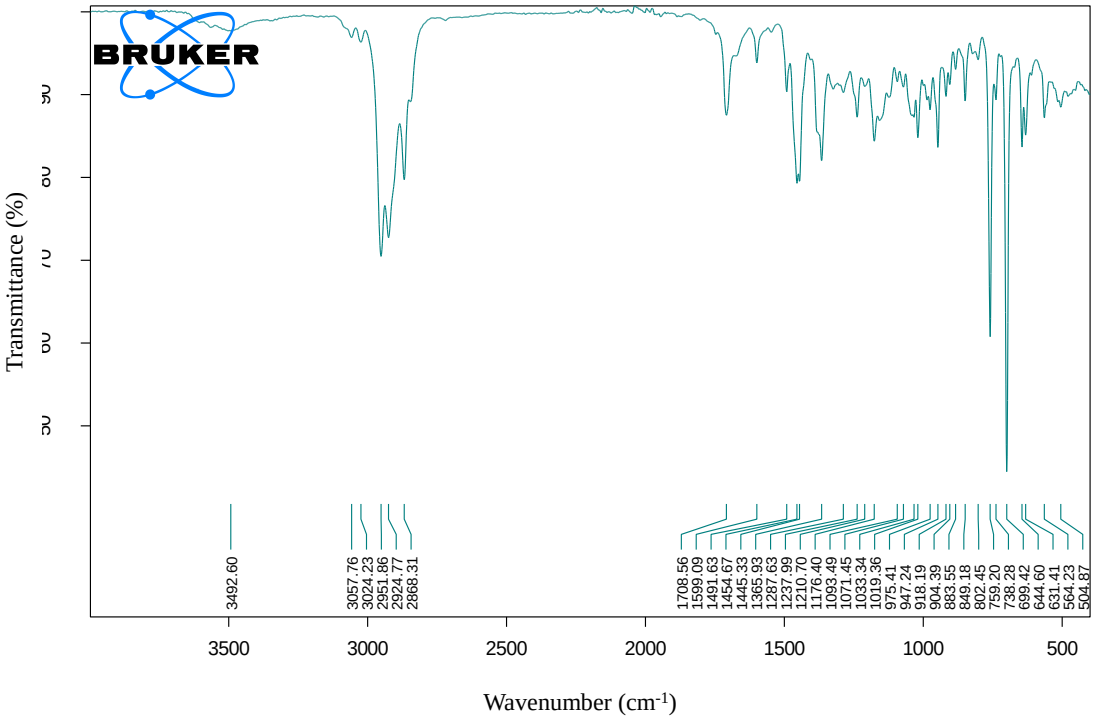

Figure 17: IR spectrum of 1-phenylmenthol synthesized according to scheme 14.

4.7. Synthesis of 1-phenylmenthol imprinted polymer and non-imprinted polymer

1-phenylmenthol imprinted polymer and non-imprinted polymer were successfully synthesized by precipitation polymerization as they settle at the bottom of the flask (Figure 18). Based on Table 2, different molar ratios of the template: functional monomer were prepared in different porogen to get the good quantity and best-working molar ratio which was found to be 1:4 MAA/EGDMA. After polymerization, the obtained MIP and NIP polymers were weighed, washed, and characterized. A modified method by Xia *et al*. [1], the template and functional monomer (MAA) were dissolved in methanol followed by cross-linker (EGDMA) and initiator (AIBN). After purging with N_2 gas flask was closed and heated at 80℃ until completion. After drying, the polymers were successfully washed with the mixture methanol: acetic acid solvent to remove the template.

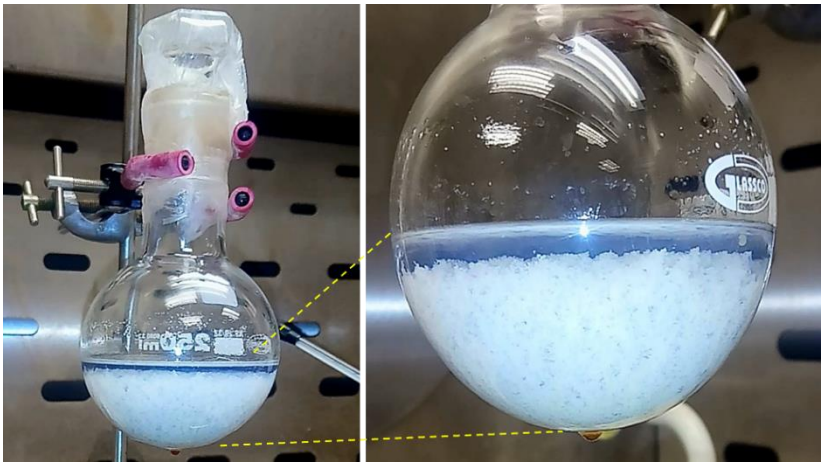

Figure 18: Synthesis of 1-phenylmenthol imprinted polymer and non-imprinted polymer.

4.8. UV/Vis absorption spectrum of 1-phenylmenthol

Figure 19 shows the absorption spectrum 1-phenylmenthol measured in the range 200 to 800 nm. Absorption of the template was done to check if the template was UV active and at what wavelength does it absorb, because this data had never been published before. A volume of 10 µL (1.32 M) template was dissolved in 250 µL methanol to make 0.0528 M concentration, then it was analysed by UV-vis spectroscopy. The results in Figure 19 indicated that the template was indeed UV active, due to chromophore benzene ring and the absorption from the antibonding -OH, which gave the maximum wavelength to be 320 nm. This UV analysis was the done after one year of synthesis and by then the compound had changed colour from light yellow to dark blue. Perhaps its chromophore breaks down into new chromophore with difference absorption wavelength. Thus, the reason why there are other peaks from 500 to 700 nm, since the compound was 1 year old, it could have broken down into fragments that resulted on those peaks. Thought it was not exposed to sunlight, it could have lost its stability over the room temperature and environment it was kept on hence.

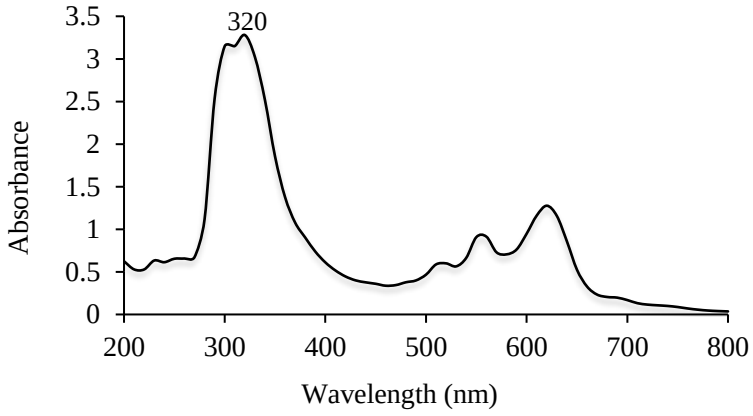

Figure 19: UV absorption spectrum of 1-phenylmenthol

4.9. Template elution

Figure 20 shows the UV/Vis spectrum of the wash-out solution analysis after removal of the template from the imprinted polymers. Although non-imprinted polymers (NIPs) were not template-imprinted they did not skip the 'removal step'. To verify the absence of template (1-phenylmenthol) into the imprinted polymer, 2 g of dried MIPs were washed with the mixture of methanol: acetic acid (90:10 v/v) for the total of 10 washing cycles. Acetic acid was chosen as the modifier as it has been used to enhance the elution strength of solvents during desorption studies. Four elution's were considered enough to wash out the template, because from wash 4 onwards the absorbance was about zero.

This step is very crucial in the synthesis of MIP due to the importance of complete template removal. However, it is known that even after exhaustive washing by different approaches (thermal annealing, microwave assisted extraction, Soxhlet extraction, and supercritical fluid template desorption), traces of template may remain in the polymer network [119, 184], because sometimes imprinted sites are formed not only on the surface of the functional monomer, but also deeply in the cross-linked polymer network structure, where organic solvent can hardly reach during the process of template elution. Thus, the remaining of template molecules in the MIP means less cavities are available for rebinding, which decreases extraction efficiency [135]. Another problem with incomplete template removal is template bleeding (bleeding of the non-extracted template), so if template could bleed during analytical applications, errors will arise and result in over estimation of analytical results (negatively impact real samples analysis) [162]. Template removal should be accurately performed in order to ensure that the maximum number of imprinted sites are free which might also reduce high concentration of template bleeding [138].

During polymerization, template, functional monomer, cross-linking agent, and initiator were dissolve in a porogenic solvent, where the functional monomer (MAA) created binding sites on the 1-phenylmenthol-imprinted polymer forming monomer-template interaction Figure 21A. In this research study the imprinting of template was achieved by non-covalent forces (hydrogen bonds) between methacrylic acid and 1-phenylmenthol. Methacrylic acid as a monomer allows the formation of hydrogen bonds between its carboxyl group and hydroxyl group from the template. Thus, the methacrylic acid was selected because it has only few polar functional groups which results in few but strong interaction with binding template to the MIPs.

In non-covalent methods, polymeric chains self-organized around the imprinting molecules through hydrogen bonding which is responsible for the molecular immobilization during the rebinding. After

polymerization, the polymer matric was washed to remove the template leaving binding cavities with a complementary geometric and chemical fitting structure, which prevent possible binding of other compounds that do not match with the template imprinted cavities Figure 21B.

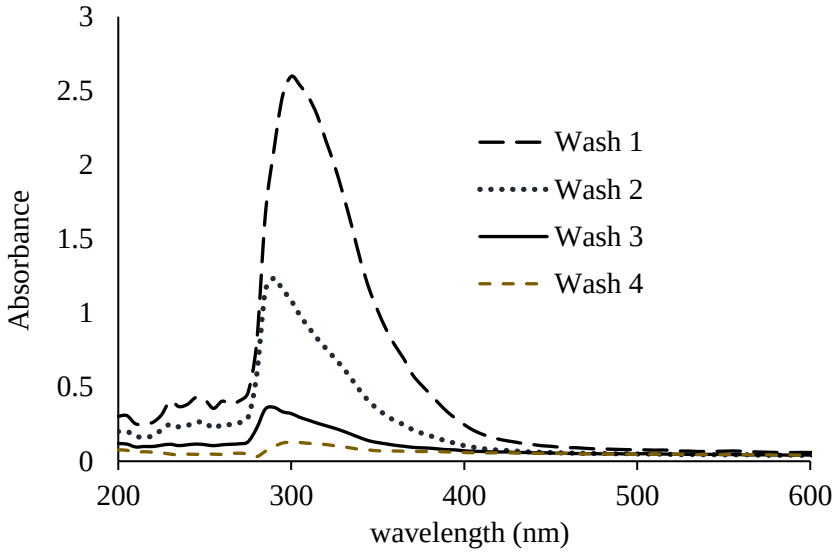

Figure 20: UV/Vis spectrum of the solution after washing of the MIP.

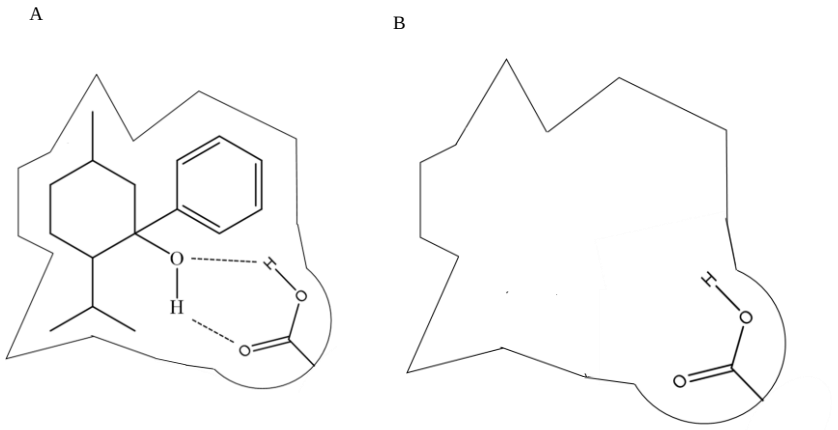

Figure 21: (a) hydrogen bonds formed between template and MAA during polymerisation (b) complementary cavity left after removal of template.

4.10. Standard calibration curve of 1-phenylmenthol

A standard calibration curve was constructed for 1-phenylmenthol to obtain the linear equation which was used to calculate the final concentration (mg L^{-1}) of the template after adsorption, which was then used to find enrichment factor (EF) according to the equation (1). For this purpose, a stock solution was prepared by dissolving a 2 µL template in 50 mL methanol to make 1225 mg L^{-1}. From this stock solution, suitable dilutions were prepared (232, 464, 580, 696, and 812 mg L^{-1}). All the standards were analysed by UV at 320 nm. The values of absorbance were recorded, and a standard curve was constructed by plotting the absorbance against concentration (Figure 22).

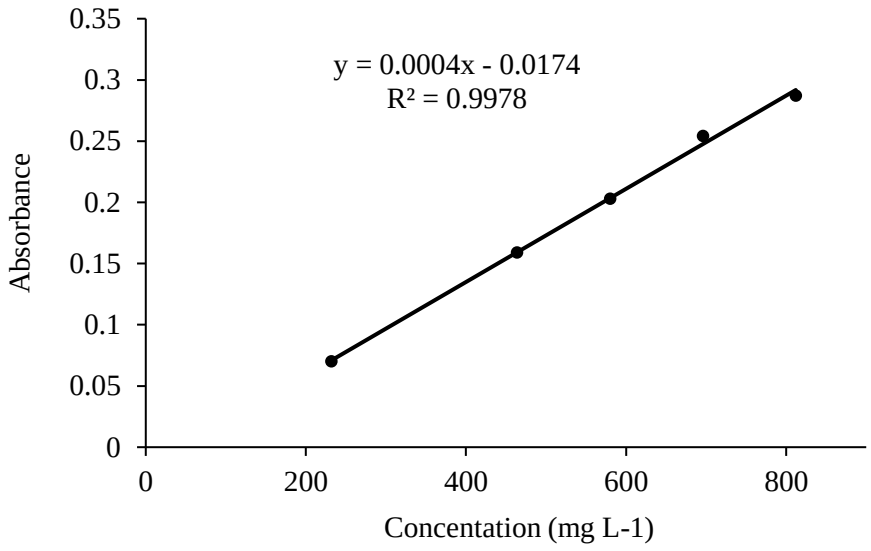

Figure 22: Standard calibration curve of 1-phenylmenthol

4.11. Characterization of prepared imprinted polymers

4.11.1. Fourier transforms infrared spectroscopy (FTIR)

FTIR spectroscopy was done to monitoring changes in functional groups of the compounds in the MIPs and NIPs. The FTIR spectrum of NIP (a), unwashed MIP (b), and washed MIP (c) are shown in Figure 23. Few peaks were observed from the spectrum of each sample. A broad -OH stretching peak at 3573 cm^{-1} for unwashed MIPs, 3545 cm^{-1} for washed MIPs, and 3519 cm^{-1} for NIPs were associated with the methacrylic acid alcohol group (OH) but, unwashed MIPs showed high wavenumber of -OH due to another alcohol from the template. The C-H peak at 2948 and 2995 cm^{-1} for unwashed MIPs, 2953 cm^{-1} for washed MIPs, and C-H, 2954 cm^{-1} for NIPs were observed and they were all due to the presence of methylene group in both MAA, EGDMA, and AIBN polymerization materials. Unwashed MIPs showed two strong C-H peaks as compared to washed MIPs due to other alkane groups from the template. Moreover, the C-H frequency or washed MIPs and NIPs are almost similar as compared to unwashed MIPs. This might be due to the absence of template in both washed MIPs and NIPs. The carbonyl group C=O strong peak at 1722 cm^{-1} in all polymers originated from MAA and EGDMA. The strong C-O peak at 1145 cm^{-1} from all the polymers were associated with aliphatic ether on EGDMA. These observations supported the successful preparation of MIPs, also the successful removal of the template. Related FTIR results were also obtained and presented by Sikiti *et al*. [185], where almost all most all the bond peaks found in their MIPs and NIPs were close to the wavenumbers presented in this study. However, their polymers were printed with 2,3,7,8-tetrachlorodibenzo-p-dioxin as a template molecule and chloroform was used as a solvent. On the other hand, Bayramoglu and Arica [186] prepared ion-imprinted polymers, using Cr (VI) as the template and 4-vinyl pyridine (4-VP) and from analysed FTIR result the same stretching bond wavenumbers were observed, though different template and functional monomer was used.

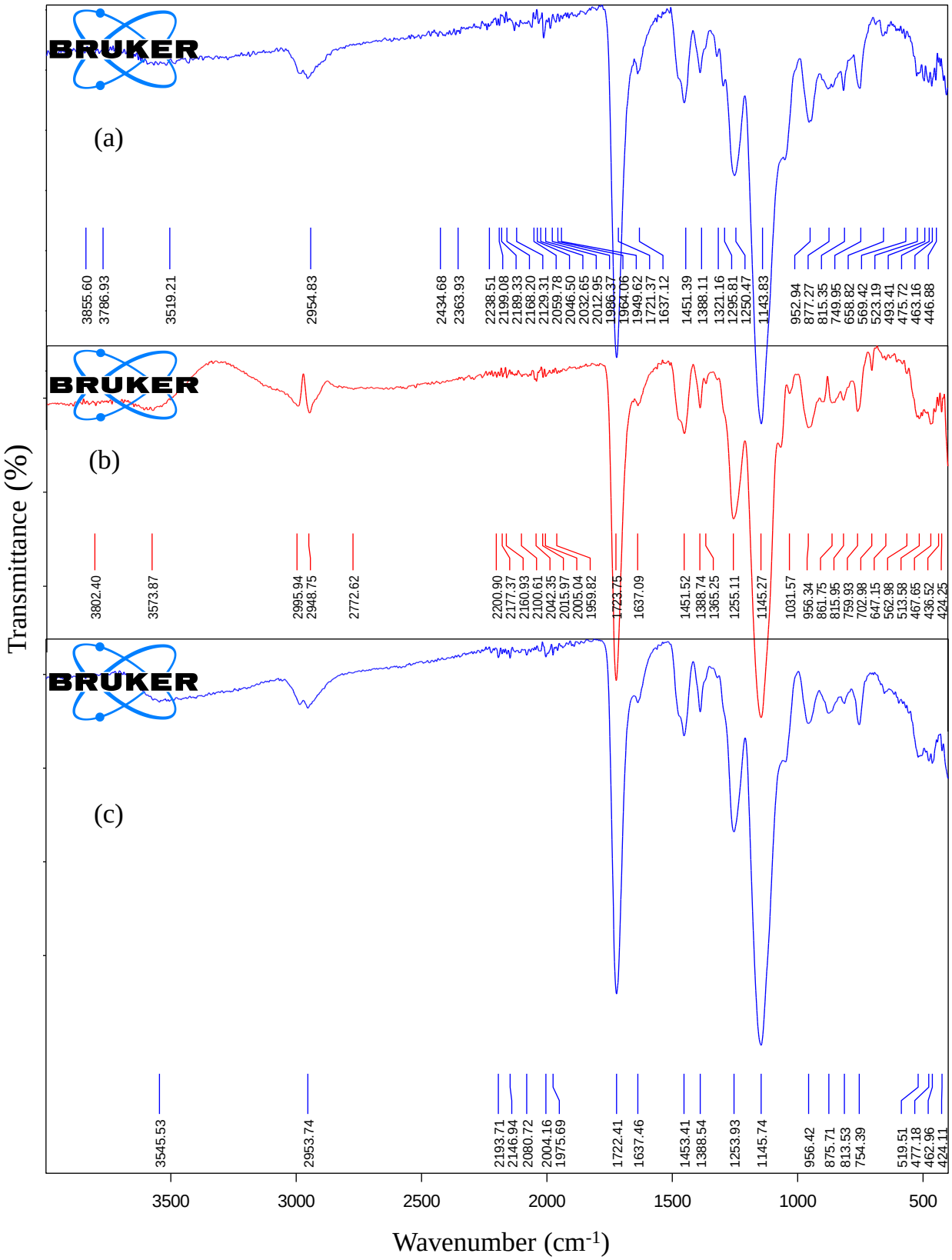

Figure 23: FTIR spectrum of washed NIP (a) unwashed MIP (b) and washed MIP (c).

4.11.2. Brunauer-Emmett-Teller (BET)

BET was done to analyse the surface area of unwashed MIPs and washed NIPs (Table 3), where the polymer surface area, pore volume, and pore diameter were measured. The surface area of MIP was found to be 17.85 m^2 g^{-1}, thus larger than that of NIP which was 10.05 m^2 g^{-1}. Although, the surface area was taken in the presence the template, it was still higher than that of NIPs, which means that the template adsorbed and saturated the pores and still leave some pores great enough to attain that surface area. The observed surface area of the NIPs might be credited to the pores left by the porogen molecules during washing. Moreover, the surface area, pore volume and pore size for MIP was also found to be larger than that of NIP. Sikiti *et al*. [185], presented related BET results for the dioxins MIPs and NIPs, the results shows the same trend of higher pore size as compared to surface area and pore volume was always the lowest. It was also found that the surface area, pore volume and pore size for MIP was higher than of the corresponding NIP. Some imprinted and non-imprinted polymer with the same BET trend of pore size greater than surface area which greater than pore volume were prepared by Xia *et al*. [1] and Tegegne *et al*. [187], but with different template molecule.

Table 3: Brunauer-Emmett-Teller (BET) results of MIPs and NIPs

Polymer	BET surface area (m^2 g^{-1})	Pore volume (cm^3 g^{-1})	Pore size (Å)
NIPs	10.05	0.018	70.69
MIPs	17.85	0.038	85.27

4.11.3. Thermogravimetric analysis (TGA)

Thermograms of the washed NIP, unwashed, and washed MIP particles are plotted in Figure 24. TGA revealed two decomposition states. The first weight loss was approximately 5% between 0 and 80°C which represents the decomposition of volatile compounds. Washed MIP and NIP were stable between 100 and 250℃, but unwashed MIP was gradually decreasing in weight between 100 and 250℃. These observations indicated that unwashed MIP was less stable as compared to washed MIP and NIP. Further rapid major thermal decomposition of all polymers was observed at 411℃ for unwashed MIP, 409℃ for washed MIP, and 415℃ for washed NIP, which was marked as the temperature where the polymer building materials collapses. A percentage of 98% of polymers were fully decomposed at 461℃ for unwashed MIP, 479℃ for washed MIP, and 465℃ for washed NIP. This was due to the thermal decomposition of the cross-linker (EGDMA) from the polymer structure. Similar results were obtained in another study by Zahedi *et al*. [139] where the polymer thermal degradation was observed at 411℃ for a washed MIP which was synthesized in the presence of dexamethasone as a template.

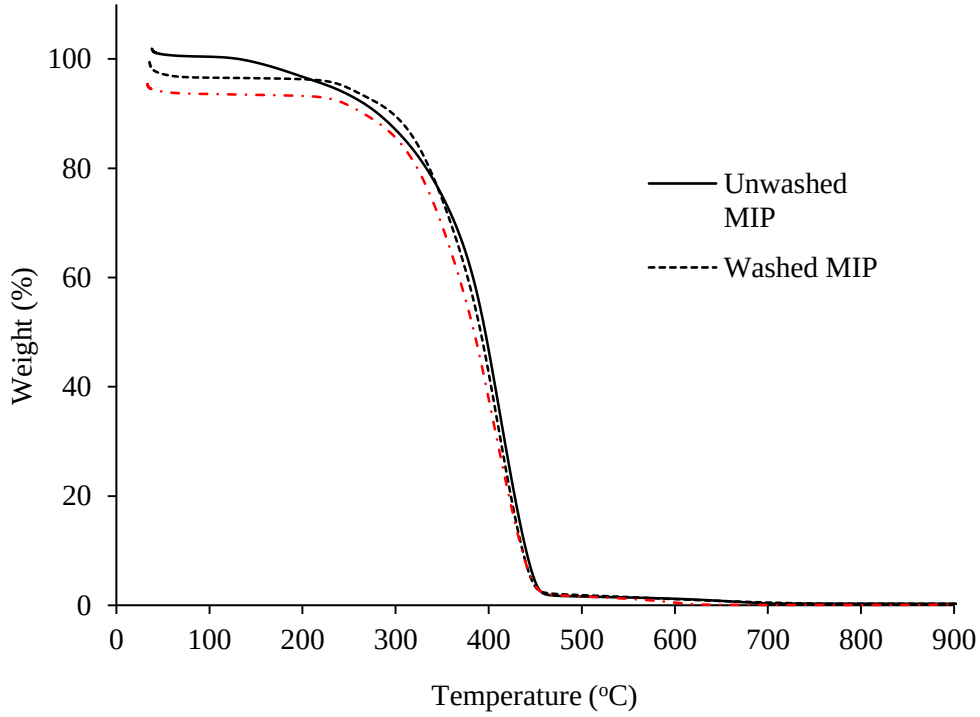

Figure 24: Thermogravimetric analysis of the washed NIPs, unwashed, and washed MIPs.

4.12. Optimization of 1-phenylmenthol

Parameters that could influence the adsorption of 1-phenylmenthol onto MIPs were optimized. Optimization was carried out by using methanol because 1-phenylmenthol (an essential oil) is insoluble in water. SPE parameters investigated include effects of sample pH, sorbent mass, concentration, and contact time at room temperature. Since the target compound is polar, methanol was used for elution from the SPE cartridge. During optimization, only one parameter was varied, and the other parameters were kept constant. Each experiment was repeated 3 times.

4.12.1. Effects of samples pH

The binding affinity of the template is highly dependent on pH of the solution; thus, the polymer pH of the solution is another important parameter for the adsorption process. So, it is very important to investigate the effect of solution pH on adsorption of 1-phenylmenthol on MIPs and NIPs. The effect of pH on 1-phenylmenthol adsorption was determined for different pH values ranging from 2 to 11, using a methanol solution (Figure 25). The pH of methanol solution was adjusted to promote the monomer-template interactions since it has been reported that the extraction is based on hydrogen bonding of the target compound and functional monomer. This is due to the chemical speciation for both active binding sites of cavities present inside the MIP and the active functional groups of the template available for bonding. Figure 25 shows that highest adsorption of template was achieved at pH 7 with an enrichment factor of 40. At optimum pH (pH 7) there are no structural changes of template and MIP configuration's so, maximum adsorption of template was observed at neutral pH and then changed as the medium turned to acidic or basic. At acidic media pH 2 or basic media pH 11 the adsorption seems to be decreasing, this might be since the synthesis of both MIP and NIP has a permanent positive charge, which causes the electrostatic repulsion and result in poor enrichment factor at pH 2. Or it might be due to the hydrophobic interactions by many competing H+ ions in acidic media that will be available for the protonation of carboxylic group result in weakening of H-bonding between template and selective binding sites of MIPs and causes a decreasing the binding capacity in acidic media. Tt higher pH values (basic media), the adsorption also seems to be decrease too which may be due to the presence of soluble hydroxyl groups and competing with the template for binding sites. MIPs had always enrichment factor than NIPs because they have specific binding sites for 1-phenylmenthol, while NIPs have no specific binding sites. A similar trend was observed by Bakhtiar *et al*. [188], who used 2-phenyl-phenol as a template to prepare MIPs. Their results showed that 99.42% was recovered at pH 7, which meant that sample pH 7 was also their optimum. Moreover Shafqat *et al*, [189] observed the same trend, using the congo red dye as a template to achieve the highest removal efficiency at pH 7.

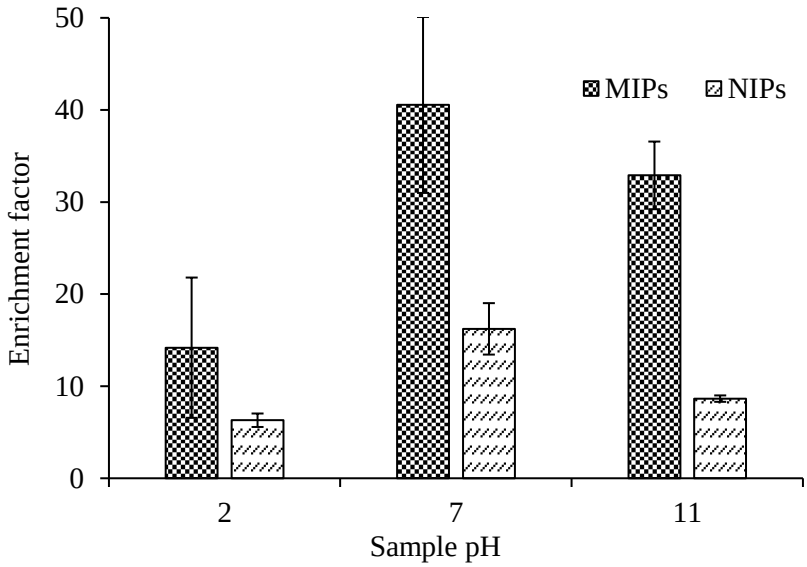

Figure 25: Effect of sample pH on the adsorption of 1-phenylmenthol (n = 3, SD). Experimental conditions: Mass of MIPs, 50 mg; mass of NIPs, 80 mg; solution volume, 30 mL; contact time, 180 min; template concentration, 11 mg L^{-1}.

4.12.2. Effects of mass

The effect mass was investigated in the range of 10 to 80 mg. Figure 26 shows that, initially, the enrichment factor of 1-phenylmenthol increased as the mass of the MIPs increased. This is because an increase in the amount of polymer, the number of the adsorption sites was increased and make a greater availability of the template to be adsorbed within the polymers. A little decrease in the enrichment factor was observed with further increased in mass of MIPs from 50 mg to 80 mg, which might be due to the aggregation of polymer particles. Therefore, aggregation of polymer particles decreased the available binding sites, and hence, lower enrichment factor. NIPs required more amount of sorbent because it had no specific binding sites for 1-phenylmenthol adsorption, hence higher enrichment factor as the mass increased. The highest enrichment factor was obtained at the mass of 50 mg for MIPs and 80 mg for NIPs. Thus, mass 50 and 80 mg were selected as optimum and used in all other experiments. The same effect of mass results was presented in a recent study by Shafqat *et al*. [189]. They synthesized MIPs in the presence of congo red dye as a template, and the effects of mass were investigated from mass of 0.1 g to 1 g. Their results indicated that percentage removal of the dye increased with the increase in the mass of MIPs up to a certain limit where further increased in mass of MIPs cause a gradual decline. A similar trend was observed for the MIPs synthesised with abacavir as template by Qwane *et al*. [190], which meant that during the increase in mass of MIPs, more binding

sites in the polymer became available, and the extraction efficiency was enhanced until the equilibrium was reached at a mass of 40 mg as their optimum mass.

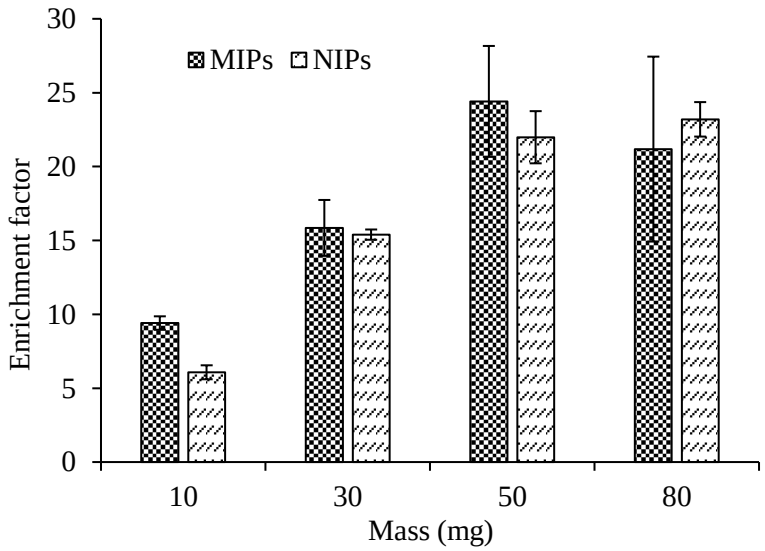

Figure 26: Effect of mass on the adsorption of 1-phenylmenthol (n = 3, SD). Experimental conditions: Sample pH 7; solution volume, 30 mL; contact time, 180 min; template concentration, 11 mg L^{-1}.

4.12.3. Effects of concentration

The experiment was carried out at a different concentration of the 1-phenylmenthol (7 to 54 mg L^{-1}). Figure 27 shows that the enrichment factor for MIPs increased with the increase of the template concentration from 7 to 11 mg L^{-1}, then decreased with further increase in concentration from 22 to 54 mg L^{-1}. This indicated that the MIP was reaching saturation at higher concentrations. However, this observation was only noticed when MIPs were used. On the other hand, when the concentration of template increased, the enrichment factor on NIPs increased from 7 to 54 mg L^{-1}. Since NIPs have limited or no binding sites, high concentration of template was needed to achieve noticeable full binding of template into the NIPs, as compared to MIPs where only 11 mg L^{-1} concentration was enough to achieve the highest enrichment factor. In other words, high adsorption at lower concentration of template with MIPs was observed, whereas high adsorption at higher concentration of template into NIPs was observed. The maximum enrichment factor was obtained at the concertation of 11 mg L^{-1} for MIPs and 54 mg L^{-1} for NIPs; therefore, they were selected as optimum and used in other optimization experiments.

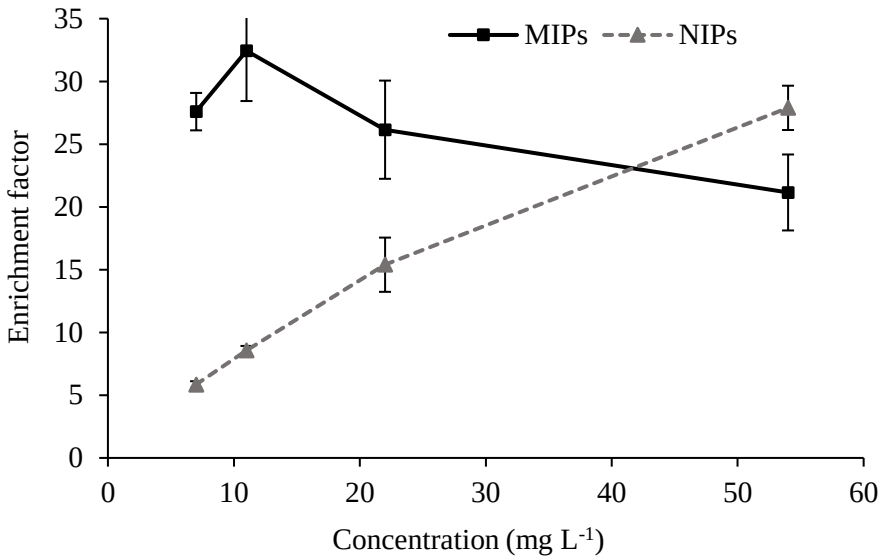

Figure 27: Effect of concentration on the adsorption of 1-phenylmenthol (n = 3, SD). Experimental conditions: Mass of MIPs, 50 mg; mass of NIPs, 80 mg; sample pH 7; solution volume, 30 mL; contact time, 180 min.

4.12.4. Effects of contact time

The relationship between the amount of 1-phenylmenthol adsorbed and contact time for the MIPs is shown in Figure 28, where 50 mg of MIPs was added into 30 mL solution (11 mg L^{-1}) at sample pH 7, the adsorption was investigated between 20 to 180 min. Figure 28 shows that there is an increase in the enrichment factor on both MIPs and NIPs from 20 to 180 min. The time 180 min was therefore selected as the optimum time in both MIPs and NIPs. The enrichment factor of the MIPs was higher than of the NIPs, because MIPs has high selectivity due to the binding sites, while NIPs had no binding sites.

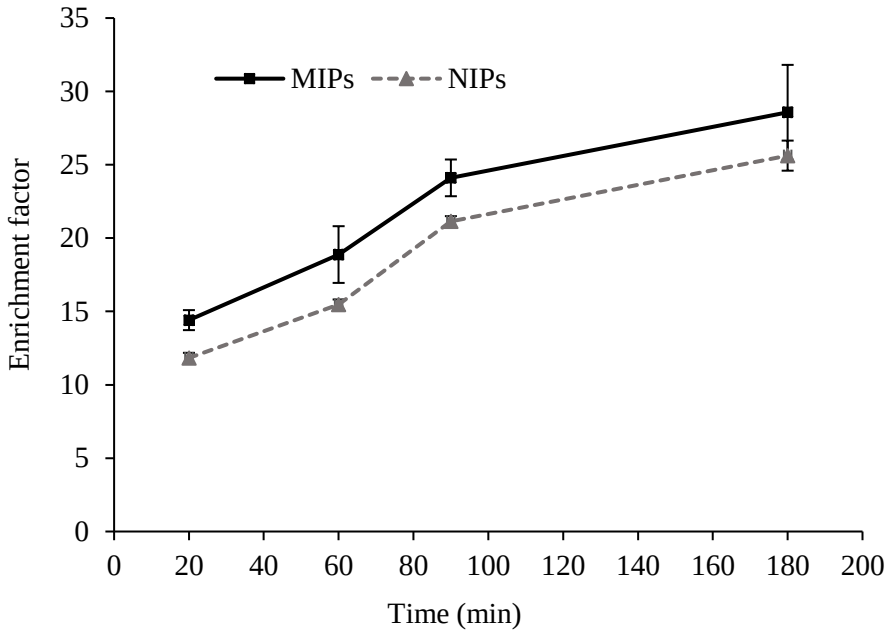

Figure 28: Effect of contact time on the adsorption of 1-phenylmenthol (n = 3, SD). Experimental conditions: Mass of MIPs, 50 mg; mass of NIPs, 80 mg; sample pH 7; solution volume, 30 mL; template concentration, 11 mg L^{-1}.

4.13. Reusability studies

The results of the reusability studies are shown in Figure 29. The reusability of imprinted polymers was done at experimental optimum conditions (mass of MIPs, 50 mg; mass of NIPs, 80 mg; sample pH, 7; solution volume, 30 mL; contact time, 180 min, template concentration, 11 mg L^{-1}). Adsorption–desorption cycles were repeated 6 times by using the same imprinted particles with fresh elution solution. An increase of enrichment factor from cycle 1 to 3 was probably due to template bleeding or memory effects, when the previous cycles of adsorption of template left some 1-phenylmenthol bound on the binding sites after washing to prepare the second cycle. After the first cycle of adsorption, they

were template molecules remaining in the MIPs thus, less cavities will be available for rebinding, which decreases the enrichment factor of the next cycles. A decrease from cycle 3 to 6 was due to the loss of polymers or some imprinted cavities were destroyed, which led to slight loss of adsorption capacity. The enrichment factors of MIPs were higher than of NIPs because MIPs has high selectivity due to the binding sites, while NIPs have no binding sites. The results of the reusability studies have shown that the MIP can be re-used up to 3 cycles, because the enrichment factor decreased by only 9 from cycle 1 to 6.

Related results for stability and reusability of MIPs were presented by Fernandes *et al*. [53], who synthesized MIPs using ascorbic acid as template. Based on their results, they have observed a little increase from cycle 2 to 3 and decrease from cycle 4 to 5. However, most of studies showed an equal uniform percentage recovery or little decrease after few cycles. Qwane *et al*. [190] synthesized abacavir imprinted polymers and reusability of the synthesized MIP for the adsorption of abacavir was done. The results showed that the extraction efficiency of MIPs was greater than 90% from cycle 1 to 6 and little decline from 6 to 10 cycles. Xu *et al*. [191] synthesized lysozyme imprinted polymers (Lyz-MIPs). The regeneration and reusability batch adsorption experiment were done, based on their results, after 6 cycles, the removal efficiency of the Lyz-MIPs for template protein was only reduced by 7.4%. Furthermore, Gao *et al*. [192] synthesized magnetic protein imprinted, and non-imprinted nanoparticles. Based on the reusability studies, they found that adsorption capacity of MP-MIPs was still maintained at stable values of 91.3% after 6 cycles, although with little decrease of 6%, whereas the extraction efficiency of NIPs remained almost unchanged.

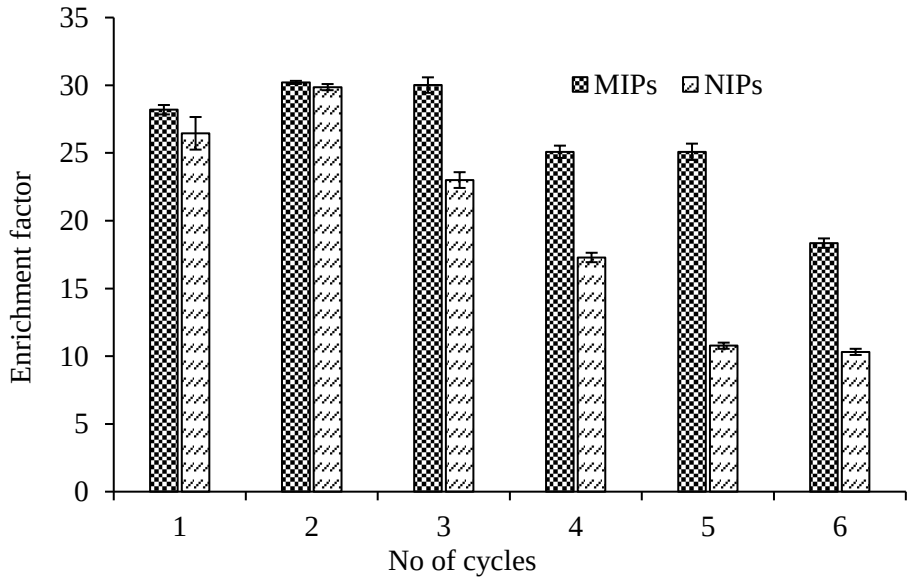

Figure 29: Reusability MIPs and NIPs (n = 3, SD). Experimental conditions: Mass of MIPs, 50 mg; mass of NIPs, 80 mg; sample pH 7; solution volume, 30 mL; contact time, 180 min; template concentration, 11 mg L^{-1}.

Chapter 5

Conclusion

This chapter conclude the aim, results, and findings of this dissertation. Challenges that were faced during the project, recommendation and future work are all discussed.

5.1. Conclusion

In this work, menthol was successfully oxidised into menthone, which was then used as starting material to synthesised 1-phenylmenthol. All organic products were purified by column chromatography and fully characterized by ^{13}C NMR, ^{1}H NMR and FTIR which showed and confirmed the structure of all successful and unsuccessful synthesized product based on the chemical shift of all carbon and hydrogen atoms. 1-phenylmenthol was then used as molecular template for the synthesis of MIPs, a robust polymeric 3D structure that was used as a sorbent on SPE. In addition, 1-phenylmenthol is a chiral organic compound that was used as a template for the first time in the synthesis of MIPs. Unlike other essential oils (menthol and menthone), 1-phenylmenthol was found to have these properties as they were never reported before: it has no minty odour, colour is yellowish and not soluble in water.

Molecularly imprinted polymer was successful synthesized using precipitation polymerization. MIP was synthesized using 1-phenylmenthol as a template, EGDMA as a cross-linking agent, methanol as a porogen, MAA as a functional monomer and AIBN as an initiator. They were characterized by FT-IR, TGA, and BET surface area analysis which indicated successful preparation of MIPs. BET analysis shows that MIP had a larger surface area, pore volume and pore size than the NIP. TGA confirmed the stability of washed MIP and NIPs up to 300℃ as compared to unwashed MIP which was gradually decreasing in weight from 100℃. FIRT spectrum showed it clearly on unwashed MIPs that there is a template as compared to washed MIPs and NIPs that did not have template. Parameters affecting adsorption of 1-phenylmenthol into polymers were optimized and calculated in terms of enrichment factors. Optimization experiments were done at different sample pH, mass of the polymer, contact time, and template concentration to find the optimum conditions. Therefore, the optimum enrichment factor was found to be at sample pH 7, mass of MIPs at 50 mg, contact time at 180 min, template concentration at 11 mg L^{-1} and mass of NIPs at 80 mg. The synthesized MIP can be re-used up to 3 cycles, because the enrichment factor decreased by only 9 from cycle 1 to 6.

5.2. Challenges, recommendation, and future work

Challenges that were encountered during the study of this research project.

- The addition of PhMgBr to menthone was quite difficult since menthone is an enolizable and hindered ketone, because of the bulky isopropyl crating 1,3 diaxial interaction, making it difficult for the Grignard addition of phenyl group to menthone.
- PhMgBr is strong nucleophile and highly reactive agent, it is sensitive to water and oxygen. Therefore, the reaction should be done in dry and inert environment because if moisture is in contact with the reagent, it will become unreactive.
- As far as synthesis of MIPs reaction was done, there were few challenges: This precipitation reaction is a condensation polymerization called endothermic reaction, thus the reaction required heat from outside. This becomes a challenge when too little or too high heat (temperature) was provided, therefore, when temperature is below 60℃ the polymerization mixture will not get enough energy to convert reactant into the desired product.
- Another challenge was when pre-polymerization mixture was purged with N_2 gas, addition of inert gas to the constant-volume reaction mixture increases the total pressure of the system. Therefore, high pressure starts to accumulate and push out the lid which closes the round bottomed flask, causing the solvent to evaporate when temperature was increased to 80℃.
- During the elution of template process, the wash out solution was analyzed by high limit detection UV-vis instrument, which could not detect the small amount of template left uneluted in the imprinted polymer matrices. Hence, the problem with incomplete template removal is template bleeding which occurred and might have caused the enrichment factors to be enhanced due over estimation of adsorption results.

Future work

- To synthesized 1-phneylmenthol considering different purification or separation methods like LC-MS to identify its molecular weight and the chirality of the product. Furthermore, some catalysts ($CeCl_3$) can be added to enhance addition of Grignard reaction and percentage yield of the product.
- To conduct one pot Grignard reaction with MIPs and determine the rate of reaction, with and without MIPs. In addition, different reducing agent (e.g., PhLi) other than PhMgBr can be used to reduce the difficulties of handling PhMgBr and increase the addition of phenyl group to menthone.

- Analyze three different imprinted polymers with SEM considering the effect of different functional monomer: cross-linker ratios. A certain functional monomer: cross-linker ratio can be used to produce MIP particles with controlled size and morphology, which can also increase the stability of polymers.
- Apart from 1-phenylmenthol used in this project as template, different commercially available organic compound can be used as template, which can dissolve in other solvents not just methanol, also to increase the reusability cycles, and selectivity of MIPs.
- Application of the prepared MIPs to real samples and analysis with the LC-MS instead of the UV.

References

[1] Xia, Q.; Yun, Y.; Li, Q.; Huang, Z.; Liang, Z. Preparation and Characterization of Monodisperse Molecularly Imprinted Polymer Microspheres by Precipitation Polymerization for Kaempferol. *Des. Monomers Polym.*, **2017**, *20* (1), 201–209.

[2] Nath, S.S., Pandey, C. and Roy, D. A near Fatal Case of High Dose Peppermint Oil Ingestion-Lessons Learnt. *Indian J. Anaesth.*, **2012**, *56* (6), 582–854.

[3] Thosar, N.; Basak, S.; Bahadure, R. N.; Rajurkar, M. Antimicrobial Efficacy of Five Essential Oils against Oral Pathogens: An in Vitro Study. *Eur. J. Dent.*, **2013**, *7* (suppl 1), S71.

[4] Schmitz, D.; Shubert, V. A.; Betz, T.; Schnell, M. Exploring the Conformational Landscape of Menthol , Menthone , and Isomenthone : A Microwave Study. *Front. Chem.*, **2015**, *300*, 31–36.

[5] Davies, S. J.; Harding, L. M.; Baranowski, A. P. A Novel Treatment of Postherpetic Neuralgia Using Peppermint Oil. *Clin. J. Pain*, **2002**, *18* (3), 200–202.

[6] Eccles, R.; Griffiths, D. H.; Newton, C. G.; Tolley, N. S. The Effects of Menthol Isomers on Nasal Sensation of Airflow. *Clin. Otolaryngol. Allied Sci.*, **1988**, *13* (1), 25–29.

[7] Balakrishnan, A. Therapeutic Uses of Peppermint –A Review. *J. Pharm. Sci. Res.*, **2015**, *7* (7), 474–476.

[8] Batool, I.; Nisar, S.; Hamrouni, L.; Jilani, M. I. Extraction , Production and Analysis Techniques for Menthol : A Review. *Int. J. Chem. Biochem. Sci.*, **2018**, *14*, 71–76.

[9] Dagli, N.; Dagli, R.; Mahmoud, R.; Baroudi, K. Essential Oils, Their Therapeutic Properties, and Implication in Dentistry: A Review. *J. Int. Soc. Prev. Community Dent.*, **2015**, *5* (5), 335–340.

[10] Oh, K. E.; Song, A. R.; Sok, S. R. Effects of Aroma Gargling, Cold Water Gargling, and Wet Gauze Application on Thirst, Halitosis, and Sore Throat of Patients after Spine Surgery. *Holist. Nurs. Pract.*, **2017**, *31* (4), 253–259.

[11] Cassel, E.; Vargas, R. M. F.; Martinez, N.; Lorenzo, D.; Dellacassa, E. Steam Distillation Modeling for Essential Oil Extraction Process. *Ind. Crops Prod.*, **2009**, *29* (1), 171–176.

[12] Hussain, A. I.; Anwar, F.; Nigam, P. S.; Ashraf, M.; Gilani, A. H. Seasonal Variation in Content , Chemical Composition and Antimicrobial and Cytotoxic Activities of Essential Oils from Four Mentha Species. *J. Sci. Food Agric.*, **2010**, *90* (11), 1827–1836.

[13] Shrigod, N. M.; Swami, N. R.; Prasad, H. R. V. Supercritical Fl Uid Extraction of Essential Oil from Mint Leaves (Mentha Spicata): Process Optimization and Its Quality Evaluation. *J. Food Process Eng.*, **2016**, *40* (3), e12488.

[14] Costa, S. S.; Gariepy, Y.; Rocha, S. C. S.; Raghavan, V. Microwave Extraction of Mint Essential Oil – Temperature Calibration for the Oven. *J. Food Eng.*, **2014**, *126*, 1–6.

[15] Hanif, M.A., Bhatti, H.N., Jamil, M.S., Anjum, R.S., Jamil, A. and Khan, M.M. Antibacterial and Antifungal Activities of Essential Oils Extracted from Medicinal Plants Using CO2 Supercritical Fluid Extraction Technology. *Asian J. Chem.*, **2010**, *22* (10), 7787–7798.

[16] Zeković, Z., Lepojević, Ž., Milić, S., Adamović, D. and Mujić, I. Supercritical CO2 Extraction of Mentha (Mentha Piperita L.) at Different Solvent Densities. *J. Serbian Chem. Soc.*, **2009**, *74* (4), 417–425.

[17] Sovova, H.; S.A Aleksovski; M. Bocevska, P. R. S. Supercritical Fluid Extraction of Essential Oils - Results of Joint Research. *Chem. Ind. Chem. Eng. Quarterly/CICEQ*, **2006**, *12* (3), 168–174.

[18] Carpinteiro, I.; Abuín, B.; Rodríguez, I.; Ramil, M.; Cela, R. Mixed-Mode Solid-Phase Extraction Followed by Dispersive Liquid – Liquid Microextraction for the Sensitive Determination of Ethylphenols in Red Wines. *J. Chromatogr. A*, **2012**, *1229*, 79–85.

[19] Kabir, A., Locatelli, M. and Ulusoy, H.I. Recent Trends in Microextraction Techniques Employed in Analytical and Bioanalytical Sample Preparation. *Separations*, **2017**, *4* (4), 36.

[20] Belay, K. Advanced Analytical Microextraction Techniques and There Applications : A Review. *Jenvironmental Pollut.*, **2016**, *6* (7).

[21] Jain, R.; Singh, R. Microextraction Techniques for Analysis of Cannabinoids. *TrAC Trends Anal. Chem.*, **2016**, *80*, 156–166.

[22] Richter, J.; Schellenberg, I. Comparison of Different Extraction Methods for the Determination of Essential Oils and Related Compounds from Aromatic Plants and Optimization of Solid-Phase Microextraction / Gas Chromatography. *Anal. Bioanal. Chem.*, **2007**, *386* (6), 2207–2217.

[23] Amlashi, H. S.; Daryasari, A. P.; Soleimani, M. Molecularly Imprinted Polymer Solid Phase Extraction Followed by High-Performance Liquid Chromatography as an Efficient and Sensitive Technique for Determination of Meropenem in Human Plasma and Urine. *South African J. Chem.*, **2019**, *72*, 32–39.

[24] Hackett, J. and Elian, A. A. Solid Phase Extraction and Analysis of THC and Metabolites from Whole Blood Using a Novel Automated Procedure Using Liquid Chromatography and Tandem Mass Spectrometry(LC-MS/MS). *J. Forensic Toxicol. Pharmacol.*, **2012**, *1* (1), 2.

[25] Cai, Y.; Cai, Y.; Shi, Y.; Liu, J.; Mou, S.; Lu, Y. A Liquid – Liquid Extraction Technique for Phthalate Esters with Water-Soluble Organic Solvents by Adding Inorganic Salts. *Microchim. Acta*, **2007**, *157* (1–2), 73–79.

[26] Scortichini, S.; Boarelli, M. C.; Fiorini, D.; Gabrielli, S.; Marcantoni, E. Development and Application of a Solid-Phase Microextraction Gas Cromatography Mass Spectrometry Method for Analysing Volatile Organic Compounds Produced during Cooking. *J. mass Spectrom.*, **2020**, *55* (11), e4534.

[27] Ochiai, N.; Sasamoto, K.; David, F.; Sandra, P. Recent Developments of Stir Bar Sorptive Extraction for Food Applications: Extension to Polar Solutes. *J. Agric. Food Chem.*, **2018**, *66* (28), 7249–7255.

[28] Bader, N. Stir Bar Sorptive Extraction as a Sample Preparation Technique for Chromatographic Analysis: An Overview. *Asian J. Nanosci. Mater.*, **2018**, *1* (2), 56–62.

[29] Silva, C.; Cavaco, C.; Perestrelo, R.; Pereira, J.; Câmara, J. S. Microextraction by Packed Sorbent (MEPS) and Solid-Phase Microextraction (SPME) as Sample Preparation Procedures for the Metabolomic Profiling of Urine. *Metabolites*, **2014**, *4* (1), 71–97.

[30] Celeiro, M.; Acerbi, R.; Kabir, A.; Furton, K. G.; Llompart, M. Development of an Analytical Methodology Based on Fabric Phase Sorptive Extraction Followed by Gas Chromatography-Tandem Mass Spectrometry to Determine UV Filters in Environmental and Recreational Waters. *Anal. Chim. Acta X*, **2020**, *4*, 100038.

[31] Kumar, R.; Gaurav; Heena; Malik, A. K.; Kabir, A.; Furton, K. G. Efficient Analysis of Selected Estrogens Using Fabric Phase Sorptive Extraction and High Performance Liquid Chromatography-Fluorescence Detection. *J. Chromatogr. A*, **2014**, *1359*, 16–25.

[32] Moradi, M.; Yamini, Y.; Baheri, T. Analysis of Abuse Drugs in Urine Using Surfactant-

Assisted Dispersive Liquid–Liquid Microextraction. *J. Sep. Sci.*, **2011**, *32* (14), 1722–1729.

[33] Abdulra'uf, L. B.; Sirhan, A. Y.; Huat Tan, G. Recent Developments and Applications of Liquid Phase Microextraction in Fruits and Vegetables Analysis. *J. Sep. Sci.*, **2012**, *35* (24), 3540–3553.

[34] Pena-pereira, F.; Lavilla, I.; Bendicho, C. Miniaturized Preconcentration Methods Based on Liquid–Liquid Extraction and Their Application in Inorganic Ultratrace Analysis and Speciation: A Review. *Spectrochim. Acta Part B At. Spectrosc.*, **2009**, *64* (1), 1–15.

[35] Bobade, V.; Eshtiaghi, N. Heavy Metals Removal from Wastewater by Adsorption Process : A Review. In *Asia Pacific Confederation of Chemical Engineering Congress 2015*; 2015; p 312.

[36] Czarna, D.; Kunecki, P.; Zmuda, R.; Wdowin, M. Synthetic Zeolites as Potential Sorbents of Mercury from Wastewater Occurring during Wet FGD Processes of Fl Ue Gas. *J. Clean. Prod.*, **2018**, *172*, 2636–2645.

[37] Guzmán, J. D.; Betancur, S.; Carrasco-Marín, F.; Franco, C. A.; Nassar, N. N.; Cortés, F. B. Importance of the Adsorption Method Used for Obtaining the Nanoparticle Dosage for Asphaltene-Related Treatments. *Energy and Fuels*, **2016**, *30* (3), 2052–2059.

[38] Ma, X.; Zhao, M.; Zhao, F.; Guo, H.; Crittenden, J.; Zhu, Y.; Chen, Y. Application of Silica-Based Monolith as Solid-Phase Extraction Sorbent for Extracting Toxaphene Congeners in Soil. *J. Sol-Gel Sci. Technol.*, **2016**, *80* (1), 87–95.

[39] Casado, N.; Morante-zarcero, S.; Pérez-quintanilla, D.; Câmara, J. S. Two Novel Strategies in Food Sample Preparation for the Analysis of Dietary Polyphenols : Micro-Extraction Techniques and New Silica-Based Sorbent Materials. *Trends Food Sci. Technol.*, **2020**, *98*, 167–180.

[40] Saleem, J.; Shahid, U. Bin; Hijab, M.; Mackey, H.; Mckay, G. Production and Applications of Activated Carbons as Adsorbents from Olive Stones. *Biomass Convers. Biorefinery*, **2019**, *9* (4), 775–802.

[41] Mendaš, G., Drevenkar, V. and Zupančič-Kralj, L. Solid-Phase Extraction with Styrene – Divinylbenzene Sorbent for High-Performance Liquid or Gas Chromatographic Determination of Urinary Chloro- and Methylthiotriazines. *J. Chromatogr. A*, **2001**, *918* (2), 351–359.

[42] Zhang, N.; Jiang, W.; Wang, T.; Gu, J.; Zhong, S.; Zhou, S.; Xie, T.; Fu, J.; Jiang, W. Facile Preparation of Magnetic Poly (Styrene- Divinylbenzene) Foam and Its Application as an Oil

Absorbent. *Ind. Eng. Chem. Res.*, **2015**, *54* (44), 11033–11039.

[43] Fathy, M., Moghny, T.A., Awadallah, A.E. and El-Bellihi, A. H. A. Study the Adsorption of Sulfates by High Cross-Linked Polystyrene Divinylbenzene Anion-Exchange Resin. *Appl. Water Sci.*, **2017**, *7* (1), 309–313.

[44] Pang, N.; Wang, T.; Cui, Y.; Hu, J. New Dispersive Solid Phase Extraction Sorbent of Graphitic Carbon Nitride for Field Evaluation and Dissipation Kinetics of Pesticides in Wheat Ecosystem by Liquid Chromatography Tandem Mass Spectrometry. *Int. J. Environ. Anal. Chem.*, **2016**, *96* (12), 1156–1169.

[45] Tan, S.C., and Lee, H.K. Graphitic Carbon Nitride as Sorbent for the Emulsification-Enhanced Disposable Pipette Extraction of Eight Organochlorine Pesticides Prior to GC-MS Analysis. *Microchim. Acta*, **2020**, *187* (2), 1–10.

[46] Sun, Y.; Ha, W.; Chen, J.; Qi, H.; Shi, Y. Advances and Applications of Graphitic Carbon Nitride as Sorbent in Analytical Chemistry for Sample Pretreatment : A Review. *TrAc Trends Anal. Chem.*, **2016**, *84*, 12–21.

[47] Cegłowski, M.; Smoluch, M.; Reszke, E.; Jerzy, S.; Grzegorz, S. Molecularly Imprinted Polymers as Selective Adsorbents for Ambient Plasma Mass Spectrometry. *Anal. Bioanal. Chem.*, **2017**, *409* (13), 3393–3405.

[48] Vasconcelos, I., da Silva, P.H.R., Dias, D.R.D., de Freitas Marques, M.B., da Nova Mussel, W., Pedrosa, T.A., e Silva, M.E.S.R., de Souza Freitas, R.F., de Sousa, R.G. and Fernandes, C. Synthesis and Characterization of a Molecularly Imprinted Polymer (MIP) for Solid-Phase Extraction of the Antidiabetic Gliclazide from Human Plasma. *Mater. Sci. Eng. C*, **2020**, *116*, 111–191.

[49] Iskierko, Z.; Sharma, P. S.; Prochowicz, D.; Fronc, K.; D'Souza, F.; Toczydlowska, D.; Stefaniak, F.; Noworyta, K. Molecularly Imprinted Polymer (MIP) Film with Improved Surface Area Developed by Using Metal-Organic Framework (MOF) for Sensitive Lipocalin (NGAL) Determination. *ACS Appl. Mater. Interfaces*, **2016**, *8* (31), 19860–19865.

[50] Tan, S. C.; Sin Leow, J. W.; Lee, H. K. Emulsification-Assisted Micro-Solid-Phase Extraction Using a Metal-Organic Framework as Sorbent for the Liquid Chromatography-Tandem Mass Spectrometric Analysis of Polar Herbicides from Aqueous Samples. *Talanta*, **2020**, *216*, 120962.

[51] Ionela, D.; Fertu, T.; Gavrilescu, M. Application of Natural Zeolites as Sorbents in the Clean-up of Aqueous Streams. *Environ. Eng. Manag. J.*, **2012**, *11* (4), 867–878.

[52] Paul, B.; Dynes, J. J.; Chang, W. Modified Zeolite Adsorbents for the Remediation of Potash Brine-Impacted Groundwater : Built-in Dual Functions for Desalination and PH Neutralization. *Desalination*, **2017**, *419*, 141–151.

[53] Fernandes, R.S., Dinc, M., Raimundo Jr, I.M. and Mizaikoff, B. Synthesis and Characterization of Porous Surface Molecularly Imprinted Silica Microsphere for Selective Extraction of Ascorbic Acid. *Microporous Mesoporous Mater.*, **2020**, *264*, 28–34.

[54] Cáceres, C., Bravo, C., Rivas, B., Moczko, E., Sáez, P., García, Y. and Pereira, E. Molecularly Imprinted Polymers for the Selective Extraction of Bisphenol A and Progesterone from Aqueous Media. *Polymers (Basel).*, **2018**, *10* (6), 679.

[55] Pardeshi, S.; Singh, S. K. Precipitation Polymerization: A Versatile Tool for Preparing Molecularly Imprinted Polymer Beads for Chromatography Applications. *Rsc Adv.*, **2016**, *6* (28), 23525-23536.

[56] Beltran, A., Borrull, F., Marcé, R.M. and Cormack, P. A. . Molecularly-Imprinted Polymers : Useful Sorbents for Selective Extractions. *TrAC Trends Anal. Chem.*, **2010**, *29* (11), 1363–1375.

[57] Fauziah, S.; Soekamto, N. H.; Taba, P.; Amran, M. B. Selectivity of β-Sitosterol Imprinted Polymers as Adsorbent. *J. Phys. Conf. Ser.*, **2018**, *979* (1), 012059.

[58] Derwich, E.; Benziane, Z.; Taouil, R. GC/MS Analysis of Volatile Compounds of the Essential Oil of the Leaves of Mentha Pulegium Growing in Morocco. *Chem Bull Politeh. Univ*, **2010**, *55* (69), 103–106.

[59] Foganholi, A.P.D.A.M., Daniel, J.F.S., Santiago, D.C., Orives, J.R., Pereira, J.P. and de Jesus Faria, T. Chemical Composition and Antifungal Activity of Pennyroyal Essential Oil in Different Stages of Development. *Semin. Agrar.*, **2015**, *36* (5), 3091–3100.

[60] Shaukat, K., Kaneez, F., Hina, Y., Hira, N., Khan, U. and Iqbal, A. Quality Control Testing of Various Samples of Peppermint Oil Collected from Local Market of Karachi Oakistan. *Baqai J. Heal. Sci.*, **2016**, *19* (1), 27–32.

[61] Croteau, R B; Davis, E M; Ringer, K L; Wildung, M. R. (−)-Menthol Biosynthesis and Molecular Genetics. *Naturwissenschaften*, **2005**, *92* (12), 562–577.

[62] Toogood, H. S.; Cheallaigh, A. N.; Tait, S.; Mansell, D. J.; Jervis, A.; Lygidakis, A.; Humphreys, L.; Takano, E.; Gardiner, J. M.; Scrutton, N. S. Enzymatic Menthol Production: One-Pot Approach Using Engineered Escherichia Coli. *ACS Synth. Biol.*, **2015**, *4* (10), 1112–1123.

[63] Reinscheid, F.; Reinscheid, U. M. Stereochemical Analysis of Menthol and Menthylamine Isomers Using Calculated and Experimental Optical Rotation Data. *J. Mol. Struct.*, **2016**, *1103*, 166–176.

[64] Ringer, K. L.; McConkey, M. E.; Davis, E. M.; Rushing, G. W.; Croteau, R. Monoterpene Double-Bond Reductases of the (-)-Menthol Biosynthetic Pathway: Isolation and Characterization of CDNAs Encoding (-)-Isopiperitenone Reductase and (+)-Pulegone Reductase of Peppermint. *Arch. Biochem. Biophys.*, **2003**, *418* (1), 80–92.

[65] Shubert, V.A., Schmitz, D. and Schnell, M. Enantiomer-Sensitive Spectroscopy and Mixture Analysis of Chiral Molecules Containing Two Stereogenic Centers - Microwave Three-Wave Mixing of Menthone. *J. Mol. Spectrosc.*, **2014**, *300*, 31–36.

[66] Albrecht, M.; Will, J.; Suhm, M. A. Chirality Recognition in Menthol and Neomenthol: Preference for Homoconfigurational Aggregation. *Angew. Chemie - Int. Ed.*, **2010**, *49* (35), 6203–6206.

[67] Hedin-Dahlström, J.; Shoravi, S.; Wikman, S.; Nicholls, I. A. Stereoselective Reduction of Menthone by Molecularly Imprinted Polymers. *Tetrahedron Asymmetry*, **2004**, *15* (15), 2431–2436.

[68] Etzold, B.; Jess, A.; Nobis, M. Epimerisation of Menthol Stereoisomers: Kinetic Studies of the Heterogeneously Catalysed Menthol Production. *Catal. Today*, **2009**, *140* (1–2), 30–36.

[69] Panev, S.; Dimitrov, V. Cerium(III) Chloride Promoted Addition of Organometallic Reagents to (-)-Menthone-Preparation of Chiral Neomenthyl Derivatives. *Tetrahedron Asymmetry*, **2000**, *11* (7), 1517–1526.

[70] Pečar, D.; Goršek, A. Oxidation of Menthol : Reaction-Rate Determination Based on Thermodynamic Profiles. *Chem. Eng. Commun.*, **2014**, *201* (11), 1548–1554.

[71] Dodero, V. I.; Giagante, N. N.; Mandolesi, S. D.; Zúñiga, A. E.; Podestá, J. C. Stereoselective Addition of Organotin Anions to R-(+)-Pulegone: A Route To8-Triorganostannylmenthols. *Arkivoc*, **2003**, *10*, 335–346.

[72] Lecomte, V.; Stéphan, E.; Jaouen, G. Improved Addition of Phenyllithium to Hindered Ketones by the Use of Non-Polar Media. *Tetrahedron Lett.*, **2002**, *43* (19), 3463–3465.

[73] Ashby, E. C.; Laemmle, J. T. Stereochemistry of Organometallic Compound Addition to Ketones. *Chem. Rev.*, **1975**, *75* (4), 521–546.

[74] Zhao, P.; Wang, Z.; Gao, X.; Guo, X.; Zhao, L. Simultaneous Enantioselective Determination of 22 Chiral Pesticides in Fruits and Vegetables Using Chiral Liquid Chromatography Coupled with Tandem Mass Spectrometry. *Food Chem.*, **2019**, *277*, 298–306.

[75] Davies, N. M.; Wei Teng, X. Importance of Chirality in Drug Therapy and Pharmacy Practice: Implications for Psychiatry. *Adv. Pharm.*, **2003**, *1* (3), 242–252.

[76] Ananthi, N.; Jayakumar, R; Vadivel, R; Ananthi, N. Role of Chirality in Drugs. *Org. Med. Chem. Int. J.*, **2018**, *5* (3), 001–006.

[77] Mukherjee, A.; Bera, A. Importance of Chirality and Chiral Chromatography in Pharmaceutical Industry : A Detailed Study. *J. Curr. Chem. Pharm. Sci.*, **2012**, *2* (4), 334–346.

[78] Cui, N.; Xu, H.; Yao, S.; He, Y.; Zhang, H.; Yu, Y. Chiral Triazole Fungicide Tebuconazole : Enantioselective Bioaccumulation , Bioactivity , Acute Toxicity , and Dissipation in Soils. *Environ. Sci. Pollut. Res.*, **2018**, *25* (25), 25468-25475.

[79] Li, L.; Gao, B.; Wen, Y.; Zhang, Z.; Chen, R.; He, Z.; Kaziem, A. E.; Shi, H.; Wang, M. Stereoselective Bioactivity , Toxicity and Degradation of the Chiral Triazole Fungicide Bitertanol. *Pest Manag. Sci.*, **2020**, *76* (1), 343–349.

[80] Nguyen, L. A.; He, H.; Pham-Huy, C. Chiral Drugs: An Overview. *Int. J. Biomed. Sci.*, **2006**, *2* (2), 85–100.

[81] Lin, G.Q., Zhang, J.G. and Cheng, J. . Overview of Chirality and Chiral Drugs. *Chiral Drugs Chem. Biol. Action*, **2011**, 456.

[82] Abualhasan, M. N.; Zaid, A. N.; Jaradat, N.; Mousa, A. GC Method Validation for the Analysis of Menthol in Suppository Pharmaceutical Dosage Form. *Int. J. Anal. Chem.*, **2017**.

[83] Ali, I.; Suhail, M.; Lone, M. N.; Alothman, Z. A.; Alwarthan, A. Chiral Resolution of Multichiral Center Racemates by Different Modalities of Chromatography. *J. Liq. Chromatogr. Relat. Technol.*, **2016**, *39* (9), 435–444.

[84] Yang, S.; Wang, Y.; Jiang, Y.; Li, S.; Liu, W. Molecularly Imprinted Polymers for the Identification and Separation of Chiral Drugs and Biomolecules. *Polymers (Basel).*, **2016**, *8* (6), 216.

[85] Toyo'oka, T. Resolution of Chiral Drugs by Liquid Chromatography Based upon Diastereomer Formation with Chiral Derivatization Reagents. *J. Biochem. Biophys. Methods*, **2002**, *54* (1–3), 25–56.

[86] Zhang, Y.; Wu, D. R.; Wang-Iverson, D. B.; Tymiak, A. A. Enantioselective Chromatography in Drug Discovery. *Drug Discov. Today*, **2005**, *10* (8), 571–577.

[87] Teixeira, J.; Tiritan, M. E.; Pinto, M. M. M.; Fernandes, C. Chiral Stationary Phases for Liquid Chromatography: Recent Developments. *Molecules*, **2019**, *24* (5), 869.

[88] Rebizi, M.; Sekkoum, K.; Belboukhari, N.; Cheriti, A.; Aboul-Enein, H. Chiral Separation and Determination of Enantiomeric Purity of the Pharmaceutical Formulation of Cefadroxil Using Coated and Immobilized Amylose-Derived and Cellulose-Derived Chiral Stationary Phases. *Egypt. Pharm. J.*, **2016**, *15* (2), 88.

[89] Fedorova, I. A.; Shapovalova, E. N.; Shpigun, O. A.; Staroverov, S. M. Bovine Serum Albumin Adsorbed on Eremomycin and Grafted on Silica as New Mixed-Binary Chiral Sorbent for Improved Enantioseparation of Drugs. *J. Food Drug Anal.*, **2016**, *24* (4), 848–854.

[90] Yang, X.; Su, L.; Hou, X.; Ding, S.; Xu, W.; Wang, B.; Fang, H. High-Performance Liquid Chromatographic Enantioseparation of 3,5-Disubstituted Hydantoins Analogs and Temperature-Induced Reversals of Elution Orders on a Polysaccharide-Based Chiral Stationary Phase. *J. Chromatogr. A*, **2014**, *1355*, 291–295.

[91] Fanali, C.; Fanali, S.; Chankvetadze, B. HPLC Separation of Enantiomers of Some Flavanone Derivatives Using Polysaccharide-Based Chiral Selectors Covalently Immobilized on Silica. *Chromatographia*, **2016**, *79* (3), 119–124.

[92] Sun, M.; Liu, D.; Shen, Z.; Zhou, Z.; Wang, P. Stereoselective Quantitation of Haloxyfop in Environment Samples and Enantioselective Degradation in Soils. *Chemosphere*, **2015**, *119*, 583–589.

[93] Hussain, S. Z.; Maqbool, K. GC-MS: Principle, Technique and Its Application in Food Science. *Int. J. Curr. Sci.*, **2014**, *13*, 116–126.

[94] Xie, S. M.; Chen, X. X.; Zhang, J. H.; Yuan, L. M. Gas Chromatographic Separation of

Enantiomers on Novel Chiral Stationary Phases. *Trends Anal. Chem.*, **2020**, *124*, 115808.

[95] Patil, R.A., Weatherly, C.A. and Armstrong, D.W. Chiral Gas Chromatography. In *Chiral Analysis*; Elsevier B.V.: Arlington, Arlington, TX, United States, 2018; pp 468–505. https://doi.org/10.1016/B978-0-444-64027-7/00012-4.

[96] Orata, F. Derivatization Reactions and Reagents for Gas Chromatography Analysis. In *Advanced Gas Chromatography - Progress in Agricultural, Biomedical and Industrial Applications*; Mohd, D. M. A., Ed.; InTech: China, 2012; pp 83–108.

[97] Koo, C.; Cox, M.; Klass, G.; Johnston, M. Stereochemical Analysis of Methorphan Using (-)-Menthyl Chloroformate. *J. Forensic Sci.*, **2012**, *57* (6), 1549–1555.

[98] Katagi, T. Isomerization of Chiral Pesticides in the Environment. *J. Pestic. Sci.*, **2015**, *37* (1), 1–14.

[99] Almalki, A. J.; Clark, C. R.; DeRuiter, J. GC–MS Analysis of Regioisomeric Substituted N-Benzyl-4-Bromo-2,5-Dimethoxyphenethylamines. *Forensic Chem.*, **2019**, *14*, 100164.

[100] White, R. L. Chromatography-IR, Methods and Instrumentation. In *Encyclopedia of Spectroscopy and Spectrometry*; John C. Lindon, Ed.; Elsevier Ltd.: Norman, OK, USA, 2016; pp 251–255.

[101] Carrão, D.B., Perovani, I.S., de Albuquerque, N.C.P. and de Oliveira, A.R.M. Enantioseparation of Pesticides A Critical Review. *Trends Anal. Chem.*, **2020**, *122*, 115719.

[102] Tao, Y.; Zheng, Z.; Yu, Y.; Xu, J.; Liu, X.; Wu, X.; Dong, F.; Zheng, Y. Supercritical Fluid Chromatography–Tandem Mass Spectrometry-Assisted Methodology for Rapid Enantiomeric Analysis of Fenbuconazole and Its Chiral Metabolites in Fruits, Vegetables, Cereals, and Soil. *Food Chem.*, **2018**, *241*, 32–39.

[103] Tarafder, A. Metamorphosis of Supercritical Fluid Chromatography to SFC: An Overview. *TrAC - Trends Anal. Chem.*, **2016**, *81*, 3–10.

[104] Li, L. Direct Enantiomer Determination of Methorphan by HPLC-MS and SFC-MS. *Forensic Chem.*, **2016**, *2*, 82–85.

[105] Harps, L. C.; Joseph, J. F.; Parr, M. K. SFC for Chiral Separations in Bioanalysis. *J. Pharm. Biomed. Anal.*, **2019**, *162*, 47–59.

[106] Yan, Y.; Fan, J.; Lai, Y.; He, J.; Guo, D.; Zhang, H.; Zhang, W. Efficient Preparative

Separation of β-Cypermethrin Stereoisomers by Supercritical Fluid Chromatography with a Two-Step Combined Strategy. *J. Sep. Sci.*, **2017**, *10*, 1–8.

[107] Heiland, J. J.; Geissler, D.; Piendl, S. K.; Warias, R.; Belder, D. Supercritical-Fluid Chromatography On-Chip with Two-Photon-Excited-Fluorescence Detection for High-Speed Chiral Separations. *Anal. Chem.*, **2019**, *91* (9), 6134–6140.

[108] Kašička, V. Capillary Electromigration Techniques. In *Capillary Electrophoresis*; Anderson, J. L., Berthod, A., Eds.; Wiley-VCH Verlag GmbH & Co. KGaA, 2015; pp 503–530.

[109] Amin, N. C.; Blanchin, M. D.; Aké, M.; Fabre, H. Capillary Electrophoresis Methods for the Analysis of Antimalarials. Part I. Chiral Separation Methods. *J. Chromatogr. A*, **2012**, *1264*, 1–12.

[110] Declerck, S.; Vander Heyden, Y.; Mangelings, D. Enantioseparations of Pharmaceuticals with Capillary Electrochromatography: A Review. *J. Pharm. Biomed. Anal.*, **2016**, *130*, 81–99.

[111] D'Orazio, G.; Fanali, C.; Asensio-Ramos, M.; Fanali, S. Chiral Separations in Food Analysis. *TrAC - Trends Anal. Chem.*, **2017**, *96*, 151–171.

[112] García, M. Á.; Menéndez-López, N.; Boltes, K.; Castro-Puyana, M.; Marina, M. L. A Capillary Micellar Electrokinetic Chromatography Method for the Stereoselective Quantitation of Bioallethrin in Biotic and Abiotic Samples. *J. Chromatogr. A*, **2017**, *1510*, 108–116.

[113] Lancioni, C.; Keunchkarian, S.; Castells, C. B.; Gagliardi, L. G. Enantiomeric Separations by Capillary Electrophoresis: Theoretical Method to Determine Optimum Chiral Selector Concentration. *J. Chromatogr. A*, **2018**, *1539*, 71–77.

[114] Ndunda, E. N.; Mizaikoff, B. Molecularly Imprinted Polymers for the Analysis and Removal of Polychlorinated Aromatic Compounds in the Environment: A Review. *Analyst*, **2016**, *141* (11), 3141–3156.

[115] Bitas, D.; Samanidou, V. Molecularly Imprinted Polymers as Extracting Media for the Chromatographic Determination of Antibiotics in Milk. *Molecules*, **2018**, *23* (2), 316–366.

[116] Madikizela, L. M.; Tavengwa, N. T.; Chimuka, L. Applications of Molecularly Imprinted Polymers for Solid-Phase Extraction of Non- Steroidal Anti-Inflammatory Drugs and Analgesics from Environmental Waters and Biological Samples. *J. Pharm. Biomed. Anal.*, **2017**, *147*, 624–633.

[117] Widstrand, C.; Björk, H.; Yilmaz, E. Analysis of Analytes: The Use of MIPs in Solid-Phase Extraction Increases Efficiency and Improves Detection Limits. *Chem. Technol.*, **2006**, 14–15.

[118] Ashley, J.; Shahbazi, M.; Kant, K.; Aaydha, V. Biosensors and Bioelectronics Molecularly Imprinted Polymers for Sample Preparation and Biosensing in Food Analysis : Progress and Perspectives. *Biosens. Bioelectron.*, **2017**, *91*, 606–615.

[119] Martín-Esteban, A. Recent Molecularly Imprinted Polymer-Based Sample Preparation Techniques in Environmental Analysis. *Trends Environ. Anal. Chem.*, **2016**, *9*, 8–14.

[120] Poliwoda, A.; Mościpan, M.; Wieczorek, P. P. Application of Molecular Imprinted Polymers for Selective Solid Phase Extraction of Bisphenol A. *Ecol. Chem. Eng. S*, **2016**, *23* (4), 651–664.

[121] Xu, S.; Lu, H.; Chen, L. Double Water Compatible Molecularly Imprinted Polymers Applied as Solid-Phase Extraction Sorbent for Selective Preconcentration and Determination of Triazines in Complicated Water Samples. *J. Chromatogr. A*, **2014**, *1350*, 23–29.

[122] Manesiotis, P.; Osmani, Q.; McLoughlin, P. An Enantio-Selective Chromatographic Stationary Phase for S-Ibuprofen Prepared by Stoichiometric Molecular Imprinting. *J. Mater. Chem.*, **2012**, *22* (22), 11201–11207.

[123] Zunngu, S. S.; Madikizela, L. M.; Chimuka, L.; Mdluli, P. S. Synthesis and Application of a Molecularly Imprinted Polymer in the Solid-Phase Extraction of Ketoprofen from Wastewater. *Comptes Rendus Chim.*, **2017**, *20* (5), 585-591.

[124] Tavengwa, N. T.; Cukrowska, E.; Chimuka, L. Application of Magnetic Molecularly Imprinted Polymers for the Solid Phase Extraction of Selected Nitroaromatic Compounds from Contaminated Aqueous Environments. *Sep. Sci. Technol.*, **2017**, *52* (3), 467–475.

[125] Sarafraz-yazdi, A.; Razavi, N. Application of Molecularly-Imprinted Polymers in Solid-Phase Microextraction Techniques. *Trends Anal. Chem.*, **2015**, *73*, 81–90.

[126] Zhang, M.; Zeng, J.; Wang, Y.; Chen, X. Developments and Trends of Molecularly Imprinted Solid-Phase Microextraction. *Chromatogr. Sci.*, **2013**, *51* (7), 577–586.

[127] Speltini, A.; Scalabrini, A.; Maraschi, F.; Sturini, M.; Profumo, A. Analytica Chimica Acta Newest Applications of Molecularly Imprinted Polymers for Extraction of Contaminants from Environmental and Food Matrices : A Review. *Anal. Chim. Acta*, **2017**, *974*, 1–26.

[128] Abdouss, M., Azodi-Deilami, S., Asadi, E. and Shariatinia, Z. Synthesis of Molecularly Imprinted Polymer as a Sorbent for Solid Phase Extraction of Citalopram from Human Serum and Urine. *J Mater Sci Mater Med*, **2012**, *23* (6), 1543–1552.

[129] Olcer, Y.A., Demirkurt, M., Demir, M.M. and Eroglu, A.E. Development of Molecularly Imprinted Polymers (MIPs) as a Solid Phase Extraction (SPE) Sorbent for the Determination of Ibuprofen in Water. *RSC Adv.*, **2017**, *7* (50), 31441–31447.

[130] Garcia, R.; Cabrita, M. J.; Maria, A.; Freitas, C. Application of Molecularly Imprinted Polymers for the Analysis of Pesticide Residues in Food — A Highly Selective and Innovative Approach. *Am. J. Anal. Chem.*, **2011**, *2* (08), 16–25.

[131] Zhao, M.; Shen, G. The Application of Molecularly Imprinted Polymers. *J. Mater. Sci. Chem. Eng.*, **2015**, *3* (07), 87–89.

[132] Włoch, M.; Datta, J. Synthesis and Polymerisation Techniques of Molecularly Imprinted Polymers. In *Comprehensive Analytical Chemistry*; 2019; Vol. 86, pp 17–40.

[133] Lorenzo, R. A.; Carro, A. M.; Alvarez-lorenzo, C.; Concheiro, A. To Remove or Not to Remove ? The Challenge of Extracting the Template to Make the Cavities Available in Molecularly Imprinted Polymers (MIPs). *nternational J. Mol. Sci.*, **2011**, *12* (07), 4327–4347.

[134] Farooq, S.; Nie, J.; Cheng, Y.; Yan, Z.; Li, J.; Asim, S.; Bacha, S.; Mushtaq, A.; Zhang, H. Molecularly Imprinted Polymers' Application in Pesticide Residue Detection. *R. Soc. Chem.*, **2018**, *143* (17), 3971–3989.

[135] Madikizela, L. M.; Tavengwa, N. T.; Tutu, H.; Chimuka, L. Green Aspects in Molecular Imprinting Technology : From Design to Environmental Applications. *Trends Environ. Anal. Chem.*, **2018**, *17*, 14–22.

[136] Shahar, T.; Tal, N.; Mandler, D. Molecularly Imprinted Polymer Particles: Formation, Characterization and Application. *Colloids Surfaces A Physicochem. Eng. Asp.*, **2016**, *495*, 11–19.

[137] Azodi-Deilami, S.; Abdouss, M.; Seyedi, S. R. Synthesis and Characterization of Molecularly Imprinted Polymer for Controlled Release of Tramadol. *Cent. Eur. J. Chem.*, **2010**, *8* (3), 687–695.

[138] Batlokwa, B. S.; Mokgadi, J.; Nyokong, T.; Torto, N. Optimal Template Removal from

Molecularly Imprinted Polymers by Pressurized Hot Water Extraction. *Chromatographia*, **2011**, *73* (5–6), 589–593.

[139] Zahedi, P.; Fallah-Darrehchi, M.; Nadoushan, S. A.; Aeinehvand, R.; Bagheri, L.; Najafi, M. Morphological, Thermal and Drug Release Studies of Poly (Methacrylic Acid)-Based Molecularly Imprinted Polymer Nanoparticles Immobilized in Electrospun Poly (ε-Caprolactone) Nanofibers as Dexamethasone Delivery System. *Korean J. Chem. Eng.*, **2017**, *34* (7), 2110–2118.

[140] Aeinehvand, R., Zahedi, P., Kashani-Rahimi, S., Fallah-Darrehchi, M. and Shamsi, M. Synthesis of Poly(2-Hydroxyethyl Methacrylate)-Based Molecularly Imprinted Polymer Nanoparticles Containing Timolol Maleate: Morphological, Thermal, and Drug Release along with Cell Biocompatibility Studies. *Polym. Adv. Technol.*, **2016**, *28* (7), 828–841.

[141] Madrakian, T.; Ahmadi, M.; Afkhami, A.; Soleimani, M. Selective Solid-Phase Extraction of Naproxen Drug from Human Urine Samples Using Molecularly Imprinted Polymer-Coated Magnetic Multi-Walled Carbon Nanotubes Prior to Its Spectrofluorometric Determination. *Analyst*, **2013**, *138* (16), 4542–4549.

[142] Yang, J.; Li, Y.; Wang, J.; Sun, X.; Cao, R.; Sun, H.; Huang, C.; Chen, J. Molecularly Imprinted Polymer Microspheres Prepared by Pickering Emulsion Polymerization for Selective Solid-Phase Extraction of Eight Bisphenols from Human Urine Samples. *Anal. Chim. Acta*, **2015**, *872*, 35–45.

[143] Huang, S.; Xu, J.; Zheng, J.; Zhu, F.; Xie, L.; Ouyang, G. Synthesis and Application of Magnetic Molecularly Imprinted Polymers in Sample Preparation. *Anal. Bioanal. Chem.*, **2018**, *410* (17), 3991–4014.

[144] Chen, L.; Li, B. Application of Magnetic Molecularly Imprinted Polymers in Analytical Chemistry. *Anal. methods ·*, **2012**, *4* (9), 2613–2613.

[145] Rutkowska, M.; Płotka-Wasylka, J.; Morrison, C.; Wieczorek, P. P.; Namieśnik, J.; Marć, M. Application of Molecularly Imprinted Polymers in Analytical Chiral Separations and Analysis. *TrAC - Trends Anal. Chem.*, **2018**, *102*, 91–102.

[146] Liao, S.; Wang, X.; Lin, X.; Wu, X.; Xie, Z. A Molecularly Imprinted Monolith for the Fast Chiral Separation of Antiparasitic Drugs by Pressurized CEC. *J. Sep. Sci.*, **2010**, *33* (14), 2123–2130.

[147] Ansell, R. J.; Kuah, J. K. L.; Wang, D.; Jackson, C. E.; Bartle, K. D.; Clifford, A. A. Imprinted Polymers for Chiral Resolution of (±) -Ephedrine , 4 : Packed Column Supercritical Fluid Chromatography Using Molecularly Imprinted Chiral Stationary Phases. *J. Chromatogr. A*, **2012**, *1264*, 117–123.

[148] Xu, X.; Zhou, G.; Li, H.; Liu, Q.; Zhang, S.; Kong, J. A Novel Molecularly Imprinted Sensor for Selectively Probing Imipramine Created on ITO Electrodes Modified by Au Nanoparticles. *Talanta*, **2009**, *78* (1), 26–32.

[149] Bai, L.; Chen, X.; Huang, Y.; Zhang, Q.-W.; Liu, Z.-S. Chiral Separation of Racemic Mandelic Acids by Use of an Ionic Liquid-Mediated Imprinted Monolith with a Metal Ion as Self-Assembly Pivot. *Anal. Bioanal. Chem.*, **2013**, *405* (27), 8935–8943.

[150] Kirsch, N.; Hedin-Dahlström, J.; Henschel, H.; Whitcombe, M. J.; Wikman, S.; Nicholls, I. A. Molecularly Imprinted Polymer Catalysis of a Diels-Alder Reaction. *J. Mol. Catal. B Enzym.*, **2009**, *58* (1–4), 110–117.

[151] Dramou, P.; Tarannum, N. Molecularly Imprinted Catalysts:Synthesis and Applications. In *Synthesis and Applications*; Elsevier Inc.: BOMBAY, INDIA, 2016; pp 35–53.

[152] Szekely, G.; Didaskalou, C. Biomimics of Metalloenzymes via Imprinting. In *Molecularly Imprinted Catalysts*; 2016; pp 121–158.

[153] Piletsky, S. A.; Piletska, E. V.; Bossi, A.; Karim, K.; Lowe, P.; Turner, A. P. F. Substitution of Antibodies and Receptors with Molecularly Imprinted Polymers in Enzyme-Linked and Fluorescent Assays. *Biosens. Bioelectron.*, **2001**, *16* (9–12), 701–707.

[154] Ye, L.; Mosbach, K. Molecularly Imprinted Microspheres as Antibody Binding Mimics. *React. Funct. Polym.*, **2001**, *48* (1–3), 149–157.

[155] Sharma, P. S.; Wojnarowicz, A.; Kutner, W.; D'Souza, F. Molecularly Imprinted Polymers as Synthetic Catalysts. In *Molecularly Imprinted Catalysts*; Elsevier Inc., 2016; pp 183–210.

[156] Yarman, A.; Jetzschmann, K. J.; Neumann, B.; Zhang, X.; Wollenberger, U.; Cordin, A.; Haupt, K.; Scheller, F. W. Enzymes as Tools in MIP-Sensors. *Chemosensors*, **2017**, *5* (2), 11.

[157] Song, X.; Xu, S.; Chen, L.; Wei, Y.; Xiong, H. Recent Advances in Molecularly Imprinted Polymers in Food Analysis. *J. Appl. Polym. Sci.*, **2014**, *131* (16).

[158] Chen, L.; Wang, X.; Lu, W.; Wu, X.; Li, J. Molecular Imprinting: Perspectives and

Applications. *Chem. Soc. Rev.*, **2016**, *45* (8), 2137–2211.

[159] Chen, L.; Xu, S.; Li, J. Recent Advances in Molecular Imprinting Technology: Current Status, Challenges and Highlighted Applications. *Chem. Soc. Rev.*, **2011**, *40* (5), 2922–2942.

[160] Gutierrez-climente, R.; Gomez-caballero, A.; Guerreiro, A.; Garcia-mutio, D.; Unceta, N.; Goicolea, M. A.; Barrio, R. J. Molecularly Imprinted Nanoparticles Grafted to Porous Silica as Chiral Selectors in Liquid Chromatography. *J. Chromatogr. A*, **2017**, *1508*, 53–64.

[161] Leonhardt, A.; Mosbach, K. Enzyme-Mimicking Polymers Exhibiting Specific Substrate Binding and Catalytic Functions. *React. Polym. Ion Exch. Sorbents*, **1987**, *6* (2–3), 285–290.

[162] Madikizela, L.; Tavengwa, N.; Pakade, V. Molecularly Imprinted Polymers for Pharmaceutical Compounds: Synthetic Procedures and Analytical Applications. *Recent Res. Polym. IntechOpen London, UK*, **2018**, 47–67.

[163] Shen, X.; Xu, C.; Ye, L. Imprinted Polymer Beads Enabling Direct and Selective Molecular Separation in Water. *Soft Matter*, **2012**, *8* (27), 7169–7176.

[164] Yang, Y.; Liu, X.; Kong, X.; Qin, Z.; Jiao, Z.; Li, S. Preparation and Evaluation of Oseltamivir Molecularly Imprinted Polymer Silica Gel as Liquid Chromatography Stationary Phase. *Molecules*, **2018**, *23* (8), 1881.

[165] Wang, X. H.; Dong, Q.; Ying, L. L.; Chi, S. S.; Lan, Y. H.; Huang, Y. P.; Liu, Z. S. Enhancement of Selective Separation on Molecularly Imprinted Monolith by Molecular Crowding Agent. *Anal. Bioanal. Chem.*, **2017**, *409* (1), 201–211.

[166] Mijangos, I.; Navarro-Villoslada, F.; Guerreiro, A.; Piletska, E.; Chianella, I.; Karim, K.; Turner, A.; Piletsky, S. Influence of Initiator and Different Polymerisation Conditions on Performance of Molecularly Imprinted Polymers. *Biosens. Bioelectron.*, **2006**, *22* (3), 381–387.

[167] Zhou, T.; Shen, X.; Chaudhary, S.; Ye, L. Molecularly Imprinted Polymer Beads Prepared by Pickering Emulsion Polymerization for Steroid Recognition. *J. Appl. Polym. Sci.*, **2014**, *131* (1).

[168] Shen, X.; Zhou, T.; Ye, L. Molecular Imprinting of Protein in Pickering Emulsion. *Chem. Commun.*, **2012**, *48* (66), 8198–8200.

[169] Szajnecki, Ł.; Gawdzik, B. Studies on Sorption of Bifenthrin and Diazinon Insecticides on

Molecularly Imprinted Polymers. *Polym. Adv. Technol.*, **2019**, *30* (7), 1595–1604.

[170] Ning, F.; Qiu, T.; Wang, Q.; Peng, H.; Li, Y.; Wu, X.; Zhang, Z.; Chen, L.; Xiong, H. Dummy-Surface Molecularly Imprinted Polymers on Magnetic Graphene Oxide for Rapid and Selective Quantification of Acrylamide in Heat- Processed (Including Fried) Foods. *Food Chem.*, **2017**, *221*, 1797–1804.

[171] Carro-Diaz, A. M.; Lorenzo-Ferreira, R. A. Molecularly Imprinted Polymers for Sample Preparation. *Handb. Mol. imprinted Polym.*, **2013**, *1*, 87–97.

[172] Regal, P.; Díaz-Bao, M.; Barreiro, R.; Cepeda, A.; Fente, C. Application of Molecularly Imprinted Polymers in Food Analysis: Clean-up and Chromatographic Improvements. *Open Chem.*, **2012**, *10* (3), 766–784.

[173] Freitas, A. F. F. L. . Synthesis and Characterization of Molecularly Imprinted Polymer Particles (MIPs) for Biomedical Applications (Doctoral Dissertation)., Politécnico de Bragança, 2015.

[174] Yan, H.; Row, K. H. Characteristic and Synthetic Approach of Molecularly Imprinted Polymer. *Int. J. Mol. Sci.*, **2006**, *7* (5), 155–178.

[175] Denderz, N.; Lehotay, J. Identification of Driving Forces for the Recognition Processes on Molecularly Imprinted Polymers. *Nov. Biotechnol. Chim.*, **2013**, *12* (2), 63–69.

[176] Fuchs, Y.; Soppera, O.; Haupt, K. Photopolymerization and Photostructuring of Molecularly Imprinted Polymers for Sensor Applications-A Review. *Anal. Chim. Acta*, **2012**, *717*, 7–20.

[177] Ansari, S.; Karimi, M. Recent Progress , Challenges and Trends in Trace Determination of Drug Analysis Using Molecularly Imprinted Solid-Phase Microextraction Technology. *Talanta*, **2017**, *164*, 612–625.

[178] Sobolewski, P.; Piwowarczyk, M. Polymer – Graphene Nanocomposite Materials for Electrochemical Biosensing. *Macromol. Biosci.*, **2016**, *16* (7), 1–14.

[179] Beyazit, S.; Tse, B.; Bui, S.; Haupt, K.; Gonzato, C. Progress in Polymer Science Molecularly Imprinted Polymer Nanomaterials and Nanocomposites by Controlled / Living Radical Polymerization. *Prog. Polym. Sci.*, **2016**, *62*, 1–21.

[180] Haupt, K., Linares, A.V., Bompart, M. and Bui, B. T. . Molecularly Imprinted Polymers. *Mol. imprinting*, **2011**, *325*, 1–28.

[181] Whitcombe, M. J.; Kirsch, N.; Nicholls, I. A. Molecular Imprinting Science and Technology. *J. Mol. Recognit.*, **2014**, *27*, 297–401.

[182] Hunsen, M. Pyridinium Chlorochromate Catalyzed Oxidation of Alcohols to Aldehydes and Ketones with Periodic Acid. *Tetrahedron Lett.*, **2005**, *46* (10), 1651–1653.

[183] McMurry, J. *Organic Chemistry 7th Edition Thomson Learning Inc*, 7th ed.; Sandra Kiselica, Ellen Bitter, S. K., Ed.; David Harris, 2008.

[184] Turiel, E.; Esteban, A. M. Molecularly Imprinted Polymers. In *Solid-Phase Extraction*; Elsevier Inc.: Madrid, Spain, 2020; pp 215–233.

[185] Sikiti, P.; Msagati, T. A. M.; Mamba, B. B.; Mishra, A. K. Synthesis and Characterization of Molecularly Imprinted Polymers for the Remediation of PCBs and Dioxins in Aqueous Environments. *J. Environ. Heal. Sci. Eng.*, **2014**, *12* (1), 1–8.

[186] Bayramoglu, G.; Arica, M. Y. Synthesis of Cr (VI) -Imprinted Poly (4-Vinyl Pyridine-Co-Hydroxyethyl Methacrylate) Particles : Its Adsorption Propensity to Cr (VI). *J. Hazard. Mater.*, **2011**, *187* (1–3), 213–221.

[187] Tegegne, B.; Chimuka, L.; Chandravanshi, B. S. Molecularly Imprinted Polymer for Adsorption of Venlafaxine , Albendazole , Ciprofloxacin and Norfloxacin in Aqueous Environment. *Sep. Sci. Technol.*, **2020**, 1–15.

[188] Bakhtiar, S.; Bhawani, S. A.; Shafqat, S. R. Synthesis and Characterization of Molecular Imprinting Polymer for the Removal of 2-Phenylphenol from Spiked Blood Serum and River Water. *Chem. Biol. Technol. Agric.*, **2019**, *6* (1), 1–10.

[189] Shafqat, S. R.; Bhawani, S. A.; Bakhtiar, S.; Nasir, M.; Ibrahim, M. Synthesis of Molecularly Imprinted Polymer for Removal of Congo Red. *BMC Chem.*, **2020**, *14*, 1–15.

[190] Qwane, S. N.; Mdluli, P. S.; Madikizela, L. M. Synthesis , Characterization and Application of a Molecularly Imprinted Polymer in Selective Adsorption of Abacavir from Polluted Water. *South African J. Chem.*, **2020**, *73*, 84–91.

[191] Xu, X.; Guo, P.; Luo, Z.; Ge, Y.; Zhou, Y.; Chang, R.; Du, W.; Chang, C.; Fu, Q. Preparation and Characterization of Surface Molecularly Imprinted Films Coated on Multiwall Carbon Nanotubes for Recognition and Separation of Lysozyme with High Binding Capacity and Selectivity. *R. Soc. Chem. Adv.*, **2017**, *7* (30), 18765–18774.

[192] Gao, R.; Zhao, S.; Hao, Y.; Zhang, L.; Cui, X.; Liu, D.; Tang, Y. Facile and Green Synthesis of Polysaccharide-Based Magnetic Molecularly Imprinted Nanoparticles for Protein Recognition. *R. Soc. Chem. Adv.*, **2015**, *5* (107), 88436–88444.

Appendix

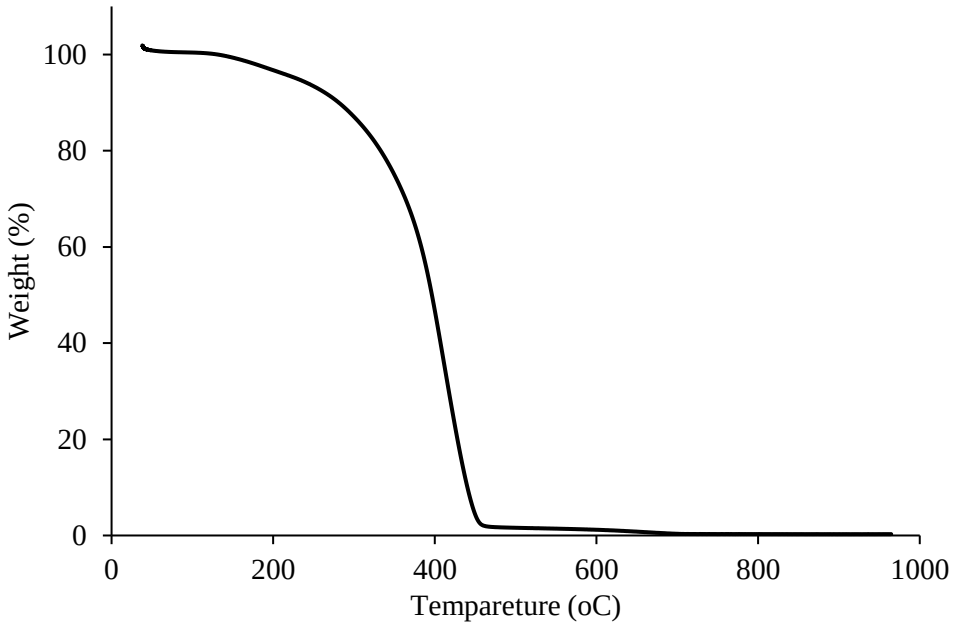

Figure A1: TGA thermograph of unwashed MIPs

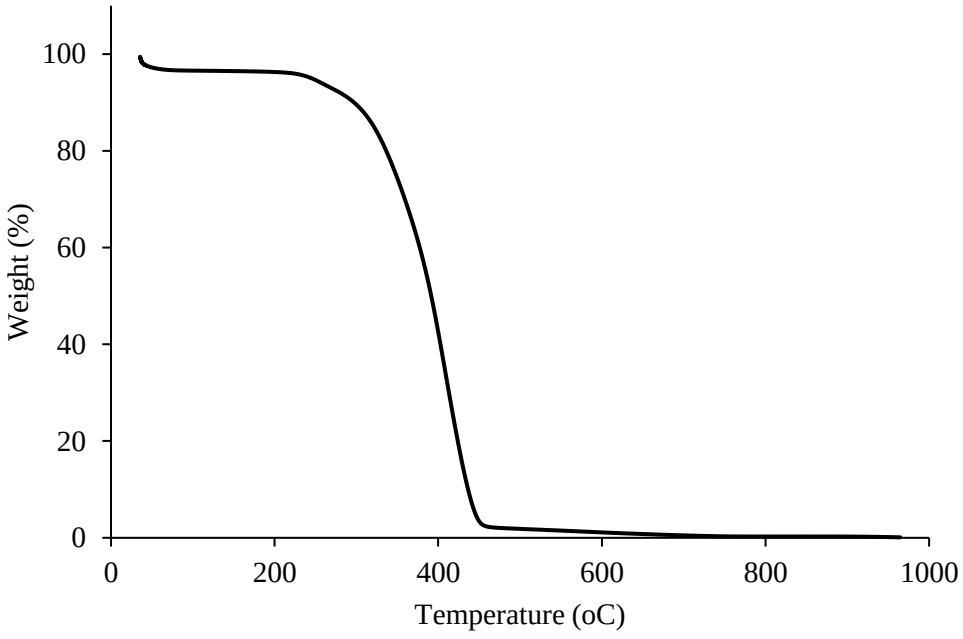

Figure A2: TGA thermograph of washed MIPs

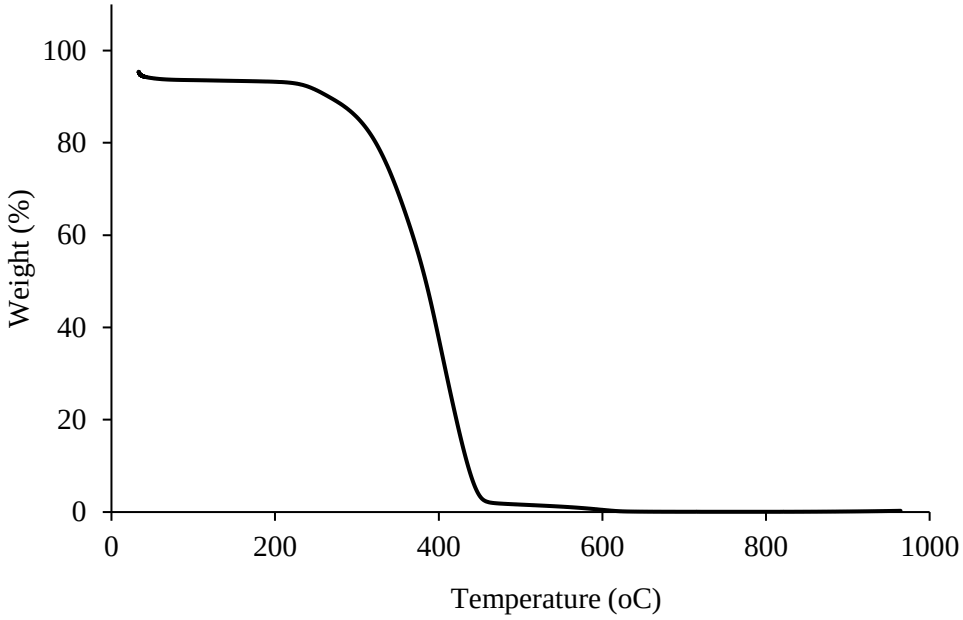

Figure A3: TGA thermograph of washed NIPs